CLIMATE AND FISHING IMPACTS ON NORTH PACIFIC FISHERIES: INSIGHTS AND PROJECTIONS FROM CONTRASTING APPROACHES TO ECOSYSTEM MODELING

A DISSERTATION SUBMITTED TO THE GRADUATE DIVISION OF THE UNIVERSITY OF HAWAIʻI AT MĀNOA IN PARTIAL FULFILLMENT OF THE REQUIREMENTS FOR THE DEGREE OF

DOCTOR OF PHILOSOPHY

IN

MARINE BIOLOGY

May 2019

By

Phoebe Anne Woodworth-Jefcoats

Dissertation Committee:

Jeffrey C. Drazen, Chairperson
Megan Donahue
Kyle Edwards
Jeffrey J. Polovina
Axel Timmermann

ACKNOWLEDGMENTS

Thank you to my advisor Jeff Drazen. Throughout my time as a graduate student you've found a balance of supporting me and challenging me. You've been an advocate for me and you ask me questions that make me think harder about my research. Thank you for taking me on as a student, seeing the value of work experience in lieu of academic background, and pushing me to work just a little bit harder.

Thank you also to Jeff Polovina who's been both a committee member and for much of my time as a student, my boss. You encouraged me to pursue my PhD and allowed me the professional space follow through. I could not ask for a better school-work balance. In addition to that, your productive curiosity is inspirational. I am extremely fortunate to have begun my career working with you.

Thank you to my other committee members: Matt Church, Megan Donahue, Kyle Edwards, and Axel Timmermann. Matt, you helped me keep the broader research community in mind in my research. Megan, your ecosystem expertise helped ensure my research was rooted in sound theory and you always managed to ask tough questions in an encouraging way. Kyle, thank you for jumping in midway through my research. You've helped me think more deeply about my modeling work and broaden my skills. Axel, your excitement about new ideas is infectious and you've helped me elevate the quality of my research.

Thank you to the Drazen Lab members both past and present. You helped me feel like a part of the Lab and a part of UH even though I was rarely in the lab. And you always made space for me when I was there. Plus, your science and your skills and your enthusiasm are inspiring. Everyone is always doing such cool stuff!

Team Lancetfish, you're awesome. Every time we assemble, you make me excited to do science. I love kicking around ideas with you guys.

Thank you to my colleagues at PIFSC for your support these last few years. Whether you were helping me sort out my work schedule, asking me how school was going, sitting in class with me, or listening to me lament my latest academic woe, thank you. Knowing I had a team of people rooting for me has been a continual source of strength. Thanks especially to Jen Raynor, Justin Hospital, Joe O'Malley, and Brian Langseth for taking the time to discuss with me

economics, fish life history, and methods for addressing the limitations of fishery-dependent data.

I owe special thanks to my master's advisor, Chidong Zhang. Chidong let me go on a three-week research cruise that had nothing to do with my (or his) meteorology research. Thank you for allowing me to do that. The more time passes, the more I realize just how pivotal that experience was in my life. It led me to my career, and along the way, to my husband Matt.

Thank you, also, to my parents. You've always been excited about my work and you're probably the only two people on the planet who've voluntarily read all of my papers.

Cecilia, you're the best sister anyone could ask for. You're always a voice of sanity and reason, yet you never make me feel silly for worrying. You're also an endless source of wit and entertainment. Thank you for being you and for being my friend.

Thank you, Matt, for more than I could possibly list. Put most simply, you've put up with me and encouraged me throughout my PhD (probably in that order). I am thankful every day that you're my husband.

Both the Fernando Gabriel Leonida Memorial Scholarship and the Denise B. Evans Fellowship in Oceanographic Research supported my research outside of NOAA. This funding made it possible for me to travel to visit collaborators, attend international meetings, and participate in extracurricular training. Thank you especially to Grace Furuya in the Hawaii Institute of Geophysics and Planetology.

I funded my return to graduate school largely with US Department of Veterans Affairs Post-9/11 GI Bill benefits. Throughout my time in school, I was continually impressed with how easy it was to access my benefits – thanks in no small part to the great liaisons in the UH Office of the Registrar. Amazingly, this component of my PhD was always the least stressful. Thank you to both UH and the VA for making this the case. And thanks especially to Chris in the Registrar's office for explaining to the VA how dissertation research works.

ABSTRACT

Climate change and fishing are among the greatest anthropogenic stressors on marine ecosystems. Ecosystem models are one tool for evaluating the effects of these stressors, and ecosystem model comparison is a particularly effective method for identifying robust projections of future ecosystem change. When fundamentally different approaches produce the same result, this increases confidence in the conclusion. Conversely, areas of model disagreement highlight topics for future research. This dissertation uses output from a suite of earth system models to determine the range of climate change effects projected for the North Pacific over the 21st century. It then pairs this output with three types of ecosystem models: a size-based, a species-based, and an integrated size- and species-based model. There is broad model agreement that climate change will lead to reduced fish biomass and fishery yield over the 21st century and that increasing fishing mortality will amplify this decline. Furthermore, Hawaii's longline fishery may move northeastward away from Hawaii in response to these changes. Examining the structure of the ecosystem models used provides insight into the mechanisms driving ecosystem change. Reduced plankton biomass is projected to reduce food availability to fish, reducing their growth and in turn, biomass. Additionally, a shift toward smaller plankton is expected to propagate through the food web leading to smaller fish body sizes. Comparison across ecosystem models also highlights areas for future research. These areas include evaluating the role that food limitation plays in fishes' foraging behavior and compiling basic life history information for species with high bycatch rates. The results of this dissertation highlight the urgent need to limit anthropogenic climate change and to account for climate change in fisheries management. We cannot hope to catch ever more fish while at the same time we erode the ecosystem's productivity and capacity.

TABLE OF CONTENTS

Acknowledgments ..... **ii**

Abstract ..... **iv**

List of Tables ..... **ix**

List of Figures ..... **x**

Chapter 1: Introduction **12**

Chapter 2: Two takes on the ecosystem impacts of climate change and fishing: Comparing a size-based and a species-based ecosystem model in the central North Pacific **17**

2.1 Introduction 18

2.2 Materials and methods 19

2.2.1 Ecopath with Ecosim 20

2.2.2 Size-based food web model 20

2.2.3 Model input and simulation scenarios 21

2.3 Results 23

2.3.1 Climate and fishing impacts on long-term changes in biomass and catch 23

2.3.2 Fishing impacts on biomass and catch 23

2.3.3 Climate change impacts on biomass and catch 24

2.3.4 Model sensitivity to top-down and bottom-up forcing 25

2.3.5 Climate and fishing impacts on interannual variability 26

2.4 Discussion 26

2.4.1 Model agreement on the broad impacts of climate change 27

2.4.2 Differences between species-based and species-blind modeling approaches 27

2.4.3 Uncertainty on the relative impacts of top-down and bottom-up forcing 29

2.4.4 Impacts of predator- vs. prey-moderated food webs on the propagation of variability 31

2.4.5 Model limitations and caveats 33

2.5 Conclusions 34

Chapter 3: Climate change is projected to reduce carrying capacity and redistribute species richness in North Pacific pelagic marine ecosystems **41**

3.1 Introduction 42
3.2 Materials and methods 43
3.2.1 Earth system models used 43
3.2.2 Data used 43
3.2.3 Pelagic habitat 44
3.2.4 Ecosystem impacts 44
3.3 Results 45
3.3.1 Pelagic habitat 45
3.3.1.1 Thermal habitat 45
3.3.1.2 Food available to fish 46
3.3.2 Ecosystem impacts 46
3.4 Discussion 47
3.4.1 Changing pelagic habitat 47
3.4.2 Ecosystem impacts of changing pelagic habitat 48
3.4.3 Caveats 51
3.4.4 Commercial fishery impacts of changing pelagic habitat 51
Chapter 4: Synergy among oceanographic variability, fishery expansion, and longline catch composition in the central North Pacific Ocean 57
4.1 Introduction 58
4.2 Materials and methods 59
4.2.1 Materials 59
4.2.2 Methods 60
4.3 Results 61
4.3.1 Fishing effort 61
4.3.1.1 Seasonal variability 61
4.3.1.2 Interannual variability 61
4.3.1.3 International competition 62
4.3.2 Oceanographic variability 62
4.3.2.1 Spatial variability 62
4.3.2.2 Temporal variability 63

4.3.3 Catch variability 63
4.3.3.1 Catch rates 63
4.3.3.2 Catch composition 64
4.4 Discussion 65
4.4.1 The role of oceanographic variability in fishery expansion 66
4.4.2 Effects of fishery expansion on catch composition 67
4.4.3 A look ahead 69
Chapter 5: Relative impacts of simultaneous stressors on a pelagic marine ecosystem 77
5.1 Introduction 78
5.2 Material and methods 79
5.2.1 Model 79
5.2.2 Model parameters and input 81
5.2.2.1 Parameters and calibration 81
5.2.2.2 Climate forcing variables 83
5.2.3 Model verification 83
5.2.4 Scenarios modeled 84
5.3 Results 85
5.3.1 Total biomass and yield 85
5.3.2 Total abundance 86
5.3.3 Large fish indicator 87
5.3.4 Mean size 87
5.4 Discussion 88
5.4.1 Outlook for future yield and ecosystem 88
5.4.2 Mechanisms driving change 89
5.4.3 Sources of uncertainty 92
5.4.4 Model limitations and future directions 94
Chapter 6: Synopsis 106
Appendix A: Ecosystem model descriptions 110
A.1 Ecopath with Ecosim 110

A.2 Size-based food web model 111
Appendix B: Species/Groups experiencing fishing mortality and their mean weights .113
Appendix C: Variance for each output time series examined in Chapter 2 114
Appendix D: Supplemental figures for Chapter 4.....115
Appendix E: Supplemental tables for Chapter 5.....119
Appendix F: Modeled and observed catch size spectra.....123
Literature Cited.....124

LIST OF TABLES

Table 2.1. Interannual variability of output time series 35

Table 3.1. Ranges of output temperatures and zooplankton densities which change in frequency of occurrence 53

Table 4.1. Significant trends in preferred thermal habitat depth 72

Table 5.1. Species-specific model parameters 95

Table B.1. Mean weights of species groups experiencing fishing mortality 113

Table C.1. Variance for each output time series examined in Chapter 2 114

Table E.1. Interaction matrix 119

Table E.2. Plankton size classes 120

Table E.3. Length-weight conversions 121

LIST OF FIGURES

Figure 2.1 Annual ESM2.1 phytoplankton densities....36

Figure 2.2 Annual mean fish catch output by each model....37

Figure 2.3 Annual mean fish biomass output by each model....38

Figure 2.4 Relative changes in fish catch....39

Figure 2.5 Relative changes in fish biomass....40

Figure 3.1 Frequency distributions of epipelagic temperature and zooplankton density....55

Figure 3.2 Multi-model median projected changes in pelagic habitat and ecosystem....56

Figure 4.1 Spatial distribution of fishing effort and average depth of preferred habitat....73

Figure 4.2 Seasonal distribution of fishing effort and its change over time....74

Figure 4.3 Annual and quarterly catch rates....75

Figure 4.4 Seasonal distribution of catch composition and its change over time....76

Figure 5.1 Illustration of longline fishing grounds....97

Figure 5.2 Schematic diagram of how temperature effects are modeled....98

Figure 5.3 Range of temperature effects for each species modeled....99

Figure 5.4 Schematic diagram of how interaction matrix is calculated....100

Figure 5.5 Change in plankton densities across earth system models....101

Figure 5.6 Percent change in biomass and yield....102

Figure 5.7 Percent change in abundance and number of fish caught....103

Figure 5.8 Time series of the large fish indicator....104

Figure 5.9 Percent change in the mean size of fish....105

Figure A.1 Schematic diagram of the Ecopath with Ecosim model....111

Figure A.2 Schematic diagram of the size-based food web model....112

Figure D.1 Correlation between logbook and observer effort 115

Figure D.2 Total Hawaii-based and international longline effort 115

Figure D.3 Annual time series of depth of preferred thermal habitat.....116

Figure D.4 Quarterly catch composition.....117

Figure D.5 Quarterly size distribution of bigeye tuna 118

Figure F.1 Size spectra of modeled and observed catch.....123

CHAPTER 1

Introduction

Climate change and fishing are two of the greatest anthropogenic stressors on marine ecosystems. Understanding their impact is critical for ensuring both ecosystem structure and function as well as food security for a growing human population. One tool for examining the effects of these stressors is ecosystem modeling. This dissertation uses several ecosystem models together with climate projections and fisheries data to investigate the pelagic central North Pacific (CNP) ecosystem's response to anthropogenic stressors.

The CNP sits at the center of the oligotrophic North Pacific subtropical gyre. Yet, it is home to international longline fleets targeting large, high trophic level fish such as tuna and billfish. It is also the source of over half the United States' tuna landings (NMFS 2018) and encompasses the fishing grounds of Hawaii's most valuable fishery. Therefore, it is important to understand the dynamics of the food web supporting these fisheries, including how it is affected by changes to the physical environment and other external stressors.

Among these stressors is anthropogenic climate change, which is expected to result in significant impacts to both the physical oceanography and biology of the CNP. Increasing ocean temperatures will result in widespread range shifts of fish (Jones and Cheung 2014). Warming oceans may also lead to decreased body size across all levels of the marine food web (Morán et al. 2010; Gardner et al. 2011; Cheung et al. 2013). Rising temperatures paired with increased vertical stratification (Sarmiento et al. 2004) are projected to lead to decreased nutrient concentrations in the euphotic zone (Rykaczewski and Dunne 2010) and in turn to reduced phytoplankton densities and a shift towards smaller phytoplankton (Polovina et al. 2011). These changes at the base of the pelagic food web are likely to lead to reduced large fish biomass and an increased abundance of small fish (Woodworth-Jefcoats et al. 2013; Lefort et al. 2015), and these changes appear to be already underway (Polovina and Woodworth 2012; Pinksy et al. 2013; Polovina and Woodworth-Jefcoats 2013).

Commercial fishing also influences the pelagic CNP ecosystem through the selective removal of large fish. This removal drives down the abundance of large fish, allowing prey populations to grow (Pauly et al. 1998; Jennings and Blanchard 2004; Polovina et al. 2009; Polovina and Woodworth-Jefcoats 2013). In fact, the catch of non-commercial, mid-trophic-

level lancetfish now exceeds target catch of bigeye tuna in Hawaii's deep-set longline fishery (Polovina and Woodworth-Jefcoats 2013).

Ecosystem modeling is one tool for assessing the potential effects of climate change and fishing on marine food webs. Ecosystem models can range from relatively simple size-based models to more complex species-based models. The former are built on the established premise that large fish generally eat smaller fish and use ecological theory to model the flow of biomass through a size-structured food web (e.g., Blanchard et al. 2009). The latter can incorporate numerous specific species, and even discretely represent their life stages (e.g., juvenile vs. adult), and use a detailed diet matrix to inform the flow of biomass through a species-structured food web (e.g., Christensen et al. 2008).

The goal of this research was to use earth system model output and commercial fishery records together with ecosystem models to determine the range of climate change and fishing impacts that can be expected in the CNP over the 21st century. Fully understanding these impacts is imperative in setting effective and sustainable fisheries management policy.

The first objective of this dissertation was to compare output from two contrasting ecosystem models, Ecopath with Ecosim (EwE) and size-based food web (SBFW), when forced with the same climate projection data and fishing scenarios. Ecosystem models are generally used singly and toward a specific question. Thus, it can be challenging to compare modeling approaches or to make robust cross-application inferences from the literature. Direct comparison of these two models' treatment of the same input and scenarios can lend insight to areas of uncertainty that are not otherwise apparent. These areas of uncertainty can be used to direct future modeling investigations as well as model development. Areas of model agreement increase confidence in projections of climate change and fishing in the CNP.

An EwE (Howell et al. 2013) and a SBFW (Blanchard et al. 2012; Woodworth-Jefcoats et al. 2013) model parameterized for the CNP were compared. Both models were forced with climate change and control scenarios, with the climate change scenario being that projected by the Geophysical Fluid Dynamics Laboratory prototype Earth System Model 2.1 (Dunne et al. 2005; Delworth et al. 2006; Gnanadesikan et al. 2006). Both models were also forced with fishing mortality ranging from 0 to 1, with and without climate change. Similarities and differences in both models' treatment of this suite of scenarios informed subsequent climate and

fishery investigations in this dissertation. Insight gained through this modeling comparison was also used in constructing an integrated size- and species-based model.

The second objective of this research was to determine the range of biophysical climate change impacts projected for the CNP. Monthly and annual model output from the fifth phase of the Coupled Model Intercomparison Project (CMIP5; Taylor et al. 2012) was used for this assessment. Models with both physical (e.g., sea surface temperature, mixed layer depth) and biological (e.g., chlorophyll, phytoplankton density, zooplankton density) output were used. CMIP5 incorporates a wide range of historical and projection runs (Taylor et al. 2012). This comparison used RCP8.5 simulations to evaluate future projections. Despite being the pathway with the greatest carbon concentrations, RCP8.5 (Riahi et al. 2011; van Vuuren et al. 2011) was used because it most closely tracks the rise in CO_2 concentrations to date (Tans and Keeling 2014) and because no substantial climate mitigation policies have yet been implemented.

A study of the projected impacts of climate change in the CNP provided a detailed analysis of what biophysical changes can be expected over the 21st century. These changes will likely have significant impacts on large fish and are consequently important from both food security and economic perspectives. Insight gained through the CMIP5 analysis was incorporated into the modeling efforts at the end of this dissertation.

The third objective of this dissertation was to investigate spatiotemporal trends in CNP longline catch. Specifically, changes in catch composition over time and in relation to proximity to the main Hawaiian Islands was investigated. Longline observer records, and logbook records to the extent possible, were used to track spatiotemporal changes in species composition over space and time as a function of proximity to land and location of fishing effort. International longline records were used to place domestic fishing effort in context with total fishing effort.

Over the past 20 years, Hawaii-based fishing effort has increased (Polovina et al. 2009) and expanded farther from the main Hawaiian Islands, particularly towards the northeast. Both empirical and size-based modeling approaches have shown that this increased fishing effort has led to increased catch of smaller and non-commercially valuable fish (Polovina and Woodworth-Jefcoats 2013). This dissertation improves upon these ecosystem modeling efforts by incorporating more spatially explicit and nuanced fishing mortality. To this end, the results from this spatiotemporal analysis were incorporated into developing the integrated model and

determining simulation scenarios. It is hoped that they can also be used to inform ecosystem-based fishery management decisions.

The fourth objective of this dissertation was to construct an integrated size- and species-based model. This model expanded on the SBFW model by including several individual commercially valuable and bycatch species such as bigeye tuna and lancetfish, respectively. Necessary model parameters such as those related to age and growth were taken from the literature. Coupling single-species size structure with the larger background pool was done by building upon existing relevant modeling packages (Scott et al. 2014). Model skill was tested with fishery data.

An integrated size- and species-based model makes the output of the size-structured model more relevant to fishery managers by including commercially valuable species. It also provides more detailed abundance estimates than are output by the EwE model, further increasing its usefulness. An integrated model also addresses shortcomings inherent to modeling the ecosystem from a purely species-based or size-based approach. For example, questions related to species abundance at size can be investigated with this model. Evaluating model skill via comparison to size- and species-specific fishery records ensured the credibility of the model's output. Climate models are routinely evaluated by their ability to replicate real systems, though this is less often the case for ecosystem models (often due to a lack of appropriate data). An integrated model that can accurately replicate both ecosystem and single-species size structure will be particularly useful in evaluating potential management strategies.

In addition to incorporating improved climate change simulations, this integrated model also incorporated insights gained through the initial model comparison and subsequent fishery analysis. These results helped guide this model's development. An updated climate change scenario and improved inclusion of fishing mortality yielded more realistic results. The integrated model also addressed limitations identified through the initial model comparison. These results – projections of climate change and fishing impacts in the CNP – may now be used by fishery managers to place current management actions in a broader context.

The integrated size- and species-based model developed in this research was a first step toward a relatively simply parameterized model which can provide fishery-relevant simulations of anthropogenic impacts in the CNP. Other modeling approaches can require quite detailed

information (e.g., Atlantis or EwE). Furthermore, the individual components of this research contributed valuable results. They summarized projected climate impacts in the CNP and their expected effects on fisheries. They also provided a comprehensive spatiotemporal examination of the movement, effort, and catch of the Hawaii-based longline fishery. The results of these components are of interest to local fishery managers such as the Western Pacific Regional Fishery Management Council. The final integrated model developed from this research is a step towards bridging the theoretical and academic application of ecosystem modeling on a multi-decadal time scale with the practical management applications on interannual time scales.

Taken together, the results presented in this dissertation show that both ecosystem carrying capacity and fisheries catch are likely to decline over the coming decades. Understanding the potential magnitude of these declines and the mechanisms driving them can help regional fishery managers plan for the future. Additionally, this dissertation illustrates a range of consequences to the choices that society as a whole will have to make with increasing frequency and urgency: whether to pursue short-term economic gain or long-term economic and ecological stability.

CHAPTER 2

Two takes on the ecosystem impacts of climate change and fishing: Comparing a size-based and a species-based ecosystem model in the central North Pacific

We compare two ecosystem model projections of 21st century climate change and fishing impacts in the central North Pacific. Both a species-based and a size-based ecosystem modeling approach are examined. While both models project a decline in biomass across all sizes in response to climate change and a decline in large fish biomass in response to increased fishing mortality, the models vary significantly in their handling of climate and fishing scenarios. For example, based on the same climate forcing the species-based model projects a 15% decline in catch by the end of the century while the size-based model projects a 30% decline. Disparities in the models' output highlight the limitations of each approach by showing the influence model structure can have on model output. The aspects of bottom-up change to which each model is most sensitive appear linked to model structure, as does the propagation of interannual variability through the food web and the relative impact of combined top-down and bottom-up change. Incorporating integrated size- and species-based ecosystem modeling approaches into future ensemble studies may help separate the influence of model structure from robust projections of ecosystem change.

Based on: Woodworth-Jefcoats PA, Polovina JJ, Howell EA, Blanchard JL, 2015. Two takes on the ecosystem impacts of climate change and fishing: Comparing a size-based and a species-based ecosystem model in the central North Pacific. Progress in Oceanography, 138: 533-545. doi: 10.1016/j.pocean.2015.04.004

2.1 Introduction

A range of climate- and fishing-induced ecosystem changes have been projected for the central North Pacific, and many of these projections are based on analysis of a single model's output (e.g., Cheung et al. 2010; Lehodey et al. 2010; Howell et al. 2013; Woodworth-Jefcoats et al. 2013). Single-model studies may make broadly comparable projections, yet their underlying fundamental differences, as well as differences in forcing scenarios, can make it difficult to directly compare projections. For example, all of the studies cited above project changes in North Pacific fish biomass over the 21st century. However, each models a different target fish population over different geographic areas. Each uses a different 21st century forcing scenario with different environmental and habitat variables considered. Fishing mortality is treated differently by each approach. Thus, while each of these studies makes a projection for North Pacific fish biomass in the face of climate change, it is not possible to compare any of these studies directly. While it is certainly not necessary for all modeling studies to be directly comparable to one another, single-model studies invite the question of how closely their results are tied to the model used and the scenario(s) being investigated.

A further challenge to projecting future ecosystem change is understanding the influence of multiple stressors, both the degree to which each impacts the ecosystem individually as well as their joint impacts. A number of modeling studies have investigated the impacts of fishing (e.g., Cox et al. 2002) and changes in primary production (e.g., Gnanadesikan et al. 2011) on pelagic food webs. However, these influences occur simultaneously in nature and it is their joint impact that will ultimately determine ecosystem changes (Perry et al. 2010). As Mackinson et al. (2009) point out, effective ecosystem-based fisheries management is reliant upon understanding the relative impacts of ecosystem influences such as fishing and primary production. Yet, gaining insight into the impacts of different degrees of fisheries exploitation through the literature is surprisingly challenging. Most studies typically use a single level of fishing mortality (e.g., Ainsworth et al. 2011) or are designed to recreate past trends in order to investigate how fishing impacted the ecosystem (e.g., Cox et al. 2002; Mackinson et al. 2009). There are some exceptions, though, which examine temporal changes in fishing mortality (Travers et al. 2010; Howell et al. 2013) or compare low and high degrees of exploitation (Blanchard et al. 2012; Gårdmark et al. 2013). In general, these studies find that higher levels of fishing mortality

reduce target species biomass and that climate change exacerbates this effect. In order to best manage fishery resources it is important we improve our understanding of these dual influences.

In this study we examine two ecosystem modeling approaches: Ecopath with Ecosim (EwE), which uses detailed species-based diet and trophic interactions (Christensen and Walters 2004; Christensen et al. 2008), and a size-based food web (SBFW) model, which uses size-based feeding interactions (Blanchard et al. 2012). Both models are forced with the same fishing and climate change scenarios. Through these scenarios, we examine each model's projected impacts of fishing and climate change on the central North Pacific ecosystem over the 21st century. We examine climate change and fishing both individually and simultaneously. Additionally, in a step towards making ecosystem model output more relevant to fishery managers, we examine a range of fishing mortality levels and attempt to tease apart the relative impacts of top-down and bottom-up forcing.

Our overarching goal is to use model comparison as a tool to examine the impacts of increasing fishing mortality and climate change on fish catch and biomass. Areas of model agreement lend confidence to our ability to model future ecosystem change, while disparities in the models' output can identify uncertainties that may not be apparent when using a single ecosystem model. Additionally, we discuss how comparing the models' projections identifies specific areas of focus for future study and model development.

2.2 Materials and methods

The models used in this comparison represent two quite different approaches to ecosystem modeling and sit at opposite ''extremes'' along the spectrum of model complexity. One, EwE, relies on detailed diet and trophic interactions. The other, SBFW, is built upon the premise that predation in the pelagic environment is largely determined by body size (Benoît and Rochet 2004; Blanchard et al. 2009, 2011; Law et al. 2009). In Sections 2.2.1 'Ecopath with Ecosim' and 2.2.2 'Size-based food web model' below we highlight the basic computational structure of each model, focusing on the key differences and similarities that are most important to this comparison. The models are described in full detail elsewhere (EwE: Christensen et al. 2008; SBFW: Blanchard et al. 2012). We discuss the scenarios modeled for comparison in Section 2.2.3 'Model input and simulation scenarios.'

2.2.1 Ecopath with Ecosim

The EwE model consists of two components: the static Ecopath component and the dynamic Ecosim component. Ecopath takes a mass-balanced approach to simulating the trophic relationships between species and/or functional groups in an ecosystem (Polovina 1984; Christensen et al. 2008). Ecosim models energy flux through a series of differential equations following the form of

$$\frac{dB_i}{dt} = g_i \sum_j Q_{ji} - \sum_j Q_{ij} + I_i - (MO_i + F_i + e_i)B_i \qquad (2.1)$$

where population growth rate of a given group, *i*, is a function of biomass (*B*), net growth efficiency (*g*), and rates of consumption (*Q*) within the group and across other groups, *j*, immigration (*I*), natural mortality (*MO*), fishing mortality (*F*), and emigration (*e*), and with prey behavior being the main moderator in trophic interactions (Christensen et al. 2008). Predator feeding rates are allowed to increase as prey increases without being restricted by handling time and, when using default EwE settings as we do, are equivalent to a linear functional response (Christensen et al. 2008). The EwE software used in this comparison is version 6.2.0.714 (Christensen and Walters 2004; Christensen et al. 2008; Howell et al. 2013).

The EwE model is that used by Howell et al. (2013), which represents multi-fleet fishing impacts in the central North Pacific (spatial domain is discussed in more detail in Section 2.2.3 'Model input and simulation scenarios' below). For straightforward comparison with the SBFW model, the EwE model was simplified in several ways. The primary simplification was to adjust fishing effort such that all exploited species/functional groups experienced equal size-dependent levels of fishing mortality. This and additional EwE adjustments are detailed in Appendix A.

2.2.2 Size-based food web model

Energy flow in the SBFW model is driven by growth resulting from size-based predation. Thus, the abundance (*N*) of a given consumer size class, *c*, at a given time is driven by continuous growth (*G*) resulting from size-based feeding and continuous mortality (*D*) resulting from size-based predation mortality, natural mortality, senescence mortality, and fishing mortality:

$$\frac{\partial N_c}{\partial t} = -\frac{\partial}{\partial m}(GN_c) - DN_c \qquad (2.2)$$

Size-based predation occurs when a fish of size *m* encounters another fish of smaller size *m'*, with the feeding kernel represented by a lognormal probability function centered around a prey with 0.01 the biomass of the predator on a linear scale (Blanchard et al. 2012). The SBFW model also uses a linear functional response (Blanchard et al. 2012).

The SBFW model used is the pelagic component of that used by Blanchard et al. (2012) modified for the North Pacific by Woodworth-Jefcoats et al. (2013) and with the treatment of fishing mortality updated as in Polovina and Woodworth-Jefcoats (2013). Additional model details are provided in Appendix A.

2.2.3 Model input and simulation scenarios

Both the EwE and SBFW models are driven by output from the National Oceanic and Atmospheric Administration Geophysical Fluid Dynamics Laboratory prototype Earth System Model 2.1 (ESM2.1). ESM2.1 couples a climate model (CM2.1; Delworth et al. 2006; Gnanadesikan et al. 2006) with a biogeochemical model (TOPAZ; Dunne et al. 2005) and is forced by the Intergovernmental Panel on Climate Change Special Report on Emission Scenario A2 (SERS A2; Nakićenović et al. 2000). ESM2.1 outputs phytoplankton density for three functional groups that span two size classes. Time series of these small (0.2–5 μm) and large (5–200 μm) phytoplankton densities are input to both ecosystem models (Fig. 2.1). ESM2.1 projects future increases in vertical stratification in the North Pacific subtropical gyre will reduce deep nutrient input into the euphotic zone. As a result, both small and large phytoplankton densities are projected to decline over the 21st century. To assess the impacts of climate change, we use both the ESM2.1 output as described above as well as a static climate scenario. The static scenario uses the ESM2.1 phytoplankton densities averaged over the years 1991–2010 at every time step.

Our study encompasses the area covered by the Hawaii-based longline fishery. This area is bounded by 170°E–150°W and 10°N–40°N, with the northern boundary set as the position of the monthly mean 17 °C sea surface temperature isotherm (Howell et al. 2013). No spatial information is input into the EwE or SBFW models, rather the ESM2.1 phytoplankton densities are averaged over this geographic area.

The ESM2.1 phytoplankton densities enter both the EwE and SBFW models in a similar fashion. For the EwE model, they enter as biomass densities for the functional groups ‘‘small phytoplankton’’ and ‘‘large phytoplankton’’. For the SBFW model, they enter as biomass densities for two broad size classes of the primary producer size spectra.

Both models were run with a range of fishing mortality values (F = 0, 0.2, 0.4, 0.6, 0.8, 1.0). As in Polovina and Woodworth-Jefcoats (2013), a gear selectivity term was used, with fish from 1 to 15 kg experiencing one quarter the level of fishing mortality as those >15 kg. This was done to more accurately reflect the size at which fish are fully exploited by the fishery. Both the EwE and SBFW models treat fishing mortality as a constant mortality term. For example, both models treat F = 0.2 as 20% mortality on the impacted groups (EwE) or sizes (SBFW). The EwE model applies fishing mortality to all species/functional groups with a mean size ≥1 kg (see following paragraph). The SBFW model applies fishing mortality to all size classes ≥1 kg.

Previous studies suggest that both climate-induced changes in phytoplankton abundance and size structure, as well as fisheries exploitation, can drive down the abundance of large fish (Pauly et al. 1998; Daufresne et al. 2009; Blanchard et al. 2012; Cheung et al. 2013; Polovina and Woodworth-Jefcoats 2013; Woodworth-Jefcoats et al. 2013). To examine how the EwE and SBFW models treat these influences, we break the catch and exploitable biomass down into small (1–15 kg) and large (>15 kg) fish. For the EwE model, which is not structured by size, we use mean weights of exploited species to assign them to either small or large categories (see Appendix B).

In addition to examining the projected trends in exploitable biomass and catch in the central North Pacific, we also examine the propagation of variability within the models. While we do examine the overall variance of each prepared output time series (Appendix C), we are more interested in the interannual variability as this can tell us how changes at the base of the food web are dampened or amplified as they propagate through larger size classes/higher trophic levels. Additionally, unlike variance, interannual variability allows us to examine variability largely free of the long-term trend imposed by climate change. To measure interannual variability, we first standardize each output time series by subtracting the mean from each value and then dividing by the standard deviation. Using these standardized time series, we calculate a 5-year running mean and sum the absolute value of the residuals between this mean and the

actual value of the year about which the 5-year mean is centered. A five year averaging period was selected as it best balanced smoothing the time series with retaining as many datum as possible (96%, 86 out of 90 years).

The EwE model uses annual mean values on a monthly time step and the SBFW model uses monthly mean values on a daily time step. To address this disparity in temporal resolution, annual mean model output is used for both models.

2.3 Results

2.3.1 Climate and fishing impacts on long-term changes in biomass and catch

Across all scenarios and all size classes, including climate change leads to a gradual decline in both catch (Fig. 2.2) and exploitable biomass (Fig. 2.3), regardless of fishing mortality. Increasing fishing mortality leads to increased small and total fish catch (Fig. 2.2). Both models project the greatest large fish catch when $F = 0.4$ and the least large fish catch when $F = 1.0$ (Fig. 2.2b and e).

The relative and combined effects of fishing and climate change are explored in more detail across the two models by looking at the time-averaged differences in biomass and catches. Catch and biomass output by each model is averaged for the final 20 years of the 21st century (2081–2100). These end-of-the-century averages are examined relative to: (i) results in the absence of fishing mortality (Figs. 2.4a, d and 2.5a, d, Section 2.3.2 'Fishing impacts on biomass and catch'), (ii) results in the absence of climate change (Figs. 2.4b, e and 2.5b, e, Section 2.3.3 'Climate change impacts on biomass and catch'), and (iii) results in the absence of both fishing and climate change (Figs. 2.4c, f and 2.5c, f, Section 2.3.4 'Model sensitivity to top-down and bottom-up forcing'). Note that in the above comparisons, biomass is examined relative to the absence of fishing mortality while catch is examined relative to the lowest level of fishing mortality ($F = 0.2$).

2.3.2 Fishing impacts on biomass and catch

Both models project fairly similar changes in catch in response to fishing mortality. Not surprisingly, increasing fishing mortality leads to increased total catch in both models (Fig. 2.4a and d). However, these increases in catch are not commensurate with the increases in fishing

mortality. This disparity is seen particularly well in small fish catch: increases in the EwE small fish catch exceed increases in fishing mortality, while increases in SBFW model small fish catch are smaller than increases in fishing mortality, particularly at the highest levels of fishing mortality (Fig. 2.4a and d). When fishing mortality increases 100% from 0.2 to 0.4, EwE small fish catch increases by about 130% while SBFW small fish catch increases by about 90%. When fishing mortality increases 400% from 0.2 to 1.0, EwE small fish catch increases by 450% whereas SBFW small fish catch increases by only about 290%. The disparity in the models' treatment of increasing fishing mortality is seen in total catch as well, though the difference is not as pronounced as that for small fish catch. Increasing fishing mortality by 100% leads to a 90% increase in EwE total catch and a 70% increase in SBFW total catch. Increasing fishing mortality by 400% leads to 260% and 210% increases in EwE and SBFW total catch, respectively.

In contrast to catch, the two models project somewhat different changes in biomass in response to fishing. The SBFW model projects biomass at all sizes to decline in response to increasing fishing mortality, with the exception of small fish biomass when F increases from 0 to 0.2 without climate change (Fig. 2.5d). For the remaining fishing scenarios, small, large, and total fish biomass decline by up to 10%, 90%, and 30%, respectively. Large fish biomass also declines as *F* increases in the EwE model, with the exception of the increase from 0 to 0.2 under the climate change scenario (not shown). At the highest level of fishing mortality, EwE-projected large fish biomass declines exceed those projected by the SBFW model. Conversely, EwE small fish biomass increases when fishing is included, with $F = 0.6$ resulting in the greatest small fish biomass (Figs. 2.3a and 2.5a). Total exploitable biomass trends are quite similar to small fish biomass trends in the EwE output, with the exception of $F = 1.0$ which results in the lowest exploitable biomass (Figs. 2.3c and 2.5a).

2.3.3 Climate change impacts on biomass and catch

There is broad model agreement on the negative impacts of climate change, with projected declines of 15–55% in both catch and exploitable biomass relative to a constant climate (across all values of *F*; Figs. 2.4b, e and 2.5b, e). However, interesting differences in the magnitude of each model's response to climate change warrant further examination. Across all

levels of fishing mortality, the EwE model projects a roughly 15% decline in total catch, while the SBFW model projects a 30% decline (Fig. 2.4b and e). Further, while the EwE model projects climate-induced declines in catch of about 15% for both small and large fish groups, the SBFW model projects declines of 25% for small fish and 45–55% for large fish (Fig. 2.4b and e). These trends in catch largely follow those of biomass: In response to climate change, the EwE model projects small, large, and total fish biomass all to decline by approximately 15%, whereas the SBFW model projects small, large, and total fish biomass to decline by approximately 20%, 50%, and 25%, respectively (Fig. 2.5b and e).

2.3.4 Model sensitivity to top-down and bottom-up forcing

In an effort to determine whether the models treat the combined forcings of fishing and climate change as amplifying, dampening, or purely additive, we compared the modeled joint forcing to the sum of the two individual forcings (Figs. 2.4c, f and 2.5c, f). Across both models and all levels of fishing mortality, three output fields were close to purely additive: small and total fish biomass (within 5% of additive) and large fish catch (within 15% of additive). For the remaining outputs (small and total fish catch, large fish biomass), the total modeled impact was about 20–85% less than additive, with the EwE-modeled joint impact being closer to additive than the SBFW-modeled impact. Across both models and all fishing scenarios, the difference between the modeled combined impact and the purely additive combined impact increased with increasing F.

The EwE model appears to be more sensitive than the SBFW model to top-down forcing from fishing mortality: The combined effects of fishing and climate change on both catch and biomass are closer to the sum of both forcings in the EwE output, particularly at increasing levels of F (Figs. 2.4 and 2.5). Yet, the SBFW model suggests more synergy between fishing and climate change impacts than the EwE model: small and large fish catch and biomass output by the SBFW model both exhibit greater declines with increasing values of F, whereas the EwE-modeled impacts of climate change appear largely unaffected by increasing fishing mortality (Figs. 2.4b, e and 2.5b, e).

2.3.5 Climate and fishing impacts on interannual variability

Model output interannual variability is shown in Table 2.1. Variability declines in both models as a function of size, going from phytoplankton to small fishes to large fishes. The interannual variability of large and total fish catch and exploitable biomass increases with increasing fishing mortality in the SBFW model, while in the EwE model it peaks at the mid-range values of $F = 0.4$ and 0.6. In both models, the interannual variability of small fish exploitable biomass is greatest in the absence of fishing mortality. The remaining model output time series do not have a clear trend in variability with respect to fishing mortality.

When model output catch (Fig. 2.2) and exploitable biomass (Fig. 2.3) are examined relative to model input (Fig. 2.1), the EwE output time series more closely follow the small phytoplankton variability while the SBFW output time series more closely follow that of large phytoplankton. These similarities can be seen both in the relationship between the climate change and static climate scenarios as well as in interannual variability, particularly the timing of peaks and troughs across time series. Additionally, large phytoplankton variability is greater than small phytoplankton variability. For all output time series, SBFW model variability is greater than that for the EwE model. SBFW small and total fish catch and exploitable biomass are up to 40% more variable than that output by the EwE model and large fish catch and exploitable biomass up to nearly 400% more variable.

2.4 Discussion

Our results show a number of areas of model agreement. First, both the EwE and SBFW models project quite similar magnitudes of exploitable biomass and catch. Both models also project a gradual decline in fish catch and biomass in response to 21st century climate change. Additionally, both models project the greatest large fish catch at a moderate level of fishing mortality ($F = 0.4$). Differences arise, however, in the models' treatment of fishing combined with climate change. While both models indicate that the combined impacts are less than additive, the EwE model is closer to additive suggesting it may be more sensitive to top-down forcing. And, unlike the EwE model, the SBFW model appears more sensitive to bottom-up change as fishing mortality increases, suggesting a greater degree of synergy between impacts at the top and bottom of the food web. Finally, while both models show that interannual variability

is dampened as it moves up the food web, the SBFW model output exhibits greater interannual variability than the EwE output. These results are discussed in further detail in Sections 2.4.1 'Model agreement on the broad impacts of climate change' through 2.4.4 'Impacts of predator- vs. prey-moderated food webs on the propagation of variability' below.

2.4.1 Model agreement on the broad impacts of climate change

In this study, climate change impacts are represented by a decrease in both small and large phytoplankton density due to increased vertical stratification and subsequent nutrient limitation. While similar trends in phytoplankton biomass are projected for North Atlantic (Morán et al. 2010) and freshwater (Yvon-Durocher et al. 2011) ecosystems, there are regions such as the California Current that are projected to see increasing phytoplankton densities (Rykaczewski and Dunne 2010). Not only does phytoplankton biomass decrease in our study, the phytoplankton community undergoes a shift towards a greater abundance of small phytoplankton (+1.3%, $p < 0.001$). A growing number of studies project that climate change will result in reduced organism size (e.g., Daufresne et al. 2009; Morán et al. 2010; Sheridan and Bickford 2011; Yvon-Durocher et al. 2011). This shift towards smaller phytoplankton, coupled with overall density declines, reduces the energy available to consumers of all sizes. Across both models and all scenarios, including the negative bottom-up impacts of climate change led to declines in biomass and catch at all sizes. Additionally, both models project large fish biomass and catch to decline when fishing is paired with climate change. That two fundamentally different modeling approaches project similar impacts is encouraging about our ability to project climate impacts on the ecosystem, and underscores the importance of including climate change as a component of ecosystem-based fisheries management.

2.4.2 Differences between species-based and species-blind modeling approaches

One goal in our study is to examine the impacts of increasing fishing mortality on fish catch and biomass, both with and without the influence of climate change. Our results appear to agree broadly with Howell et al. (2013) in that both models projected the greatest large fish (i.e., target fish) catch at a moderate level of fishing mortality, $F = 0.4$. The ability of reduced fishing mortality to partially mitigate climate change impacts (Howell et al. 2013) does not appear in our

results for either model. Rather, climate change results in decreased catch and biomass at all levels of fishing mortality (Figs. 2.2 and 2.3), aligning broadly with the results presented by Blanchard et al. (2012) and Gårdmark et al. (2013). Our results may differ from those of Howell et al. (2013) despite using the same model because we hold fishing mortality constant over time whereas Howell et al. (2013) examined the effects of reducing fishing mortality to one half historic levels. Thus, Howell et al. (2013) capture a rebuilding of biomass that appears to overcome the negative impacts of climate change. This result suggests the central North Pacific ecosystem may be more sensitive to top-down than bottom-up stressors, though see Section 2.4.3 'Uncertainty on the relative impacts of top-down and bottom-up forcing' for further discussion of the relative influence of these impacts.

Looking more specifically at increasing fishing mortality, the impacts seem highly model-dependent. In the SBFW model, biomass decreases as F increases, whereas in the EwE model, this impact is somewhat obscured by species-based interactions. As a result of the complex food web used in the EwE model, changes at the base and apex of the food web are moderated by predator–prey relationships and impact different species/functional groups at different time scales and to different degrees (Watters et al. 2003; Essington 2007; Travers et al. 2010). For example, despite preying on similar species/functional groups, 74% of blue sharks' diet is composed of large fish, 19% of small fish, and 7% of unexploited species, whereas for the ''Other Shark'' functional group these values are 49% large fish, 34% small fish, and 17% unexploited species.

In this study, the EwE model most clearly captures the impacts of prey release as fishing mortality increases, with small fish biomass peaking when $F = 0.6$ (Figs. 2.3 and 2.5). Conversely, SBFW model small fish biomass does not appear to respond in kind (Fig. 2.3). However, the apparent lack of prey release in the SBFW output is an artifact of presenting the results in terms of biomass rather than abundance. Both empirical (Blanchard et al. 2005; Ward and Myers 2005b) and modeling studies (Polovina and Woodworth-Jefcoats 2013) show that as fishing mortality increases, the abundance of large fish decreases while the abundance of small fish increases. This shift in abundance alters the size structure of the consumer spectra, with greater numbers of smaller fish. When viewed purely in terms of biomass at size, as is done in this study, change in size structure projected by the SBFW model is obscured. Additionally,

because the EwE model assumes species/functional groups to be of a set size, it is not able to capture this change in size structure. Rather, size is fixed throughout the modeled time span.

The above discussions illustrate several important differences between the two modeling approaches discussed in this study. First, they illustrate the impact that inter-species relationships can have in species-based ecosystem models and which are not captured in a size-based approach. They also illustrate the potential shortcomings of a detailed species-specific diet; without the possibility for species to broaden their diet composition beyond those prey specified in the initial input, changes in a single population can have a large effect on the entire ecosystem. While such changes may indeed occur in nature at times (Steneck et al. 2002), it is also possible that individuals would adjust their diet and/or behavior based on the abundance of other individuals (Olson et al. 2014) – a scenario that is tacitly implied in purely size-based approaches. In other words, size-based models envision ecosystems to be fully resilient to shifts in species composition within size classes, whereas species-based models envision ecosystems with limited or no resiliency to changes in species composition across trophic pathways. Additionally, the species-specific catch in the EwE model may fail to fully incorporate the effects of bycatch while the species-blind catch in the SBFW model may fail to capture the effects of targeted species removal. These shortcomings highlight the need for modeling approaches that incorporate both species-based and size-based predation and fishing, such as those by Travers et al. (2009), Speirs et al. (2010), Shin et al. (2004), and Blanchard et al. (2014). Through incorporating such approaches into ensemble studies that encompass the full range of ecosystem models, it may be possible to improve our understanding of the roles size structure and species composition play in changing ecosystems. Future studies should also move towards quantifying models' uncertainty and skill. The results of such work would help answer questions related to the influence of model structure, and would likely raise new questions.

2.4.3 Uncertainty on the relative impacts of top-down and bottom-up forcing

Both fishing and climate change will impact the central North Pacific ecosystem simultaneously. Thus, we attempt to tease apart the relative impacts of these forcings. While there are some clear cross-model examples of both top-down (greater declines in large fish biomass with increasing fishing mortality) and bottom-up (decreased exploitable biomass and

catch in response to climate change) forcing, their relative impacts on exploitable biomass and catch remain uncertain. Our results seem to indicate that, across both models, increasing levels of fishing mortality had a diminishing impact on catch and biomass even when considered in conjunction with climate change (Section 2.3.4 'Model sensitivity to top-down and bottom-up forcing'). While this conclusion is in line with points raised by Perry et al. (2010), it appears to contradict the results discussed by Blanchard et al. (2012), who found that higher levels of fishing mortality left the ecosystem more vulnerable to top-down forcing. The particular aspects of increased fishing mortality and climate change to which each model responds raises further questions about how ecosystems will respond to these forcings. For example, the EwE model suggests a shift toward more small fish biomass in response to fishing and suggests that fishing does not necessarily exacerbate biomass declines resulting from climate change, whereas the SBFW model suggests an overall biomass decline in response to increased fishing (though see Section 2.4.2 'Differences between species-based and species-blind modeling approaches' for the implications of measuring biomass vs. abundance at size) and suggests that fishing mortality clearly compounds biomass declines resulting from climate change. From the bottom-up perspective, the models' results raise questions about which aspects of climate change will have the greatest ecosystem impacts. The ESM2.1 output projects small and large phytoplankton densities to decline by 9.6% and 19.6% respectively. Given that small phytoplankton density is roughly ten times greater than large phytoplankton density (Fig. 2.1), coupling these declines leads to a greater impact on phytoplankton size structure than on overall phytoplankton density. In this context, the climate change impacts presented in Section 2.3.3 'Climate change impacts on biomass and catch' and model-specific trends in interannual variability presented in Section 2.3.5 'Climate and fishing impacts on interannual variability' suggest that the SBFW model shows greater sensitivity to changes in primary producer size structure, while the EwE model shows greater sensitivity to changes in phytoplankton abundance. Jennings and Brander (2010) suggest that, even from a size-based perspective, changes in phytoplankton abundance will ultimately drive ecosystem changes, and further work including differently structured ecosystem models and additional climate change scenarios could help elucidate the primary drivers of bottom-up ecosystem change.

Further complicating the investigation of relative impacts are fundamental differences between the models' computational structures. The slope and intercept of the SBFW model's primary producer size spectra are determined by the abundances of small and large phytoplankton (Woodworth-Jefcoats et al. 2013). Because there are only two size classes, both parameters are quite sensitive to even small changes in these densities. Additionally, consumer abundance is sensitive to changes in the slope and intercept of the primary producer spectra, and to increases in slope in particular (Woodworth-Jefcoats et al. 2013, S4). The climate change scenario used in this study results in steepening primary producer spectra slopes and thus may overestimate the SBFW model's sensitivity to bottom-up impacts. EwE's structure also influences the relative impacts of ecosystem forcing. For example, Kearney et al. (2013) show that changes at the base of the food web are carried through to higher trophic levels more readily under linear rather than quadratic non-predatory mortality relationships. Such a linear relationship is used in our EwE model and may, in part, explain the nature of bottom-up sensitivity in our results. The degree to which these aspects of model structure affect bottom-up sensitivity could potentially be quantified through further scenario testing. For example, scenarios could be created to examine declines in phytoplankton biomass without changes in size structure and vice versa. Additionally, the EwE model could be run with a variety of non-predatory mortality relationships. Structural disparities in the influence of top-down impacts are discussed above in Section 2.4.2 'Differences between species-based and species-blind modeling approaches.'

2.4.4 Impacts of predator- vs. prey-moderated food webs on the propagation of variability

Predator–prey interactions are moderated quite differently in the two models: feeding interactions in the EwE model are a function of predator avoidance by prey (Christensen et al. 2008) whereas feeding interactions in the SBFW are a function of predator preference and search area (Blanchard et al. 2012). Thus, only a portion of total prey biomass is available to predators in the EwE model and availability of a given prey is not necessarily a function of its abundance but rather its vulnerability to a given predator. Conversely, all suitable prey in a given search area are equally available to predators in the SBFW model. Because of this disparity, changes at

the base of the food web in the SBFW model are carried up through larger size classes much more readily than are changes at the base of the food web in the EwE model.

Variability propagation in the SBFW model is also a function of the primary producer spectra (as explained in Section 2.4.3 'Uncertainty on the relative impacts of top-down and bottom-up forcing' above). While there is some dampening of the input variability in the consumer size spectra, much of it is transmitted through the food web. Top-down forcing also propagates readily in the SBFW model, through it is dampened considerably as size decreases due to the inverse relationship between size and abundance; as size decreases abundance increases exponentially and predation impacts an increasingly smaller proportion of the prey population (Andersen and Pedersen 2010; Polovina and Woodworth-Jefcoats 2013). There is also evidence to suggest that increasing fishing mortality of large fish destabilizes the consumer spectra and amplifies variability (Rochet and Benoît 2012). Our results appear to support this (Table 2.1).

An important EwE parameter is vulnerability; it ultimately controls the relative strength of bottom-up vs. top-down effects and we know almost nothing about how to actually parameterize it from real systems. In this comparison, we set all EwE vulnerabilities to the default value of two. This was done for several reasons. First, setting all vulnerabilities to the same value should help minimize the impacts of species-specific interactions that have the potential to confound the model comparison. Second, by setting all values to the default value of two the EwE model is fairly equally sensitive to top-down and bottom-up forcing (Mackinson et al. 2009). Despite using the default vulnerability value, a great deal of variability in the phytoplankton densities is dampened in the EwE model. Additionally, small phytoplankton, which have a lower interannual variability than large phytoplankton, are the dominant biomass input (Fig. 2.1) and are more directly linked to higher trophic levels than are large phytoplankton. Finally, factors such as the degree of cannibalism (Essington 2007) and biomass recycling (Vasconcellos et al. 1997) can also affect variability propagation in EwE. Detailed sensitivity testing of a range of vulnerability parameterization schemes may help quantify the uncertainties associated with EwE's vulnerability (Morris et al. 2014).

Understanding the degree to which variability propagates through the marine food web is essential when attempting to assess the impacts of ENSO cycles and other forms of interannual

variability. Additionally, factors such as species and/or size composition and targeted fishery exploitation can influence how resilient ecosystems are to interannual variability (Watters et al. 2003). In this comparison, propagation of interannual variability is largely tied to each model's computational structure through features such as EwE's vulnerability and SBFW's parameterization of the primary producer spectra. Further work is needed to determine how fluctuations in the phytoplankton community structure and abundance impact consumers, at what time scales, to what degree these impacts are a function of consumer community composition, and what role fishing plays in variability propagation. Comparative and ensemble modeling studies are an ideal method for separating the influence of model structure from broadly applicable ecosystem projections (Essington 2007; Smith et al. 2011; Evans et al. 2013; Gårdmark et al. 2013; Jones and Cheung 2014).

2.4.5 Model limitations and caveats

There are important caveats to how well ecosystem forcing can be evaluated by each modeling approach. The fishing scenarios carried out in this study are quite simplistic in that they assume constant fishing mortality over time, which is likely not realistic. Constant fishing mortality also precludes the ability to examine the impact of top-down variability, both independent of and in combination with bottom-up variability. Additionally, with the exception of several multi-stanza tuna species in the EwE model, the models do not incorporate dynamic reproduction. Thus, the removal of larger, mature individuals does not lead to a reduction in offspring.

There are caveats related to the investigation of climate change impacts in this study as well. We examine the presence and absence of only one climate change scenario. Examining additional climate models and scenarios would provide insight on a fuller range of projected climate impacts in the central North Pacific. Additionally, only two size classes of phytoplankton are used in this study's approach. As discussed in Section 2.4.3 'Uncertainty on the relative impacts of top-down and bottom-up forcing', this can lead to potential overestimation of the impacts of relative changes in phytoplankton size structure. It would be ideal to have phytoplankton biomass discretized into a greater number of narrower size classes. The recent release of a suite of new climate model output (Taylor et al. 2012), including models

with several classes of phyto- and zooplankton, presents an excellent opportunity to address some of these caveats through future ecosystem modeling work.

An aspect beyond the scope of this study is how maximum body size (both within species and for the ecosystem as a whole) might change as a result of, or independent of, fishing, climate change, or both. Cheung et al. (2013) project that maximum fish body size could decrease by as much as 10 – 20% by 2050 in the central North Pacific as a result of climate impacts. And recent work suggests that shifts in predator and prey size relationships can occur independent of direct climate change impacts (Wirtz 2012). Finally, rising ocean temperatures will likely have a significant impact on ecosystem structure (Burrows et al. 2011; Pinsky et al. 2013) and should be included in future studies.

2.5 Conclusions

We compare a size-based and a species-based model's treatment of the same fishing and climate scenarios. Such a comparison sheds light on the differences between each approach by highlighting the influence model structure can have on model output. In addition to differences in the structure of these models, they also make very different assumptions about how organisms interact. Future ensemble studies that incorporate the full suite of marine ecosystem models may enable the uncertainty stemming from differences in model structure to be captured. However, model assumptions and predictions also need to be tested. In the future, ensembles should aim to move beyond model comparison and towards quantifying uncertainty and assessing model skill both within and across models.

Our study concludes that the propagation of interannual variability, mechanisms responsible for bottom-up change, and relative impacts of combined top-down and bottom-up change are all linked to model structure. This link makes it difficult to confidently project some aspects of ecosystem change. Conversely, model agreement regarding the negative impacts of both climate change and increased fishing mortality supports the need for comprehensive and forward-looking ecosystem-based approaches to fisheries management.

Table 2.1. Interannual variability (sum of the absolute value of residuals from a 5-year running mean) for each output time series listed[a]. Time series include climate change and are standardized prior to calculating the running mean and residuals.

F:	Ecopath with Ecosim						Size-based Food Web					
	0	0.2	0.4	0.6	0.8	1.0	0	0.2	0.4	0.6	0.8	1.0
Catch												
Small	-	13.5	14.6	12.7	11.7	11.8	-	15.1	15.0	15.1	15.2	15.5
Large	-	4.5	4.8	9.9	8.9	2.3	-	8.7	9.5	10.2	10.8	11.3
Total	-	10.1	11.9	12.3	11.6	10.9	-	11.9	12.9	13.7	14.3	14.9
Exploitable Biomass												
Small	14.7	13.5	14.6	12.7	11.7	11.8	17.2	16.6	16.3	16.2	16.3	16.5
Large	5.9	4.5	4.8	9.9	8.9	2.3	7.7	8.7	9.5	10.2	10.8	11.3
Total	13.4	12.3	13.7	12.6	11.7	11.5	13.9	14.5	15.0	15.4	15.7	16.0

[a] Input interannual variability with climate change: Small phytoplankton: 40.1; Large phytoplankton: 43.5.

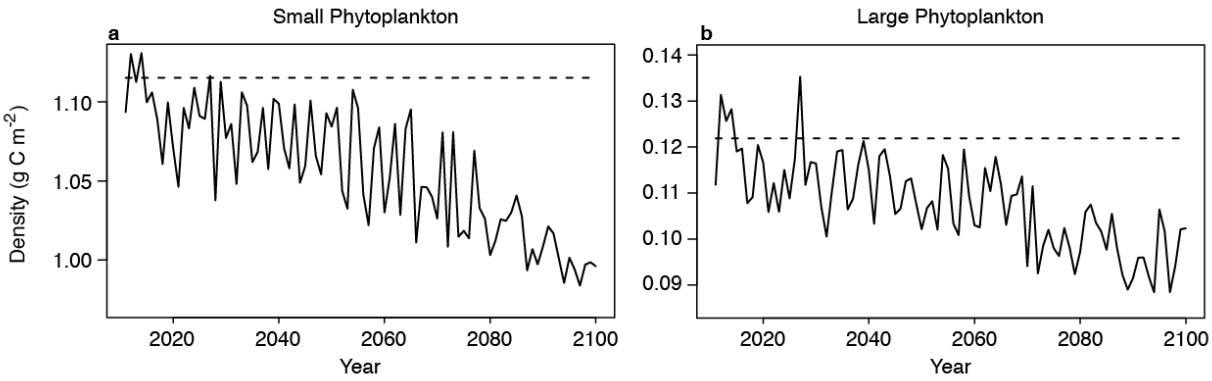

Figure 2.1 Annual mean (a) small and (b) large phytoplankton density from ESM2.1. Solid lines represent climate change scenario and dashed lines represent static climate scenario.

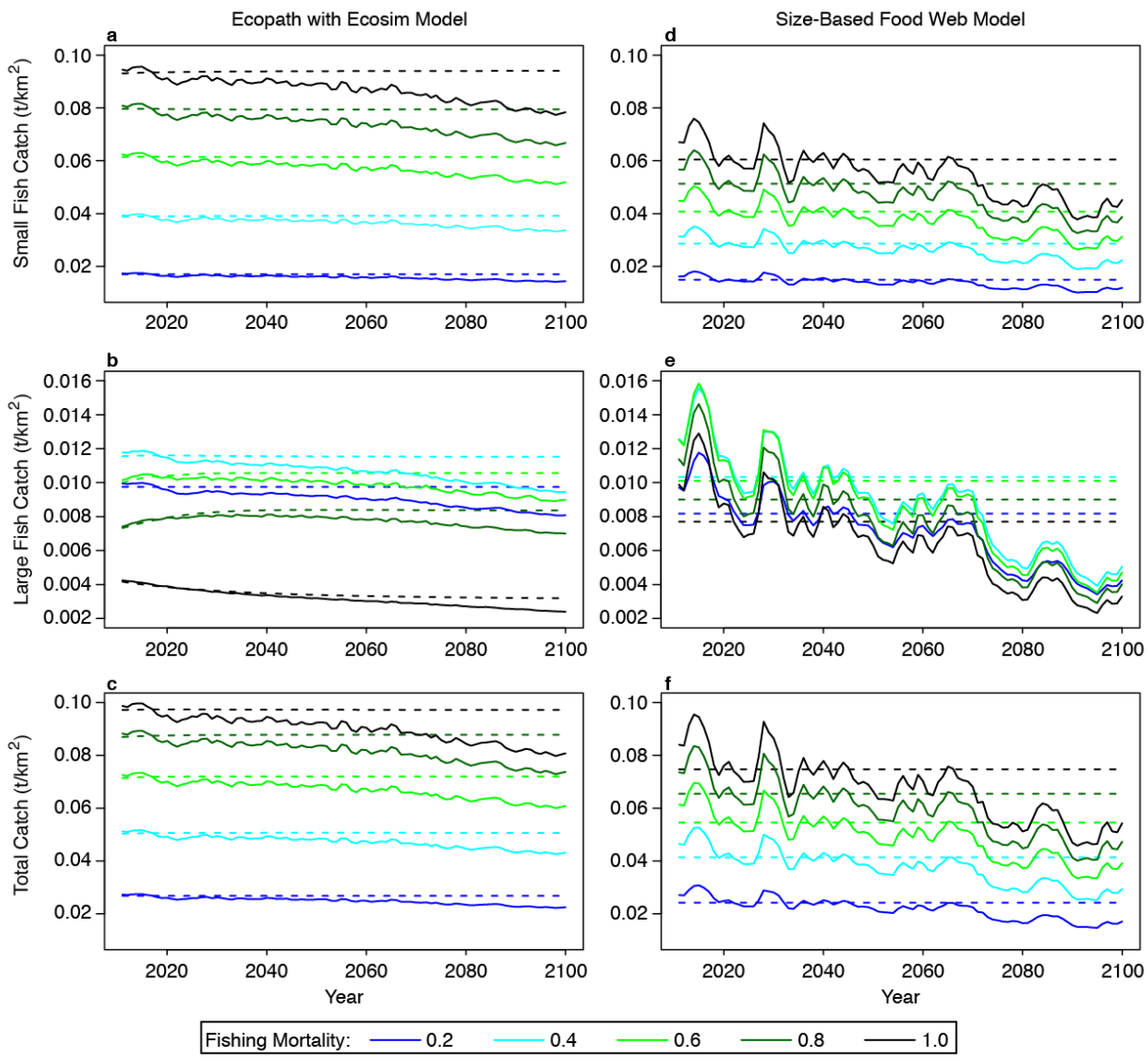

Figure 2.2 Annual mean (a, d) small fish catch, (b, e) large fish catch, and (c, f) total catch for both models. EwE output is shown on the left (a–c) and SBFW on the right (d–f). Solid lines represent climate change scenario and dashed lines represent static climate scenario.

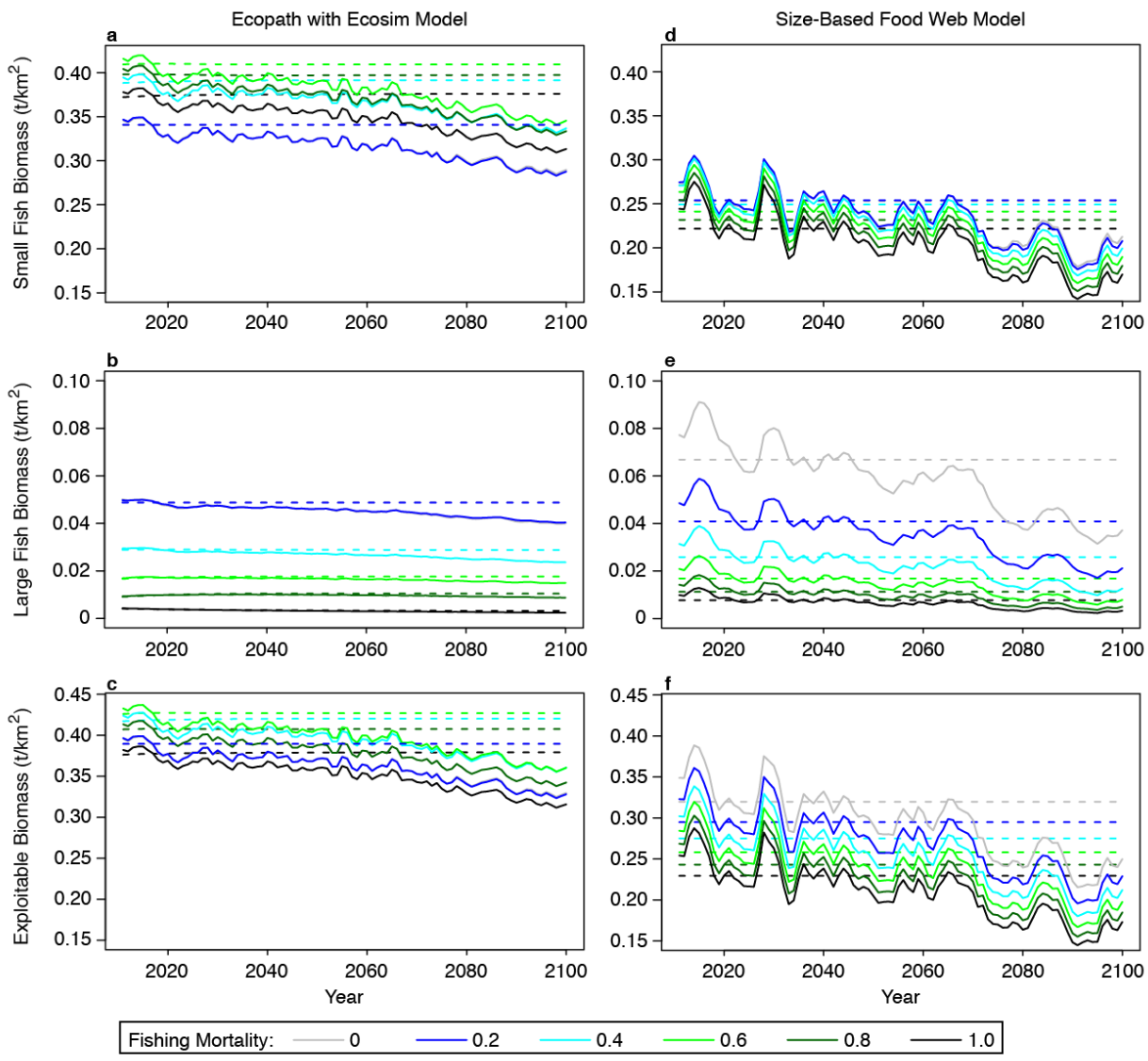

Figure 2.3 Annual mean (a, d) small fish biomass, (b, e) large fish biomass, and (c, f) total exploitable biomass for both models. EwE output is shown on the left (a–c) and SBFW on the right (d–f). Solid lines represent climate change scenario and dashed lines represent static climate scenario. Note that the F = 0 line is obscured by the F = 0.2 line in panels a, b, and c.

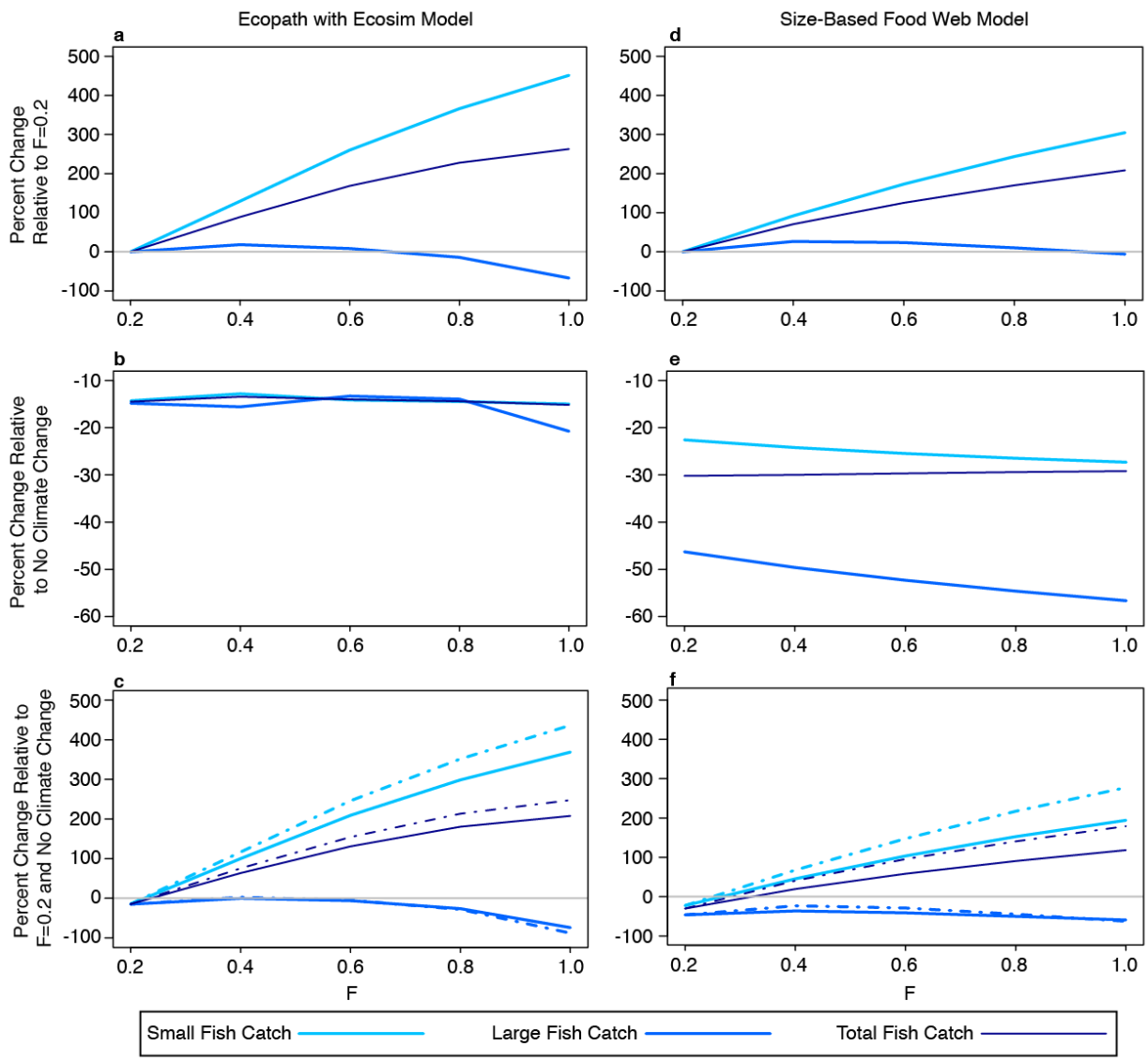

Figure 2.4 Using 2081–2100 mean catch, the effects of (a, d) increasing fishing mortality, (b, e) climate change at each F value, and (c, f) both increasing fishing mortality and climate change combined. The percent change in catch at each level of fishing mortality is shown relative to (a, d) F = 0.2, (b, e) no climate change, and (c, f) F = 0.2 and no climate change. In (c) and (f), the modeled combined effect of fishing and climate change is shown with a solid line and the mathematically combined effect of fishing and climate change (i.e., (a) + (b), (d) + (e)) is shown with a dot-dash line. Note that panels (b) and (e) are scaled differently from the other four panels.

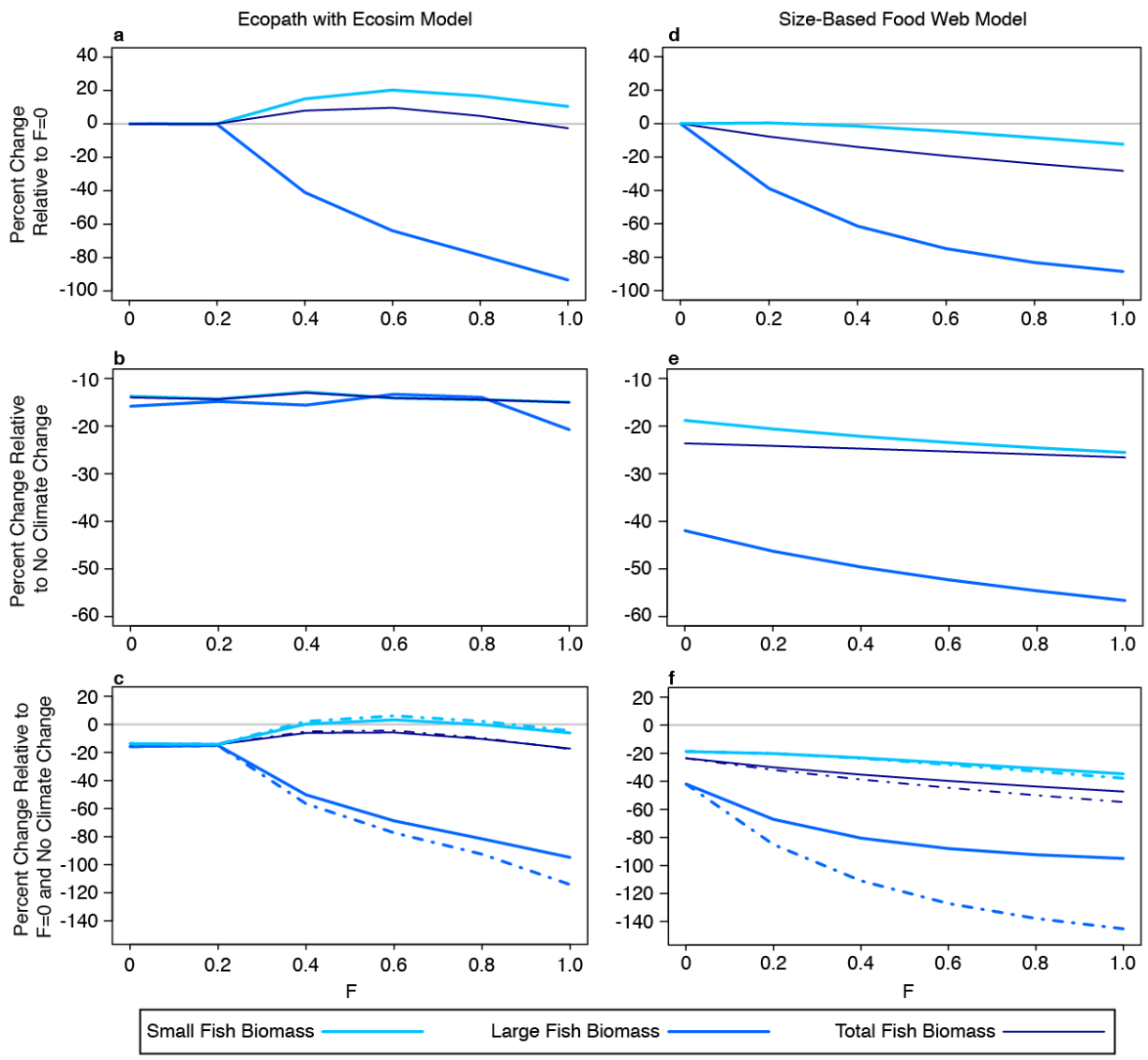

Figure 2.5 Using 2081–2100 mean biomass, the effects of (a, d) increasing fishing mortality, (b, e) climate change at each F value, and (c, f) both increasing fishing mortality and climate change combined. The percent change in biomass at each level of fishing mortality is shown relative to (a, d) F = 0, (b, e) no climate change, and (c, f) F = 0 and no climate change. In (c) and (f), the modeled combined effect of fishing and climate change is shown with a solid line and the mathematically combined effect of fishing and climate change (i.e., (a) + (b), (d) + (e)) is shown with a dot-dash line. Note that each row of panels is scaled differently.

CHAPTER 3

Climate change is projected to reduce carrying capacity and redistribute species richness in North Pacific pelagic marine ecosystems

Climate change is expected to impact all aspects of marine ecosystems, including fisheries. Here, we use output from a suite of 11 earth system models to examine projected changes in two ecosystem-defining variables: temperature and food availability. In particular, we examine projected changes in epipelagic temperature and, as a proxy for food availability, zooplankton density. We find that under RCP8.5, a high business-as-usual greenhouse gas scenario, increasing temperatures may alter the spatial distribution of tuna and billfish species richness across the North Pacific basin. Furthermore, warmer waters and declining zooplankton densities may act together to lower carrying capacity for commercially valuable fish by 2–5% per decade over the 21st century. These changes have the potential to significantly impact the magnitude, composition, and distribution of commercial fish catch across the pelagic North Pacific. Such changes will in turn ultimately impact commercial fisheries' economic value. Fishery managers should anticipate these climate impacts to ensure sustainable fishery yields and livelihoods.

Based on: Woodworth-Jefcoats PA, Polovina JJ, Drazen JC, 2017. Climate change is projected to reduce carrying capacity and redistribute species richness in North Pacific pelagic marine ecosystems. Global Change Biology, 23(3): 1000-1008. doi: 10.1111/gcb.13471

3.1 Introduction

Pelagic marine habitat is projected to experience a number of impacts from climate change (e.g., Bopp et al. 2013). As earth system models improve with each model generation, confidence in their projections has increased and a community consensus is coalescing around several projected impacts. Of these, two of the most significant impacts to epipelagic habitat are likely to be ocean warming (Bopp et al. 2013) and the expansion of the oligotrophic subtropical gyres (Sarmiento et al. 2004; Steinacher et al. 2010; Polovina et al. 2011; Cabré et al. 2015b). Ocean warming is a direct result of ocean heat uptake in response to atmospheric warming driven by increasing greenhouse gas concentrations. Gyre expansion is projected as the result of two physical mechanisms. Ocean heating leading to increased vertical stratification is expected to further reduce nutrient concentrations in the euphotic zone of oligotrophic gyre waters (Xu et al. 2012; Cabré et al. 2015b). Additionally, changes in atmospheric circulation may result in a poleward displacement of both the descending branch of the Hadley circulation and midlatitude storm tracks (Chang et al. 2012; Scheff and Frierson 2012; Yongyun et al. 2012; Cabré et al. 2015b). These changes in atmospheric circulation will in turn alter ocean surface wind stress curl, primarily along the gyres' poleward boundaries, contributing to gyre expansion.

Change in the biophysical marine environment will impact many marine organisms, as well as fisheries and those who rely on fishery services. Catch from pelagic fisheries in the North Pacific is largely comprised of tuna, including skipjack (*Katsuwonus pelamis*), yellowfin (*Thunnus albacares*), and bigeye (*Thunnus obesus*), as well as other species (FAO 2012). Tunas occupy specific thermal habitats at different life stages and have a high metabolic demand (Lehodey et al. 2011, 2013). Thus, changes to either thermal habitat or ocean productivity are likely to impact tunas, as well as other commercially valuable fish. We examine these climate change impacts through a suite of models included in the fifth phase of the Coupled Model Intercomparison Project (CMIP5; Taylor et al. 2012), focusing on the two habitat parameters that most directly influence ecosystem productivity and capacity: temperature and food availability. We aim to make broad projections of climate change impacts on marine fisheries that can be used by fishery managers when drafting ecosystem-based fisheries management plans. Previous studies have suggested that climate change may have a substantial impact on commercial fish catch, independent of fishing (Cheung et al. 2010; Lehodey et al. 2011, 2013; Bell et al. 2013;

Howell et al. 2013; Woodworth-Jefcoats et al. 2015). Therefore, it is essential that these potential impacts be incorporated into management plans so that both fishery resources and livelihoods can be sustained well into the future.

3.2 Materials and methods

3.2.1 Earth system models used

We examine 11 earth system models included in CMIP5. Models used are presented in Table 3.1. Models selected are those with two trophic levels (phyto- and zooplankton) of output available at time of download. All data were downloaded from the CMIP5 data portal (http://cmip-pcmdi.llnl.gov/cmip5/data_portal.html). Spherical interpolation (for curvilinear grids) and nearest coordinate regridding (for rectilinear grids) were used to regrid output to a common 1° × 1° rectilinear grid spanning 0–66°N and 120°E–70°W, with the Bering Sea and Sea of Okhotsk excluded. We note that output from two additional models, HadGEM2-CC and HadGEM2-ES (Collins et al. 2011), was available but not used in our analysis due to unrealistic negative plankton densities across much of the central North Pacific.

3.2.2 Data used

Both historical and projected data are examined. All projections are from the representative concentration pathway (RCP) 8.5 scenario, 'a relatively conservative business as usual case... with no explicit climate policy' (Riahi et al. 2011). We focus on two 20-year time periods representing the beginning and end of the 21st century: 1986–2005 and 2081–2100. The beginning of the 21st century is captured by the last 20 years of the historical runs and the end of the 21st century by the last 20 years of the 21st century in the RCP8.5 projection.

Data are vertically integrated across the epipelagic zone, represented as the upper 200 m of the water column. Vertical resolution varies by model, and we integrated across all depths of 200 m or less. We examine potential temperature, phytoplankton carbon density, and zooplankton carbon density output by each model. Data are examined as a model ensemble to address the possible influence of individual model drift (Sen Gupta et al. 2013).

Vertically integrated (upper 200 m) ocean temperatures from the World Ocean Atlas 2013 (WOA13; Locarnini et al. 2013) were used as baseline temperatures when calculating projected ecosystem impacts. The temperature increase projected by each model was then added to the WOA13 data to determine projected ecosystem change.

3.2.3 Pelagic habitat

We examine changes in thermal habitat by comparing probability frequency distributions of pooled 20-year, monthly epipelagic temperatures. Because so much of the literature is focused on sea surface temperature (SST), we also present projected changes in SST though these changes are not the focus of our analysis. In both cases, monthly temperatures were used in an effort to fully capture seasonal extremes and distributions are binned in 0.5 °C bins. Change in zooplankton densities is similarly compared, although annual densities are used as this is the only temporal scale available for three-dimensional biogeochemical data through the CMIP5 data portal. Distributions are binned in 0.05 g C m^{-2} bins. Twenty-year means from the beginning and end of the 21st century are used to evaluate the absolute change in epipelagic temperature and percent change in both phyto- and zooplankton densities.

3.2.4 Ecosystem impacts

We assess two measures of ecosystem impact: tuna and billfish species richness and carrying capacity. Species richness captures the total number of tuna and billfish species present and carrying capacity the total number of fish the ecosystem can support. Species richness (*SR*) is a function of epipelagic temperature, following equation 3.1 as determined by Boyce et al. (2008),

$$SR = -0.0033T^3 + 0.1156T^2 - 0.4675T \qquad (3.1)$$

where T is epipelagic temperature in °C. Carrying capacity (K) is determined from ecological theory, following equation 3.2,

$$K \propto [R]M^{-3/4} e^{E/kT} \qquad (3.2)$$

where $[R]$ is limiting resource supply, which we take as zooplankton density, M is target fish mass, E is activation energy (0.63 eV; Brown et al. 2004), k is Boltzmann's constant (8.62×10^{-5} eV K^{-1}; Brown et al. 2004; Jennings et al. 2008), and T is epipelagic temperature in Kelvin

(Brown et al. 2004). Given that equation 3.2 is a proportional relationship, we evaluate relative changes in the right-hand side of the equation and refer to these as changes in potential carrying capacity (K_p). Twenty-year means from the beginning and end of the 21st century are used to evaluate changes in SR and K_p. We hold M constant over both periods so the resulting change in K_p is independent of M. To assess whether R or T has a greater influence on K_p, we examine the difference between the absolute percent change in both R and $e^{E/kT}$ following equation 3.3,

$$|\%\Delta R| - |\%\Delta e^{E/kT}| \qquad (3.3)$$

with positive results indicating that changes in zooplankton density have the greatest influence on K_p and negative results indicating that changes in T have the greatest influence on K_p.

3.3 Results

3.3.1 Pelagic habitat

3.3.1.1 Thermal habitat

Across all models, sea surface and epipelagic temperatures are projected to increase (Table 3.1, Figs 3.1a and 3.2a). Additionally, all model scenarios project the emergence of new, warmer temperatures by the end of the 21st century. Emerging SSTs (i.e., temperatures not present at the beginning of the 21st century that are present at the end of the 21st century) range from 31.5 to 38 °C and epipelagic temperatures from 29 to 35 °C. Change in thermal habitat is also captured through the difference between frequency distributions over time. Epipelagic temperatures that comprise the majority of the North Pacific at the beginning of the 21st century (15.6–23.7 °C on average) decline in frequency and warmer temperatures come to dominate by the end of the century (24.5–32.9 °C on average).

Our results focus on the warmest temperatures in the North Pacific as these temperatures cover the largest area. However, it is important to note that there is a similar distributional shift in the coolest temperatures. Here, too, there is model consensus on a shift toward warmer temperatures, as well as a loss of the coolest temperatures by the end of the 21st century (Fig. 3.1a). Across all models, disappearing epipelagic temperatures range from -1.5 to 2 °C. Three models (IPSL-CM5B-LR, MPI-ESM-LR, and MPI-ESM-MR) project a loss of the coolest SSTs, ranging from -2.0 to -1.0 °C.

3.3.1.2 Food available to fish

We take zooplankton density to be a proxy for food available to fish. Across all models, the distribution of zooplankton densities is projected to shift toward lower values (Table 3.1, Figs. 3.1b and 3.2b). Densities that comprise the majority of the North Pacific at the beginning of the 21st century (0.50–1.10 g C m^{-2} on average) decline in frequency and lower densities come to dominate by the end of the century (0.18–0.49 g C m^{-2} on average).

Not only do the models used in our study project zooplankton densities to decline across much of the North Pacific, but they also project these declines to be amplified relative to declines in phytoplankton densities (Fig. 3.2c, warm colors represent waters where zooplankton declines are projected to be greater than phytoplankton declines). When declining zooplankton densities are examined in relation to projected phytoplankton changes, we find that zooplankton declines exceed phytoplankton declines to a large degree. All models but three (CanESM2, GISS-E2-H-CC, and GISS-E2-R-CC) place such waters across much of the North Pacific excluding only subpolar waters, and in some cases equatorial and California Current upwelling waters. Projected declines in zooplankton exceed those of phytoplankton by 10–30% on average, with individual model maxima of 25–50% found along the periphery of the North Pacific subtropical gyre (NPSG).

3.3.2 Ecosystem impacts

Changes in predicted tuna and billfish species richness (*SR*) follow projected changes in epipelagic temperature. Across all models, the area of maximum *SR* shifts northward and eastward. Species richness declines across much of the central and western subtropics and increases in temperate and subpolar waters, with the magnitude of change increasing with distance toward the western tropical Pacific and temperate latitudes, peaking at approximately four species lost or gained (Fig. 3.2d). Most models project potential carrying capacity (K_p) for commercially valuable fish to decline by 20–50% across the North Pacific, or by roughly 2–5% per decade over the 21st century (Fig. 3.2e). As with trophic amplification, the areas projected to see the greatest declines in K_p are found along the periphery of the NPSG. Declining K_p is a result of both increasing epipelagic temperature and declining zooplankton density, with the primary driver varying across the North Pacific. In the western equatorial Pacific and NPSG,

declining zooplankton density has a stronger impact on K_p, while in the eastern equatorial Pacific and at temperate latitudes, increasing epipelagic temperature is the stronger driver (Fig. 3.2f).

3.4 Discussion

The CMIP5 projections presented in this study suggest a number of changes to North Pacific pelagic habitat. Broadly, thermal habitat is projected to warm and be spatially redistributed. Zooplankton densities are projected to decline and to an amplified degree relative to phytoplankton declines. When these projections are examined more finely and in relation to one another, they suggest that commercial fisheries in the central North Pacific may see catch decline by 20–50% and be comprised of three to four fewer tuna and billfish species.

3.4.1 Changing pelagic habitat

While warming epipelagic temperatures might be expected to unfold as a straightforward poleward creep of present-day conditions, we find that this is not the case (Fig. 3.2a, d). Rather, warmer temperatures appear to emerge from the western equatorial Pacific and expand eastward and northward as moderate temperatures retreat in kind. Over time, this results in a reshaping of pelagic thermal habitat. For example, thermal habitat associated with adult tuna foraging is displaced by thermal habitat more commonly associated with tuna spawning grounds, and spawning habitat is replaced by temperatures that exceed even the warmest temperatures associated with commercially valuable fish (Boyce et al. 2008; Lehodey et al. 2011, 2013). Evidence suggests that fish and other pelagic organisms will relocate to maintain residence in preferred thermal habitat in both freshwater (Grenouillet and Comte 2014) and marine (Pinsky et al. 2013; Montero-Serra et al. 2015) environments, and with relocations varying over different life history stages (Walsh et al. 2015). Some fish may simply be able to spend more time in deeper, cooler waters. However, such an adaptation comes at a cost. For example, fish may forage less successfully at the lower light levels found below the epipelagic realm. Organisms that are unable to exploit deeper habitat will be forced to relocate geographically. Such vertical and geographic relocations could ultimately alter predator–prey dynamics.

The emergence of new thermal habitat also raises questions, as it is projected to exceed current maximum temperatures. It remains unknown how or whether pelagic organisms will

adapt to these temperatures. Storch et al. (2014) suggest there are firm limits on temperatures to which animals can adapt. They find that due to constraints posed by cellular complexity, the highest SST that allowed multicellular Eukaryea to grow was 40 °C, close to temperatures projected to occur over the North Pacific in our study. The unprecedented rate at which climate is changing (Doney et al. 2014) adds further uncertainty to questions surrounding adaptation.

In addition to changes in thermal habitat, we also project a shift toward lower zooplankton densities over the 21st century. Spatially, the lowest zooplankton densities are associated with the oligotrophic NPSG. Declining densities are manifested as both an expansion of the NPSG and lower densities in NPSG waters (Fig. 3.2b). While we examine the oligotrophic NPSG from the perspective of zooplankton densities, our results are similar to those from other studies focused on phytoplankton that project the gyre's expansion (Sarmiento et al. 2004; Steinacher et al. 2010; Polovina et al. 2011; Cabré et al. 2015b).

Not only do the models used in our study project zooplankton densities to decline across much of the North Pacific, but they also project these declines to be amplified relative to declines in phytoplankton densities. Stock et al. (2014) link trophic amplification to declining zooplankton growth efficiency as food resources (net primary production) decline, while Chust et al. (2014) link trophic amplification to nonlinear coupling of phytoplankton and zooplankton biomass. It remains unclear whether this amplification in the plankton community will propagate further up through the food web; however, modeling work suggests that it will be amplified by some micronekton (Bell et al. 2013) and possibly throughout the size spectrum (Lefort et al. 2015). If trophic amplification does indeed carry through the food web, an amplification of roughly 20% at each trophic linkage could result in apex predator density (trophic level 4–5) declining by up to 50–60% by the end of the century, or by 5–6% per decade.

3.4.2 Ecosystem impacts of changing pelagic habitat

The projected impacts of climate change in the North Pacific extend beyond the immediate changes to temperature and food availability. Increasing epipelagic temperature is projected to lead to a redistribution of tuna and billfish *SR* (Fig. 3.2d). There is strong model agreement of a decline of up to 3–4 species across much of the subtropics with an increase of similar magnitude projected for temperate latitudes. These projected changes in *SR* largely, and

not surprisingly given equation 3.1, mirror the changing footprint of thermal habitat in the North Pacific. Based solely on thermal tolerance, much of the subtropical North Pacific is projected to become less hospitable to adult commercially valuable tuna and billfish. While a decline of only a few species may not seem very substantial, the longline fisheries in these waters target only a small number of species, primarily bigeye tuna and swordfish (*Xiphias gladius*), and also catch several commercially valuable, nontarget species such as skipjack tuna, yellowfin tuna, shortbill spearfish (*Tetrapturus anguistorostris*), and striped marlin (*Tetrapturus audax*). Thus, even a small decline in SR could significantly impact catch composition, magnitude, and value. Likewise, at the northern limits of the fishery, the small increase in species diversity could potentially benefit fishermen. Whether this potential benefit would be offset by the increased expense of traveling further from port to fish is unknown. Fishermen may also shift their homeport based on target catch relocation, as some in the Hawaii-based longline fishery have already done.

Increasing epipelagic temperatures combined with largely declining zooplankton densities are projected to act together to lower North Pacific K_p over the 21st century. We find strong model agreement that K_p is projected to decline by roughly 20–50% across the North Pacific (Fig. 3.2e). Despite our measure of K_p being a simple relationship based on ecological theory, this projection is in line with previous studies that have projected similar declines in exploitable high-trophic-level biomass as the result of climate change (Lefort et al. 2015; Woodworth-Jefcoats et al. 2015). We also find that declines in K_p exceed those of zooplankton densities, further suggesting that trophic amplification in the plankton community may propagate up through the food web. Additionally, K_p is projected to decline even in regions where plankton densities are projected to increase (Fig. 3.2b, e). This suggests that potential increases in biomass at the base of the food web would not be enough to compensate for the metabolic costs of increasing temperatures. Further examination of the impact of temperature vs. zooplankton on K_p shows that the dominant driver of change varies spatially (Fig. 3.2f). In subtropical regions where zooplankton declines are projected to be greatest, these declines seem to have the greater impact on K_p. In the eastern North Pacific and at temperate latitudes, waters seeing the greatest increase in epipelagic temperature, temperature increases drive K_p declines.

Potential carrying capacity is projected to decline most in and around the central North Pacific. This has the potential to particularly impact longline fisheries operating in this area. Potential fisheries' yields could decline by up to 50% over a time when the Food and Agriculture Organization of the United Nations projects that food resources will need to increase by roughly 70% to meet the demands of a growing human population (UN 2011). Such an increase in demand could further strain the ecosystem, as the heavy removal of large fish has the potential to drive down exploitable biomass independent of any bottom-up impacts (Blanchard et al. 2005; Ward and Myers 2005b; Polovina and Woodworth-Jefcoats 2013).

The areas of greatest trophic amplification and declining K_p occur around the boundaries of the NPSG (Fig. 3.2c, e). To the north of the NPSG lies the North Pacific transition zone, a narrow area used as a migration and foraging corridor by a number of pelagic species (Polovina et al. 2001; Hazen et al. 2013). To the south of the NPSG are spawning grounds for a number of tropical tuna species (Lehodey et al. 2011, 2013). Thus, the areas likely to see the greatest declines in food availability are areas crucial to specific life history stages of pelagic species. Such a mismatch in resource demand and supply could amplify climate impacts on species exploiting these regions. Furthermore, given that organisms from around the North Pacific target these areas, changes here have the potential to impact the entire basin. These maxima of declining phyto- and zooplankton densities are not flanked by corresponding areas of increasing densities, suggesting that productive regions around the NPSG are not simply relocating. Or, if productive regions are relocating, they are still experiencing overall declines in phytoplankton densities. The importance of these regions bordering the NPSG, along with their relatively small size, makes them ideal areas for monitoring climate change as it unfolds. Survey (Howell et al. 2015; Polovina et al. 2015) and tagging (Block et al. 2011) efforts already in place in these regions may provide insight into how organisms across the food web are responding to climate change.

One question we are unable to address in this study is how regions bordering the NPSG may be impacted by changes in phenology. The transition zone in particular moves meridionally with the seasons. The phenology of both the seasonal migration of the transition zone (Hazen et al. 2013) and its associated productivity (Polovina et al. 2011) may change as a result of climate change. Thus, organisms targeting the region at specific times of the year may have to migrate

farther or to different locations. Both finer temporal resolution projections and tagging data may help address such phenology questions.

3.4.3 Caveats

Our study focuses on the two primary influences on ecosystem capacity: temperature and food availability. These are far from the only influences, however. Other variables such as oxygen concentration, pH, and exploitation can influence pelagic carrying capacity. Given that changes in many of these variables are projected to have negative impacts in the North Pacific (Koslow et al. 2011; Bopp et al. 2013), they are likely to exacerbate the impacts of warming temperatures and declining food availability.

We also assume that physical climate influences will be the primary determinants of ecosystem capacity. However, species and trophic interactions are also influential. In some cases, these interactions can have a larger impact than physical climate drivers (Grenouillet and Comte 2014; Ockendon et al. 2014). Additionally, changes in temperature and food availability can alter foraging range and create new competition (Bond and Lavers 2014). Such changes in predator–prey interactions could have large impacts on commercial fisheries and could potentially be examined through species-based ecosystem modeling approaches and network theory.

In this study, we examine only the epipelagic realm, although many commercially valuable fish also inhabit mesopelagic depths (Howell et al. 2010; Abecassis et al. 2012). Future impact studies could examine a broader vertical habitat range. For example, Lefort et al. (2015) suggest that fishes able to migrate between epi- and mesopelagic depths may fare better in the face of climate change than fishes restricted to either realm. Finally, we examine only one climate change scenario. By examining RCP8.5, we hopefully project the upper limits of potential climate change impacts. Future work could examine more optimistic RCPs, potentially providing motivation to take mitigating actions by presenting goals for limited impacts.

3.4.4 Commercial fishery impacts of changing pelagic habitat

Through examining a suite of CMIP5 earth system models, we find that climate change may significantly alter North Pacific epipelagic habitat over the 21st century. Warming thermal

habitat and declining zooplankton densities are projected to lower potential carrying capacity, and in turn fishery yield, by approximately 2–5% per decade. Additionally, based on changing thermal habitat alone, species richness across much of the subtropics is projected to decline by up to four tuna and billfish species by the end of the century. Together, these changes have the potential to significantly impact commercial fish catch in the North Pacific. Fishery managers can use these projections to place current yields and management actions in a broader climate-based context. For example, early warning thresholds for changing catch composition or yield could be based on projected climate impacts. Such strategic management plans would ensure that the ecosystem is not further stressed by unsustainable removals.

Table 3.1. For each model, the SST and epipelagic temperature ranges that decrease in frequency, increase in frequency, and emerge by the end of the 21st century followed by the zooplankton density ranges that increase and decrease in frequency by the end of the century. [a]Output not used in analysis due to unrealistic negative plankton densities in the central North Pacific.

Model and Scenario	Sea Surface Temperature (°C)			Epipelagic Temperature (°C)			Zooplankton Density (g C m^{-2})	
	Decreases	Increases	Emerges	Decreases	Increases	Emerges	Increases	Decreases
Canadian Centre for Climate Modelling and Analysis Earth system model[1] (CanESM2)	20.0–30.0	30.0–38.0	34.0–38.0	14.5–21.5	21.5–32.5	30.5–32.5	0.05–0.20	0.20–0.40
NOAA Geophysical Fluid Dynamics Laboratory Earth System Model Generalized ocean layer dynamics[2] (GFDL-ESM2G)	20.0–29.5	29.5–35.0	32.5–35.0	13.0–18.5	24.5–32.0	30.0–32.0	0.50–0.90	0.90–1.85
NOAA Geophysical Fluid Dynamics Laboratory Earth System Model Modular Ocean Model 4[2] (GFDL-ESM2M)	20.0–30.0	30.0–35.0	33.0–35.0	15.0–25.5	25.5–32.5	30.0–32.5	0.40–0.95	0.95–1.75
NASA Goddard Institute for Space Studies ModelE2 Earth System Model with carbon cycle coupled to the HYCOM ocean model[3, 4] (GISS-E2-H-CC)	22.0–30.0	30.0–34.5	32.0–34.5	17.5–23.0	23.0–32.5	31.0–32.5	0.00–0.10	0.10–1.00
NASA Goddard Institute for Space Studies ModelE2 Earth System Model with carbon cycle coupled to the Russell ocean model[3, 4] (GISS-E2-R-CC)	20.0–30.5	30.5–34.5	32.5–34.5	16.5–26.5	26.5–33.0	31.5–33.0	0.00–0.15	0.15–0.85
HadGEM2 of the Met Office Hadley Centre Unified Model Coupled Carbon Cycle[5, a] (HadGEM2-CC)	-	-	-	-	-	-	-	-

Table 3.1. (**continued)** For each model, the SST and epipelagic temperature ranges that decrease in frequency, increase in frequency, and emerge by the end of the 21st century followed by the zooplankton density ranges that increase and decrease in frequency by the end of the century. [a]Output not used in analysis due to unrealistic negative plankton densities in the central North Pacific.

Model and Scenario	Sea Surface Temperature (°C)			Epipelagic Temperature (°C)			Zooplankton Density (g C m^{-2})	
	Decreases	Increases	Emerges	Decreases	Increases	Emerges	Increases	Decreases
HadGEM2 of the Met Office Hadley Centre Unified Model Full Earth System[5, a] (HadGEM2-ES)	-	-	-	-	-	-	-	-
Institut Pierre-Simon Laplace Low Resolution CM5A[6] (IPSL-CM5A-LR)	21.0–30.0	30.0–36.0	32.5–36.0	15.5–26.0	26.0–34.0	30.0–34.0	0.30–0.45	0.60–1.10
Institut Pierre-Simon Laplace Medium resolution CM5A[6] (IPSL-CM5A-MR)	21.5–31.0	31.0–36.5	33.0–36.5	15.5–26.0	26.0–34.0	31.0–34.0	0.30–0.65	0.65–0.95
Institut Pierre-Simon Laplace Low resolution CM5B[6] (IPSL-CM5B-LR)	21.5–30.0	30.0–35.5	32.0–35.5	17.5–24.0	26.5–32.5	31.0–32.5	0.25–0.35	0.35–0.70
Max-Planck-Institute für Meteorologie Earth System Model low resolution[7] (MPI-ESM-LR)	20.0–30.0	30.0–37.0	34.0–37.0	14.5–22.0	22.0–33.5	31.5–33.5	0.10–0.75	0.75–1.50
Max-Planck-Institute für Meteorologie Earth System Model medium resolution[7] (MPI-ESM-MR)	20.0–30.0	30.0–36.5	34.0–36.5	16.0–21.0	21.0–35.0	32.5–35.0	0.10–0.70	0.70–1.55
Meteorological Research Institute Earth System Model Version 1[8] (MRI-ESM1)	21.0–29.5	21.0–34.5	31.5–34.5	16.5–27.0	27.0–30.5	29.0–30.5	0.00–0.20	0.20–0.40

[1]Christian et al. 2010 [2]Dunne et al. 2013 [3]Romanou et al. 2014 [4]Schmidt et al. 2014 [5]Collins et al. 2011 [6]Dufresne et al. 2013 [7]Giorgetta et al. 2013 [8]Yukimoto et al. 2011

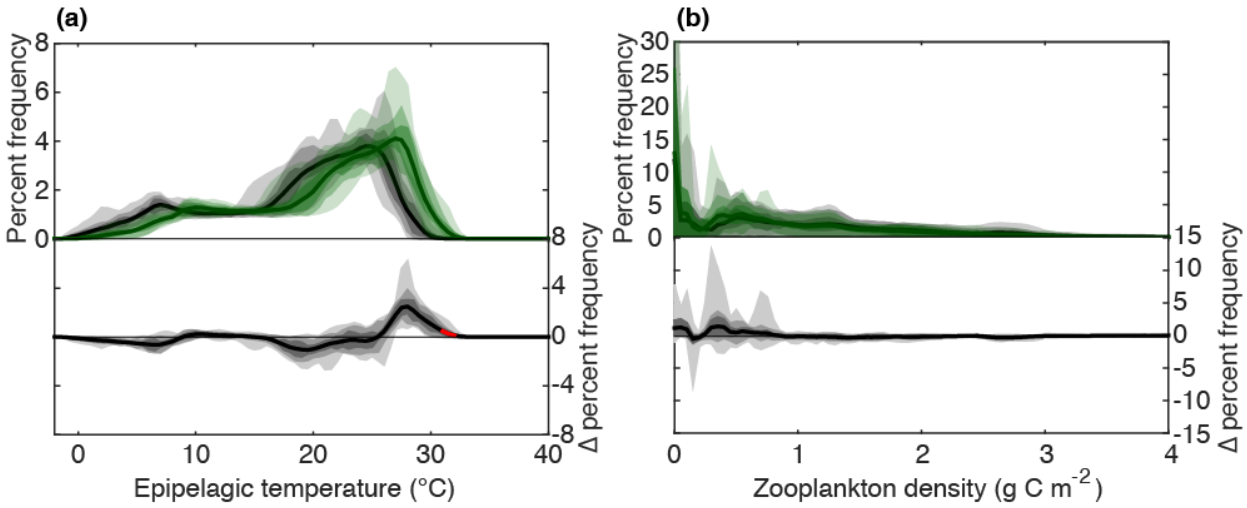

Figure 3.1 Percent frequency distributions of 20-year pooled epipelagic temperatures (a) and zooplankton densities (b) from the beginning (gray) and end (green) of the 21st century are plotted above the difference between the two distributions. Solid lines show multi-model means. Terciles encompassing 33%, 67%, and 100% of the models are shaded progressively lighter. The red line in the lower panel of (a) indicates the temperature range over which at least half the models project the emergence of new thermal habitat.

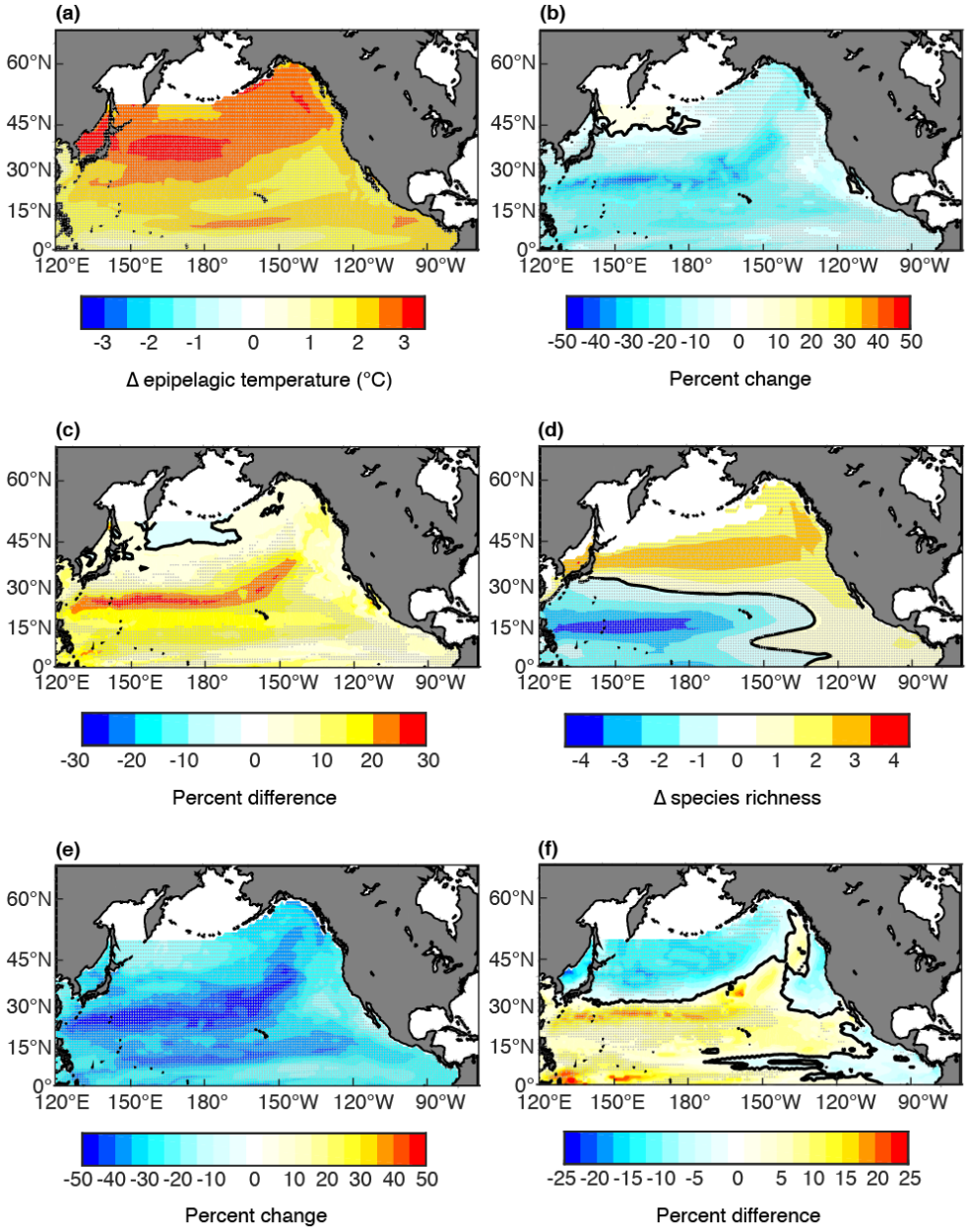

Figure 3.2 Multi-model median projected change in epipelagic habitat (a and b) and resulting degrees of ecosystem impact (c–f) over the 21st century: projected change in epipelagic temperature (a) and zooplankton density (b), degree of trophic amplification (indicated by warm colors) or the difference between projected phytoplankton and zooplankton percent declines (c), projected change in tuna and billfish species richness for waters within the bounds of a positive solution to equation 3.1 (5–30 °C) (d), projected percent change in potential carrying capacity (e), and the difference in the strength of changing zooplankton density (warm colors) vs. changing epipelagic temperature (cool colors) as drivers of change in potential carrying capacity (f). In (a–e), stippling indicates areas where at least 80% of the models used project a change of the same sign. In (f), stippling indicates areas where at least 80% of the models used indicate the same dominant driver.

CHAPTER 4

Synergy among oceanographic variability, fishery expansion, and longline catch composition in the central North Pacific Ocean

The fishing ground of the Hawaii-based longline fleet spans over 13 million km^2 in the central North Pacific Ocean. We investigated over 20 years of commercial logbook and observer data to gain an understanding of how the magnitude and composition of the fleet's catch varies on both intra- and interannual scales. We found that the fishery follows a quarterly geographic migration and that the fishery has expanded over time, with a five-fold increase in effort and a spatial expansion primarily to the northeast of Hawaii in the third quarter of the year. World Ocean Atlas and ocean reanalysis data indicate that waters to the northeast of Hawaii are a particularly efficient fishing ground because of the vertical overlap of preferred thermal habitat and fishing gear. Furthermore, we found that the Hawaii-based fleet faced little international competition in this region. The fishery's expansion has also impacted catch composition, resulting in discard rates exceeding target catch rates. Understanding how catch varies as a result of oceanographic variability and fleet movement can lead to a more efficient, resilient, and cost-effective fishery.

Based on: Woodworth-Jefcoats PA, Polovina JJ, Drazen JC, 2018: Synergy among oceanographic variability, fishery expansion, and longline catch composition in the central North Pacific. Fishery Bulletin. 116(3): 228-239. doi:10.7755/FB.116.3.2

4.1 Introduction

The Hawaii-based longline fishery is among the most economically valuable fisheries in the United States, ranked 6th in 2015 (NMFS 2016b). Its footprint spans over 13 million km^2 in the central North Pacific, ranging from the dateline to 120°W and from equatorial waters to roughly 40°N. The Hawaii-based fleet focuses on two fisheries, a shallow-set fishery targeting swordfish (*Xiphias gladius*) and a deep-set fishery targeting bigeye tuna (*Thunnus obesus*). The deep-set fishery is the dominant fishery by far, with both effort and catch (magnitude and value) being an order of magnitude greater than that of the shallow-set fishery (NMFS 2016a). For this reason, we focused on the deep-set fishery in this study.

The deep-set fishery operates largely during the day (Bigelow et al. 2006). Hooks are primarily set between 100–400 m below the surface, with a median hook depth of 250 m (Boggs 1992; Bigelow et al. 2006). This depth range coincides with the daytime vertical habitat of bigeye tuna; tagging data indicate they spend much of the day 200–400 m below the surface (Boggs 1992; Ward and Myers 2005a; Howell et al. 2010) in waters with a temperature range of 8–14°C (Howell et al. 2010) and oxygen concentrations over 1.0 mL/L (Boggs 1992; Lehodey et al. 2010).

Although bigeye tuna are the target of the deep-set fishery, the catch also includes a number of other species, some of which are also of commercial value. These commercially valuable, non-target species include mahi mahi (*Coryphaena hippurus*), yellowfin tuna (*Thunnus albacares*), striped marlin (*Kajikia audax*), sickle pomfret (*Taractichthys steindachneri*), and opah (*Lampris guttatus*). This fishery also catches but discards several non-commercially valuable species, such as lancetfish (*Alepisaurus ferox*) and snake mackerel (*Gempylus serpens*). Recent studies have noted increased catch rates of these non-commercial species concurrent with declines in the catch rate for the target species. These changes have been attributed to increasing fishing effort (Ward and Myers 2005b; Polovina et al. 2009) and prey release of the often smaller, non-commercial fish as larger target species are removed (Polovina and Woodworth-Jefcoats 2013). These studies support the previous identification that longline fisheries function as a keystone predator in the central North Pacific (Kitchell et al. 2002).

Despite spanning millions of square kilometers, pelagic fisheries have often been examined as a spatial aggregate (e.g., Cox et al. 2002; Kitchell et al. 2002; Sibert et al. 2006).

Previous studies of the Hawaii-based longline fishery, for example, have used spatially averaged trends focused on the core region of the fishery's operating area (12–27°N; Polovina et al. 2009; Polovina and Woodworth-Jefcoats 2013). Shifting spatial patterns in fishing effort and the influence these changes may have on catch in the central North Pacific are under-explored in the primary literature (although see Gilman et al. 2012; Walsh and Brodziak 2015). Additionally, the effect that international competition has had on the movement of the Hawaii-based fleet has not been explored. In this study, we aimed to determine how both the changing spatial footprint of the fishery and oceanographic variability have influenced catch magnitude and composition, the understanding of which is essential for ensuring a sustainable and cost-effective fishery.

4.2 Materials and methods

4.2.1 Materials

We used both logbook and observer records in this study. Logbook data are reported by fishing vessel masters and contain records of all hooks set (time, date, and location) as well as all commercially valuable catch. Observer data cover an average of roughly 17% of the fishing effort in the study period and contain records of all hooks set (time, date, and location) as well as all catch regardless of commercial value. The distribution of observer data correlates well with that of the logbook data (Fig. D.1), and taken together the two data sets provide a robust measure of both effort and catch from 1995 through 2015. Logbook data are complete through 2015 and observer data through 2014. We used all deep-set fishery data, which span the area of 16°S–42°N and 179–120°W. We defined deep sets as those with ≥10 hooks/float (Polovina et al. 2009; Polovina and Woodworth-Jefcoats 2013). Logbook data are collected by the Pacific Islands Fisheries Science Center. Observer data are collected by the Pacific Islands Regional Office.

We used publicly available data for longline effort from the Western and Central Pacific Fisheries Commission (WCPFC) and the Inter-American Tropical Tuna Commission (IATTC) to place Hawaii-based effort in an international context. These data are available at a 5° × 5° horizontal and monthly temporal resolution through 2014. The WCPFC provides data for areas west of 150°W, and the IATTC provides data for areas east of 150°W. This 150°W boundary divides the two fishing convention areas of the Hawaii-based fishery.

Global Ocean Data Assimilation System (GODAS) reanalysis data (Saha et al. 2006) provide modeled monthly temperature at depth across the fishing grounds for the entire period studied. The GODAS data used in this study were provided by the Physical Sciences Division of the NOAA Earth System Research Laboratory in Boulder, Colorado, and downloaded from the Asia Pacific Data Research Center's OPeNDAP server. World Ocean Atlas 2013 (WOA13) data (Garcia et al. 2013) provide a 3-dimensional climatological reference of oxygen concentration. The WOA13 oxygen data were downloaded from the National Centers for Environmental Information's OPeNDAP server. Both the GODAS and WOA13 data sets are based on in situ observations such as those from Argo floats (Saha et al. 2006) and discrete water samples (Garcia et al. 2013).

4.2.2 Methods

All data (fishery and environmental) except those from the WCPFC and IATTC were transformed into a common 1° × 1° grid matching that of the WOA13 data. The GODAS data were changed from their native 0.33° × 1° resolution using nearest coordinate regridding. In this study, we examined data at regional and quarterly resolutions (e.g., quarter one includes January, February, and March).

We assessed several measures of catch magnitude and composition, all in terms of numbers of fish caught as opposed to weight. Catch rates were measured as catch per unit of effort (CPUE), which we defined as the number of fish caught per 1000 hooks set. We focused primarily on catch rates of the target species, bigeye tuna, and the primary bycatch species, lancetfish. Our assessment of catch composition used the 21 most commonly caught species identified by Polovina and Woodworth-Jefcoats (2013). We also followed their method for measuring discard rate (measured as the ratio of catch of lancetfish, snake mackerel, pelagic stingray (*Pteroplatytrygon violacea*), and 95% of sharks to total catch).

We have defined preferred thermal habitat for bigeye tuna as waters with temperatures of 8–14°C. Tagging data from Howell et al. (2010) indicate that when bigeye tuna are at depth during the daytime, which is when the fishery for bigeye tuna operates, they are primarily in waters with this thermal range. The GODAS data were used to determine the minimum, maximum, and median depths of preferred thermal habitat for bigeye tuna in two ways. One,

these depths were determined for all grid cells (each 1° × 1°) with fishing effort at any point in the time series. Two, quarterly GODAS data were weighted by the number of hooks set in each grid cell in each quarter. We then used standard linear regression to evaluate whether there are significant (p<0.05) linear trends in both unweighted and weighted median depths of preferred thermal habitat. Where significant trends were found, we used linear regression to determine how the depth of preferred thermal habitat changed over the years studied.

4.3 Results

4.3.1 Fishing effort

4.3.1.1 Seasonal variability

The Hawaii-based longline fishery exhibits strong seasonal movement during the period studied, 1995–2015. Fig. 4.1A shows the temporally averaged meridional and zonal distribution of effort (number of hooks set) each quarter. Following this distribution, as well as the 150°W boundary between the two fishing convention areas of the Hawaii-based fishing grounds, we divided the fishery into the five regions shown in Fig. 4.1B: northeast (NE), northwest (NW), central west (CW), southwest (SW), and southeast (SE). Together, Figs. 4.1A and 4.2 show the fishery's movement by quarter throughout the year. In the first quarter of the year, most of the effort take place in the SW region north of 10°N and in the CW region. During the second quarter, effort is concentrated in the SW and NW regions. The fishery then undergoes a large geographic shift in the third quarter, with most of its effort set in the NE region. Effort occurs closest to Hawaii in the CW region during the fourth quarter. There was virtually no fishing effort in the SE region; therefore, it was not included in our analysis.

4.3.1.2 Interannual variability

In 1995, nearly all (97.1%) of the Hawaii-based longline effort occurred west of 150°W and south of 26°N in the CW and SW regions. Over time, the fishery has expanded, and in 2015 41.3% of the longline fishing effort was either north of 26°N or east of 150°W in the NW and NE regions. Total effort also increased, with the total number of hooks set increasing steadily from nearly 8.4 million in 1995 to over 47 million in 2015. This increase in fishing effort has

been greatest in the NE region (Fig. 4.2). Time series of total effort in each region and quarter (Fig. 4.2) show that effort increased in the CW and SW regions up until about 2004. After this time, and with the exception of the CW region in the first quarter, effort in these regions has remained roughly stable, while effort in the NW and NE regions has increased steadily.

Fishery expansion is detailed in Fig. 4.2. It shows that, over the past 21 years, the fishery has changed its geographic focus substantially. Across all quarters, the proportion of total annual effort in the CW and SW regions declined by about 1–8%. At the same time, the proportion of total annual effort in both northern regions increased by 2–13%, with a strong maximum in the NE region during the third quarter (13% versus 7%, the next closest value).

4.3.1.3 International competition

The ratio of Hawaii-based effort to international effort varied by region (Fig. D.2). Hawaii-based effort accounted for nearly all effort recorded in the CW region, with little to no competition from international fisheries. For the grid cells in the SW region that had Hawaii-based effort, international fisheries' effort was roughly equal to the effort of the Hawaii-based fishery. However, the ratio of Hawaii-based effort to international effort has increased steadily in the first quarter of the year over the years studied. For grid cells in the NW region with Hawaii-based effort, there was little competition from international fisheries during the second and third quarters. In the first and fourth quarters, the ratio of Hawaii-based effort to international effort has increased over the past decade, and the efforts of the two groups are now roughly equal. With the exception of the first and fourth quarters in the first five years of the time series, there was virtually no international effort in the NE region.

4.3.2 Oceanographic variability

4.3.2.1 Spatial variability

A great deal of spatial variability across the fishing grounds was observed in the median depth and vertical extent of the preferred thermal habitat of bigeye tuna (8–14°C) (Fig. 4.1B). Median thermal habitat depth was at its maximum in the CW region, at about 350–400 m below the surface, and it was shallowest in the NE region where it occurred within about 300 m of the surface. In the SW and NW regions, median thermal habitat depth ranged from 400 m to the

surface at the northernmost latitudes. The full vertical extent of preferred thermal habitat of bigeye tuna also varied by region (Fig. D.3). The extent of this habitat was greatest in the SW and NW regions (depth: 200–450 m), least in the CW region (depth: 300–425 m), and shallowest in the NE region (depth: 200–350 m).

Across the CW and NW regions, as well as much of the NE region, the depth of threshold oxygen concentration (1.0 mL/L) for bigeye tuna was below 500 m. In the SW region, this threshold was shallowest along 10°N (depth: 100–200 m) and progressed to depths below 500 m at the meridional extremes of the region. The oxygen concentration threshold for bigeye tuna was shallowest in the SE region, generally above 500 m and above 100 m along 10°N (Fig. 4.1B).

4.3.2.2 Temporal variability

Across all grid cells where fishing occurred at some point during the time series, the median depth of preferred thermal habitat for bigeye tuna shoaled at a rate of 0.55–0.71 m/year, or by 12–15 m from roughly 280 to 265 m between 1995 and 2015 (Table 4.1). Shoaling was significant and greater when the depths of these temperatures were weighted by total quarterly effort (1.78–3.11 m/year or 37–65 m overall in the second–fourth quarters, shoaling from depths of 320–340 m to depths of 270–315 m; Table 4.1). Significant shoaling within each region is presented in Table 4.1.

We lack sufficient data to examine variability in oxygen concentration over time. However, given that the oxygen concentration threshold of bigeye tuna was found below 500 m across much of the area where the fishery operates, it is unlikely that low oxygen concentrations have affected bigeye tuna in the study area.

4.3.3 Catch variability

4.3.3.1 Catch rates

Annual catch rates of bigeye tuna declined until 2009, but have increased in subsequent years (Fig. 4.3A). Catch rates of lancetfish, on the other hand, have increased over the past two decades, especially after 2004. For the past decade, catch rates of lancetfish have exceeded those of bigeye tuna (Fig. 4.3A).

Quarterly catch rates of bigeye tuna and lancetfish were considerably variable across the four regions of the fishery included in our analysis (Fig. 4.3B). The variability in catch rates of bigeye tuna was most striking in the third quarter, when the rates were notably higher in the NW and NE regions than in the SW and CW regions. Catch rates of lancetfish were highest in the NW region and lowest in the SW region throughout the year. The quarterly and regional catch rates of mahi mahi, skipjack tuna (*Katsuwonus pelamis*), yellowfin tuna, and striped marlin are also presented in Fig. 4.3B. The highest catch rates for these species, with the exception of mahi mahi, generally occurred in the SW and CW regions.

4.3.3.2 Catch composition

The contribution of bigeye tuna to total catch varied by both quarter and region as did the proportion of catch that was discarded (Fig. D.4). In general, bigeye tuna composed nearly 20% of the total catch, although their contribution ranged from as low as 8% (CW region, second and third quarter averages) to over 21% (CW and SW regions, fourth quarter averages). Discard rates had more variability, with the lowest rates in the SW region in the first and second quarters (<30% on average) and the highest rates in the third and fourth quarters across all regions (40–55% on average).

In looking at catch composition, we found that each of the 11 species in Fig. 4.4 accounted for at least 5% of the total annual catch at some point in the time series. Their contribution to total catch is broken down in that figure by quarter for the beginning and end of the time series. These distributions indicate that the seasonal timing of catch of bigeye tuna shifted from the first and fourth quarters to the third and fourth quarters, but that the overall contribution of this species to the annual catch changed little. Conversely, the contribution of lancetfish to total annual catch increased by about 14%, primarily in the third quarter. The proportion of blue shark (*Prionace glauca*), yellowfin tuna, and striped marlin in total annual catch has declined by 4–6% while the proportion of sickle pomfret, snake mackerel, and escolar (*Lepidocybium flavobrunneum*) has risen by 4–6% over the time series.

4.4 Discussion

Over the 21-year period examined in this study, the Hawaii-based longline fishery increased its effort more than five-fold. A growing proportion of this effort occurred in the NE region of the fishing grounds, particularly during the third quarter of the year. The GODAS reanalysis and WOA13 data indicate that oceanographic conditions are favorable for bigeye tuna across much of the fishery's footprint. Although increasing effort should correlate with fisher's desire to catch more fish, the shift in the seasonal and spatial deployment of effort raises several biologically pertinent questions. Why did the spatial footprint of the fishery expand, as opposed to simply setting more hooks across the CW and SW regions? Why did it expand, primarily, into the NE region and only during the third quarter of the year?

The expansion of the fishery into the NE region during the third quarter is likely the result of several factors. One possibility is that the CW and SW regions were already supporting maximum effort. Effort was rather stable in these regions after about 2004 (Fig. 4.2), and previous work has documented that the catch rates of large, high-trophic-level, commercially valuable fish were declining in these waters as a result of increased fishing effort (Polovina et al. 2009; Polovina and Woodworth-Jefcoats 2013). Furthermore, competition from international fisheries may have precluded additional Hawaii-based effort in the SW region. The NW and NE regions, on the other hand, had comparably little Hawaii-based effort and little to no competition from international fisheries.

Specifically during the third quarter, less than 10% of the total annual catch was caught during this portion of the year at the beginning of the time series (Fig. 4.4). Furthermore, in the CW and SW regions, target catch rates were lowest (9% and 14% on average, respectively) and discard rates highest (56% and 44% on average, respectively; Fig. D.4) during the third quarter, possibly explaining why fishers may have been willing to change fishing locations. These low target catch rates may also explain why effort was lowest in the third quarter at the beginning of the time series, and why, unlike in other quarters, effort was not concentrated in a specific region (prior to focus of the fishery on the NE region).

Considering the distribution of fishing effort together with catch rates, we found that trends in catch rates are strongly correlated with the shift in effort location. Comparison of quarterly CPUE of bigeye tuna with the proportion of annual effort in each region and quarter

indicates that the third quarter CPUE of bigeye tuna was strongly correlated with the proportion of effort in the NE region (Pearson correlation coefficient, $r = 0.66$) and negatively correlated with third quarter effort in the CW and SW regions ($r = -0.56$ and -0.46, respectively). No other significant correlations were found ($p<0.5$). Given the above correlations and the trends in catch composition, we conclude that the shift in fishing effort was a response to low target species catch rates in the CW and SW regions during the third quarter. The NE region proved to be a particularly efficient fishing ground with high catch rates of target species, relatively low discard rates, and little competition from international fishing fleets. As a result, a large portion of annual catch of bigeye tuna occurred in the third quarter by the end of the time series (Fig. 4.4).

Although the fishery's movement toward the NE region was greatest in the third quarter, the fishery does operate in this region throughout the year, if to a lesser degree (Fig. 4.2). As discussed above, catch rates of target species in the SW and CW regions were generally higher during the rest of the year, possibly explaining why there was less fleet movement outside the third quarter.

4.4.1 The role of oceanographic variability in fishery expansion

The enhanced fishery yield in the NE region can be explained by the region's oceanography. It has the largest area in which preferred thermal habitat for bigeye tuna closely overlaps vertically with both deep-set hooks (100–400 m) and waters with suitable oxygen concentrations (>1.0 mL/L; Fig. 4.1B). The time series of the depths of preferred thermal habitat show that in the NE region, the preferred daytime habitat of bigeye tuna was consistently and completely within the depth range of deep-set hooks (Fig. D.3). Oceanographic variability also explains why the fishery did not expand into the SE region. This region encompasses the eastern tropical Pacific's oxygen minimum zone. Across much of the SE region, the oxygen concentration threshold of 1.0 mL/L occurred at depths shallower than the depths of both bigeye tuna's preferred thermal habitat and deep-set gear (Fig. 4.1B), rendering it poor habitat for bigeye tuna and poor longline fishing grounds.

Effort-weighted trends in the depth of preferred habitat of bigeye tuna indicate the fishery's movement into the NE region's more favorable oceanographic conditions. At the

beginning of the time series, the fishery was operating largely in waters where the median depth of preferred thermal habitat for bigeye tuna was roughly 320–340 m below the surface. However, by the end of the time series, the fishery was operating in waters where the median depth of preferred thermal habitat was 270–315 m below the surface and more closely aligned with the median depth of deep-set gear (250 m; Boggs 1992; Bigelow et al. 2006). These trends in effort-weighted depth of preferred thermal habitat indicate that fishers were either targeting regions where preferred thermal habitat is more closely aligned with their gear or where thermal habitat shoaling was greatest (or employing a combination of these two tactics). Across the entire fishing ground, the preferred thermal habitat of bigeye tuna shoaled by only about 12–15 m. Yet, when weighted by quarterly effort, the shoaling increased to roughly 37–65 m. Without information on depth of capture, it is difficult to determine the degree to which this shoaling actually influenced the fishery's yield. However, given the vertical distributions of both deep-set gear and preferred daytime thermal habitat of bigeye tuna, shoaling could increase the degree to which these overlap. It could also compress the total vertical habitat that bigeye tuna occupied. Both scenarios would increase the catchability of bigeye tuna, and in turn, the fishery's yield.

4.4.2 Effects of fishery expansion on catch composition

During the period studied, the spatial expansion and seasonal shift of the fishery influenced the seasonal timing of both the catch and catch composition. Although the fishery's primary target species, bigeye tuna, consistently was about 20% of the total annual catch, the bulk of the annual catch shifted from the first and fourth quarters to the third and fourth quarters. A combination of factors could have contributed to this shift. The foremost factor was the increase in effort deployed in the NE region during the third quarter (Fig. 4.2), where catch rates of bigeye tuna were consistently high over time (Fig. 4.3B). Additionally, by the end of the period examined, less effort was deployed in the SW region in the first quarter than in the CW region during the fourth quarter (Fig. 4.2). First quarter catch rates of bigeye tuna in the SW region declined over the past two decades (Fig. 4.3B), whereas fourth quarter catch rates of bigeye tuna in the CW region remained consistently high. In summary, by 2015, the fishery deployed most of its effort in the regions and quarters where catch rates of bigeye tuna are highest. It is interesting to note that these regions are also those where preferred thermal habitat

for bigeye tuna completely overlaps with deep-set gear (NE region) and where preferred thermal habitat for bigeye tuna is most compressed (CW region) (Fig. D.3).

It is possible that the shift in when and where the bulk of the year's bigeye tuna were caught can be attributed to changes in fishing gear, although we found no evidence that this was the cause. Using the number of hooks per float as a proxy for hook depth, we found no significant differences between gear set in the SW region in the first quarter, in the NE region in the third quarter, and in the CW region in the fourth quarter (5% significance level, Wilcoxon–Mann–Whitney rank-sum tests).

The shift in the annual timing of catch of bigeye tuna could also be attributed to fish movement or changes in population dynamics. Stock assessments from both fishing convention areas (west of 150°W, WCPFC, Harley et al. 2014; east of 150°W, IATTC, Aires-da-Silva and Maunder 2015), along with tagging data (Schaefer et al. 2015), indicate that there is extensive zonal movement by bigeye tuna. At low latitudes (e.g., 15°S–15°N), there is more eastward movement than westward movement (Aires-da-Silva and Maunder 2015; Schaefer et al. 2015). However, a lack of tagging data for areas farther north makes it difficult to determine whether bigeye tuna make the same directional movement in our study area. If they do, the high catch rates in the NE region noted in our study may have been fueled in part by fish moving into the region. The role of population dynamics is also unclear. Although it is likely that large-scale population dynamics impact interannual changes in CPUE of bigeye tuna (Harley et al. 2014; Aires-da-Silva and Maunder 2015), size structure (and presumably age structure) of bigeye tuna was fairly consistent across the fishing ground (Fig. D.5), echoing earlier work (Kume 1969).

For other commercially valuable species, such as yellowfin tuna and striped marlin, the spatial shift in effort exacerbated declining catch rates. Although CPUEs for both species declined across the fishing grounds, catch rates for these species were greatest in the SW and CW regions despite the movement of the fishery away from these regions (Fig. 4.3B). Catch rates for skipjack tuna, although not declining, were generally highest in the SW and CW regions (Fig. 4.3B). Therefore, the fishery's changing footprint likely contributed to an overall decline in the contribution of skipjack tuna to total annual catch (Fig. 4.4).

Discard rates also were influenced by the spatiotemporal shift in effort. In the core region of the fishery (12–27°N), rising discard rates were linked to increased fishing effort

(Polovina and Woodworth-Jefcoats 2013). At the same time, catch rates of lancetfish in particular rose as a result of the fishery's northward expansion and increased focus on the third quarter. Catch rates of lancetfish were not only highest in the NW region but also highest within-region in the third quarter (Fig. 4.3B). Therefore, the fishery deployed more effort in a region where lancetfish were more commonly caught and during the season when catch rates were highest. As a result, catch of lancetfish, all of which was discarded, has exceeded catch of target species for the past decade (Fig. 4.3A). The same spatiotemporal shift in effort also explains the change in the contribution of mahi mahi to annual catch (Figs. 4.3B and 4.4), although mahi mahi are retained by the fishery and sold.

As with bigeye tuna, it is possible that both fish movement and population dynamics could have influenced changes in total composition of the catch. Tagging data and stock assessments are lacking for many of the species caught by the Hawaii-based longline fishery, especially the non-commercial species. Future work examining the seasonal timing, location, and size structure of this catch may provide insight into such questions.

When using observer data to determine catch composition as we did, there is a possibility that observer error could influence results. Such errors in the reporting of rare or cryptic species have been noted for individual longline sets and they can influence results at fine spatiotemporal resolutions (e.g., months and single degrees) and when observer coverage is low (Walsh et al. 2002; Walsh et al. 2005). However, it's not clear that such errors would be distinguishable when observer data are aggregated more broadly, such as on a quarterly and regionally basis. Additionally, our results indicate strong agreement between observer and logbook reported catch rates of bigeye tuna (Fig. 4.3A) and, thus, consistent species identification of target species. The observed increase in catch of lancetfish is corroborated by the fishery's regional expansion: catch rates of lancetfish were much higher in the NW region than elsewhere (Fig. 4.3B), and, in the early years of our study, the fishery was not operating in the NW region (Fig. 4.2A). Therefore, we conclude that the impacts of fishery expansion on catch composition are robust.

4.4.3 A look ahead

We have detailed how both fishery expansion and oceanographic variability have influenced catch of the Hawaii-based longline fishery. In particular, we found that the fishery

has expanded into a region that has proven to be an efficient fishing ground by virtue of its local oceanography. With this perspective on past catch, can the fishery expect CPUEs to continue to rise into the future? Likely not. The results of previous work indicate that sustained increases in fishing effort drive down the abundance of large, high-trophic-level fish, such as those targeted by the Hawaii-based longline fishery (Ward and Myers 2005b; Polovina et al. 2009; Polovina and Woodworth-Jefcoats 2013). We also note that, although bigeye tuna are not considered to be subject to overfishing in the NE region (Aires-da-Silva and Maunder 2015), overfishing of bigeye tuna is documented to be occurring in the three western regions (Harley et al. 2014). This disparity creates the potential for further eastward displacement of fishing effort (both Hawaii-based and international) and hastening removals of bigeye tuna. Therefore, it is possible that catch rates in the NE region will eventually diminish as did the catch rates in the SW and CW regions over the past 20 years.

Another change that will affect the fishery in coming years is the recent expansion of the Papahānaumokuākea Marine National Monument. In August 2016, the monument boundaries were expanded to encompass the full U. S. exclusive economic zone west of 163°W, moving the boundaries an additional 150 nm from land (Federal Register 2016). This expansion bars commercial fishing over a portion of the fishing grounds, with the greatest impact on the CW region. On average, 21% of the effort in the CW region in the fourth quarter (when fishing effort in this region is the greatest) and 25% of the bigeye tuna caught in the CW region during the fourth quarter are from waters that will now be off limits to the fishery. It is uncertain how the fishery will adjust, possibly by simply relocating fourth quarter effort outside the monument or by shifting the allocation of that effort to another quarter or region.

Finally, climate change can be expected to impact the Hawaii-based longline fishery in a number of ways, potentially driving productive fishing grounds even farther from Hawaii. As ocean temperatures continue to rise, the preferred thermal habitat of bigeye tuna will be displaced northward (Lehodey et al. 2010; Bopp et al. 2013; Woodworth-Jefcoats et al. 2017). Additionally, the oxygen minimum zone that covers much of the SE region (Fig. 4.1B) has expanded over the past 50 years (Stramma et al. 2008). Although climate projections of further expansion are mixed (Stramma et al. 2008; Bopp et al. 2013; Cabré et al. 2015a), continued

expansion potentially would encroach on the NE region and render a larger portion of the SW region inhospitable to bigeye tuna.

We have shown how the Hawaii-based longline fishery's own movement, particularly its seasonally focused expansion to the NE region, has helped shape the composition, magnitude, and seasonal timing of its catch. This information, together with previous studies of the fishery's impact on the ecosystem, future climate projections, and socioeconomic data such as trip cost and catch value, has the potential to help guide future fishery management actions. For example, recent increases in CPUE of bigeye tuna can be placed in the context of the high catch rates the fishery saw in the late 1990s. Climate models could be used to project future changes to bigeye tuna's habitat. Additionally, the impact of the fishery's continued expansion away from Hawaii can be assessed in relation to other factors, such as future fuel prices. Such context and analyses can help fishery managers ensure that the Hawaii-based longline fishery remains both ecologically and financially sustainable.

Table 4.1. Significant linear trends (P<0.05) in the median depth of the preferred thermal habitat of bigeye tuna (*Thunnus obesus*) (8–14 °C) based on logbook records of the Hawaii-based longline fishery and ocean temperatures obtained from the Global Ocean Data Assimilation System for 1995 through 2015. These records were transformed into a grid, and the values in this table were determined by using all grid cells with fishing effort at any time (any effort) and by weighting grid cells by total quarterly effort (effort-weighted). A dash denotes the lack of a significant trend. Each trend value is followed by the depth for 2005 from the linear regression or, in the absence of a significant trend, by the mean depth of the time series. Results are presented for the full fishing ground, as well as for the northeast (NE), northwest (NW), central west (CW), and southwest (SW) regions individually.

		Any effort		Effort weighted	
Region	Quarter	Trend (m/yr)	Depth (m)	Trend (m/yr)	Depth (m)
NE	Q1	−1.36	255.46	–	302.59
	Q2	−1.38	256.66	–	301.29
	Q3	−1.17	254.00	−2.64	291.71
	Q4	−0.96	251.55	–	292.45
NW	Q1	–	264.21	–	346.42
	Q2	–	263.20	−3.49	328.70
	Q3	–	262.85	−3.69	290.24
	Q4	–	262.92	−1.71	336.40
CW	Q1	−1.52	367.35	−0.85	358.42
	Q2	−1.64	369.48	−1.15	357.56
	Q3	−1.76	365.06	−1.63	352.98
	Q4	−1.75	361.89	−2.07	348.46
SW	Q1	–	265.83	–	292.62
	Q2	–	265.43	−1.47	292.82
	Q3	−0.48	266.78	–	302.72
	Q4	−0.69	264.76	−2.14	320.98
Full fishing ground	Q1	−0.55	272.21	–	319.58
	Q2	−0.71	272.67	−1.78	303.25
	Q3	−0.63	271.92	−3.11	300.54
	Q4	−0.70	269.91	−2.23	336.08

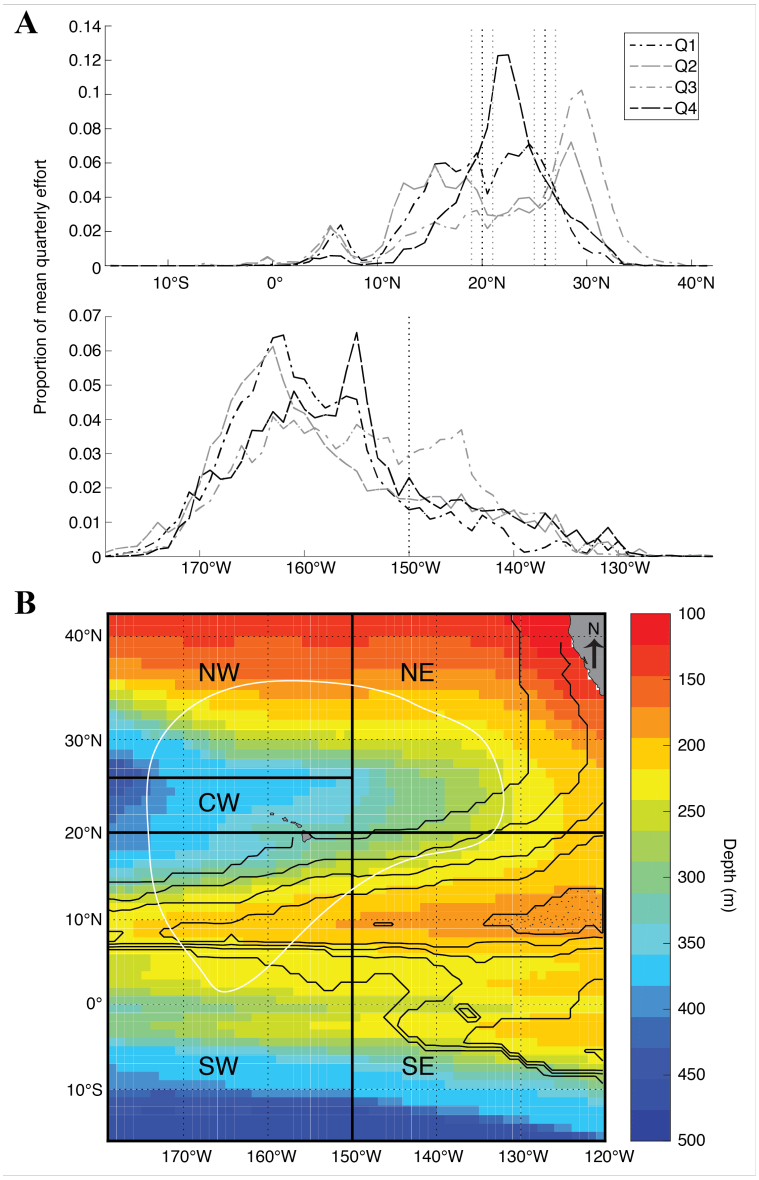

Figure 4.1 (A) The meridional (top) and zonal (bottom) distributions of quarterly effort of the Hawaii-based longline fishery, averaged across the full time series (1995–2015). Dashed black vertical lines are drawn at 20°N and 26°N (top) and at 150°W (bottom) and delineate the divides between the SE and NE regions and the SW, CW, and NW regions, and dashed gray lines are drawn at ±1° for comparison of alternate options (top). (B) Illustration of the five regions by which the Hawaii-based longline fishery was examined overlaid on the climatological (1995–2015) median depth of preferred thermal habitat of bigeye tuna (*Thunnus obesus*) (8–14°C) obtained from Global Ocean Data Assimilation System (shaded) and the depth of the 1.0 mL/L oxygen-concentration threshold from World Ocean Atlas 2013 data (contoured every 100 m from 100 to 500 m, with stippling where the depth is less than 100 m). The white line in panel B encompasses grid cells with fishing effort from at least 3 vessels over the full time series. Effort in panel A is from logbook data.

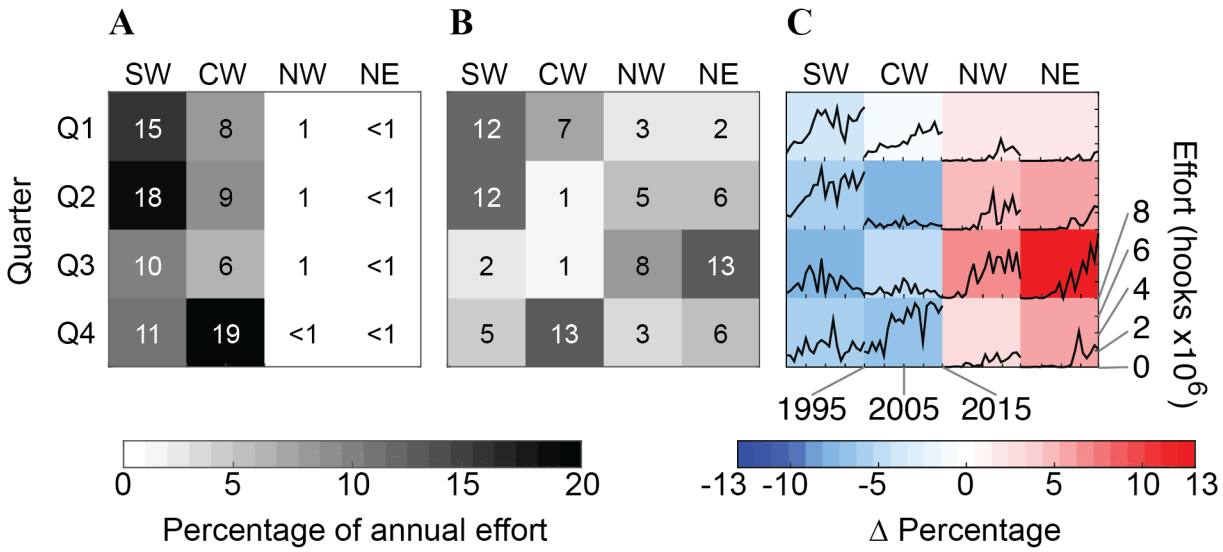

Figure 4.2 The mean percentages of total annual effort that occurred in each quarter and region at the (A) beginning (1995–1997) and (B) end (2013–2015) of the time series from logbook data examined in this study of the Hawaii-based longline fishery. (C) The change in the percentage of total annual effort that occurred in each quarter and region is shaded in color and overlaid with the total annual effort set in each region and quarter in black. Four regions were used in these analyses: southwest (SW), central west (CW), northwest (NW), and northeast (NE).

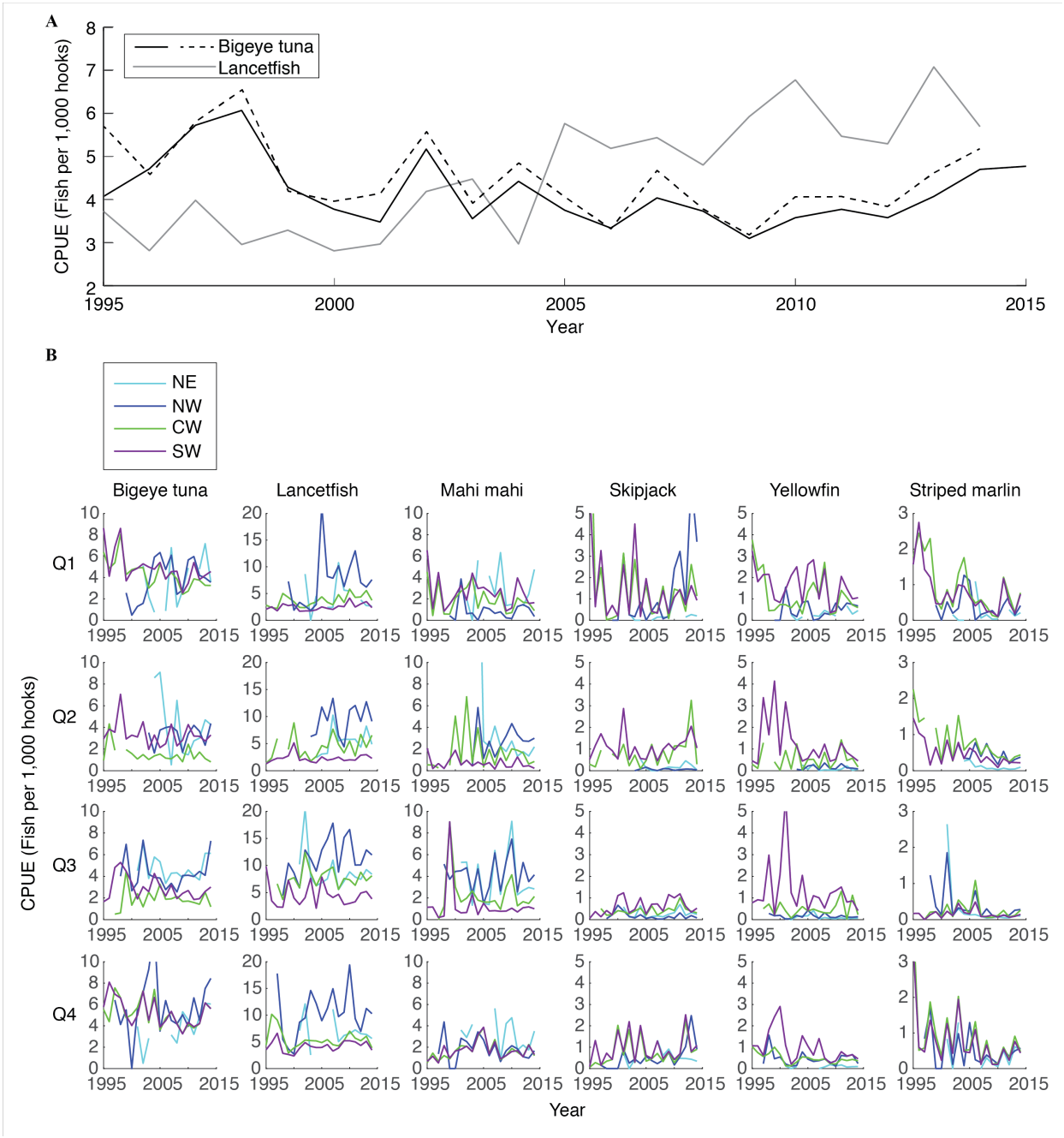

Figure 4.3 (A) Annual catch per unit of effort (CPUE) for bigeye tuna (*Thunnus obesus*; black lines) and lancetfish (*Alepisaurus ferox*; gray line) for the Hawaii-based longline fishery from 1995 through 2015. The CPUE for bigeye tuna was calculated from both logbook records (solid black line), which are complete through 2015, and observer records (dashed black line), which are complete through 2014. The CPUE of lancetfish was calculated from observer records. (B) Quarterly and regional CPUE, based on observer data, of bigeye tuna; lancetfish; mahi mahi (*Coryphaena hippurus*); skipjack tuna (*Katsuwonus pelamis*), yellowfin tuna (*Thunnus albacares*), and striped marlin (*Kajikia audax*). Note that the scales of the y-axes vary by species.

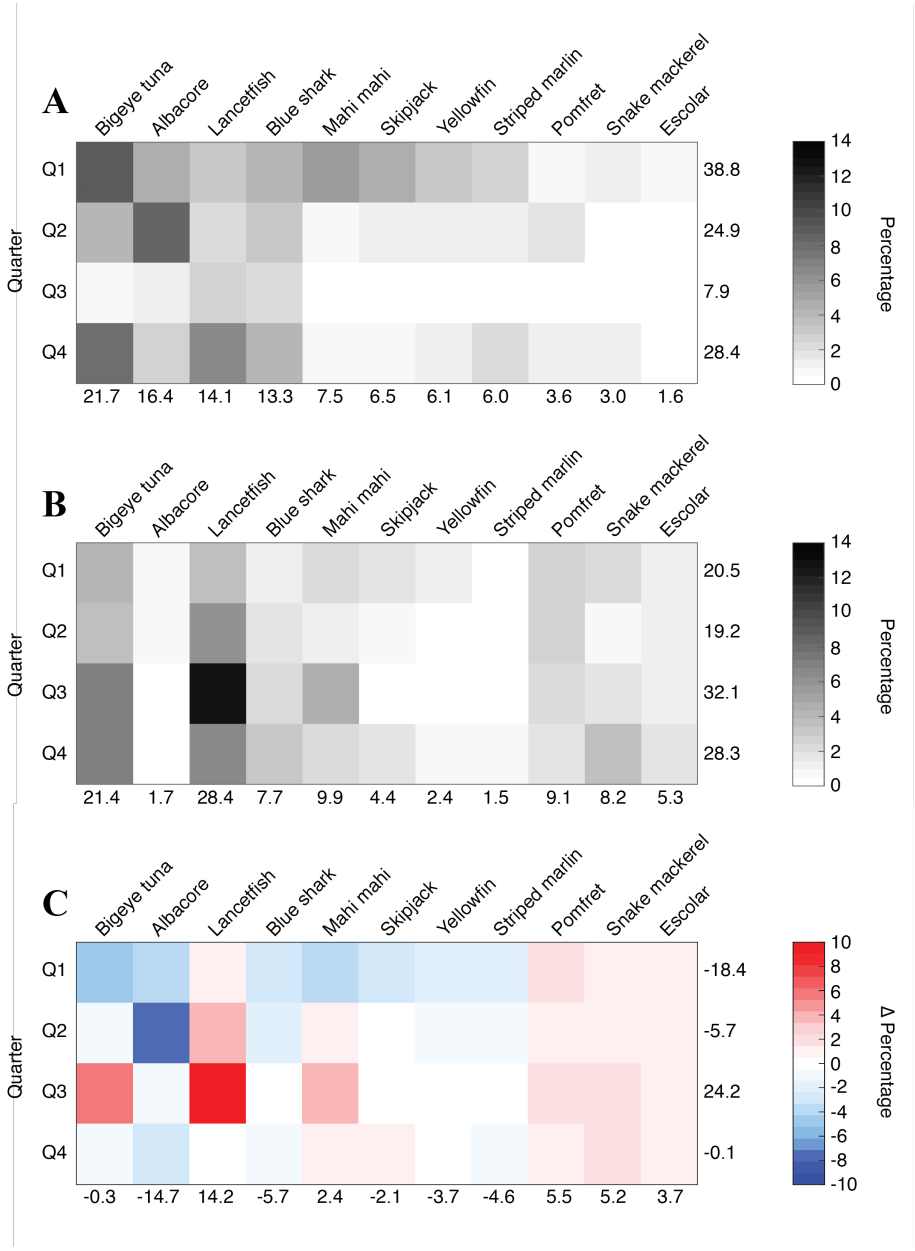

Figure 4.4 The mean percentages of total annual catch of the Hawaii-based longline fishery to which 11 species contributed each quarter, shaded for (A) the beginning (1995–1997) and (B) the end (2012–2014) of the time series of observer data, and (C) the differences between these percentages. The species were the following: bigeye tuna (*Thunnus obesus*), albacore (*Thunnus alalunga*), lancetfish (*Alepisaurus ferox*), blue shark (*Prionace glauca*); mahi mahi (*Coryphaena hippurus*), skipjack tuna (*Katsuwonus pelamis*), yellowfin tuna (*Thunnus albacares*), striped marlin (*Kajikia audax*), sickle pomfret (*Taractichthys steindachneri*), snake mackerel (*Gempylus serpens*), and escolar *(Lepidocybium flavobrunneum*). In graphs A and B, the total annual contribution of each species is listed below each column, and the total annual contribution from each quarter is listed along the right-hand side of each row. In graph C, the difference in total annual contribution is listed below each column and along each row.

CHAPTER 5

Relative impacts of simultaneous stressors on a pelagic marine ecosystem

Climate change and fishing are two of the greatest anthropogenic stressors on marine ecosystems. We investigate the effects of these stressors on Hawaii's deep-set longline fishery for bigeye tuna (*Thunnus obesus*) and the ecosystem which supports it using a size-based food web model that incorporates individual species and captures the metabolic effects of rising ocean temperatures. We find that when fishing and climate change are examined individually, fishing is the greater stressor. This suggests that proactive fisheries management could be a particularly effective tool for mitigating anthropogenic stressors either by balancing or outweighing climate effects. However, modeling these stressors jointly shows that even large management changes cannot completely offset climate effects. Furthermore, when climate change and fishing are considered together, their effects are to some degree synergistic. Our results suggest that a decline in Hawaii's longline fishery yield may be inevitable. The effect of climate change on the ecosystem depends primarily upon the intensity of fishing mortality. Management measures which take this into account can both minimize fishery decline and support at least some level of ecosystem resilience.

Based on: Woodworth-Jefcoats PA, Blanchard JL, Drazen JC, 2019: Relative impacts of simultaneous stressors on a pelagic marine ecosystem. Frontiers in Marine Science, In Review.

5.1 Introduction

Climate change and fishing are two of the greatest anthropogenic stressors on marine ecosystems and commercial fisheries. Additionally, these stressors are impacting marine systems simultaneously, potentially exacerbating one another. Given that current carbon emissions are outpacing the most emission-heavy scenario being used in climate models (RCP8.5; Riahi et al. 2011) and that a growing human population derives nearly one-sixth of its animal protein from the sea (Pentz et al. 2018), it is imperative that we understand the effects of these joint stressors now and in the future (Perry et al. 2010). Furthermore, we need to do so in an ecosystem context in order to understand the full ramifications of these stressors' effects (e.g., Pikitch et al. 2004; Brander 2007). In this study, we examine the effects of climate change and fishing on Hawaii's longline fishery for bigeye tuna (*Thunnus obesus*) and its supporting ecosystem. This fishery operates largely outside the United States exclusive economic zone (EEZ), extending from equatorial waters to the northern limits of the North Pacific subtropical gyre (35–40°N) and from the dateline to the outer limits of the California Current region (roughly 125°W), excluding the eastern tropical Pacific's oxygen minimum zone (Fig. 5.1). Yet, a sizeable portion of the fishery operates in waters with little to no international competition (Woodworth-Jefcoats et al. 2018). This means that local management measures have the potential to effect broad ecosystem change. Additionally, Honolulu ranks 6th among United States commercial fishing ports in terms of the value of fish landed ($106 million; NMFS 2017) and over half the nation's tuna landings are from this fishery (NMFS 2018). These factors create a strong incentive to ensure the fishery's future ecological and economic viability.

Commercial fishing has reduced the abundance of large high-trophic level predators in this ecosystem by over 20% (Ward and Myers 2005b) and at the same time has led to increasing catch rates of smaller mesopredator species (Polovina et al. 2009). Modeling studies have replicated these historical observations using both species-based (Cox et al. 2002; Kitchell et al. 2002) and size-based (Polovina and Woodworth-Jefcoats 2013) models. Similar modeling approaches have projected future effects of fishing and/or climate change over the 21st century. These approaches range from highly specific single species models (Lehodey et al. 2010, 2013; Del Raye and Weng 2015) to multi-species ecosystem (Howell et al. 2013; Woodworth-Jefcoats et al. 2015) and dynamic bioclimate envelope (Cheung et al. 2010) models to size-based

approaches without species-level resolution (Woodworth-Jefcoats et al. 2013, 2015; Lefort et al. 2015). Collectively, they suggest climate-driven declines in food availability may reduce fish body size (Lefort et al. 2015; Woodworth-Jefcoats et al. 2015) and biomass (Howell et al. 2013; Lefort et al. 2015; Woodworth-Jefcoats et al. 2015), as well as future fishery yields (Howell et al. 2013; Woodworth-Jefcoats et al. 2015). The location of spawning and fishing grounds may also change with climate change (Cheung et al. 2010; Lehodey et al. 2010, 2013). A number of these studies included the effects of increasing temperatures. Multi-species or species-blind approaches relied on statistical relationships (Cheung et al. 2010) or monotonically increasing costs of metabolism (Woodworth-Jefcoats et al. 2013), while species-specific models were able to incorporate more complex temperature effects. These include linking spawning to ocean temperature (Lehodey et al. 2010, 2013) and incorporating temperature into physiological rates (Lefort et al. 2015).

Despite the array of approaches discussed above, there has not been, to our knowledge, a multi-species approach that includes both size and species resolution as well as the physiological effects of rising ocean temperatures. In this study, we use a food web model that integrates both size and species. This approach allows us to examine species-specific change in terms of biomass, abundance, and size structure. The model also incorporates temperature's effects on metabolism as well as aerobic scope, providing more realistic future projections. Aerobic performance is closely linked to temperature (e.g., Pörtner and Peck 2010; Pörtner 2012) and affects fishes' ability to forage. Our simulations include climate change's effects on two variables which most directly affect fishes' fitness: food supply, via changes to the plankton community, and temperature. We also examine a range of future fishing scenarios. Our results offer insight into the simultaneous effects of these stressors, and the modeling framework we developed offers a new tool for supporting strategic management decision-making in this and other regions.

5.2 Material and methods

5.2.1 Model

We developed the size-based food web model *therMizer*, which is a modification of *mizer*, a well-documented multi-species size spectrum model (Blanchard et al. 2014; Scott et al.

2014). Such models describe predation, mortality, reproduction, and physiological processes at the individual level and scale them up to population and community levels (Blanchard et al. 2017). They track the flow of biomass through fully resolved body size classes (size measured in mass) via growth and size-based predation (Blanchard et al. 2017). In *mizer*, the smallest fish size classes feed upon a background resource size spectrum that exhibits semi-chemostat growth dynamics (Blanchard et al. 2014; Scott et al. 2014). Our model *therMizer* contains two key modifications from *mizer*. The primary modification is incorporating the effect of ocean temperature on metabolic scope. Temperature dependencies are absent in *mizer*. We also replace *mizer*'s semi-chemostat background resource with a resource that is input at each time step.

The effect of temperature on metabolic scope is determined by including temperature's effect on both metabolic rate and prey encounter rate. This is incorporated into the model by scaling both rates as described below and illustrated in Fig. 5.2. In all cases, temperature is averaged over each species' depth range.

As temperature increases, metabolic rate increases. To capture this relationship, we model temperature's effect on metabolic rate, *TEM*, following equation 5.1:

$$TEM = e^{25.22-\frac{E}{kT}} \qquad (5.1)$$

where T is vertically averaged temperature in Kelvin, k is Boltzmann's constant (8.62×10^{-5} eV K^{-1}), and E is activation energy (0.63 eV; Brown et al. 2004; Jennings et al. 2008). *TEM* is then scaled to *TEM′*, a value ranging from 0 to 1, following equation 5.2:

$$TEM' = (TEM - Min_{sp}) / R_{sp} \qquad (5.2)$$

where Min_{sp} and R_{sp} are the minimum value and range, respectively, of *TEM* for each species (Fig. 5.2). *TEM′* is then used as a multiplier for standard metabolic rate. This has the effect of standard metabolic rate being at its minimum at the lower limit of a species' thermal range and at its maximum at the upper limit of a species' thermal range.

We incorporate temperature into prey encounter rate to capture the effect of temperature on movement via aerobic scope (*sensu* Pörtner and Peck 2010). The effect of temperature on encounter rate, *TER*, is modeled using a generic polynomial rate equation (van der Heide et al. 2006):

$$TER = T(T - T_{min})(T_{max} - T) \qquad (5.3)$$

where T is vertically averaged temperature, T_{min} is a species' minimum thermal tolerance, and T_{max} is a species' maximum thermal tolerance (Fig. 5.2). All temperatures in equation 5.3 are in °C. TER is then scaled to TER', a value ranging from 0 to 1, by dividing by Max_{sp}, the maximum value of TER for each species (Fig. 5.2). TER' is then used as a multiplier for encounter rate. This has the effect of species being able to realize peak aerobic performance and encounter the maximum amount of prey possible when they are at their optimal temperature. Foraging success declines to either side of this temperature.

The joint effects of temperature on metabolic rate and prey encounter rate (TEM' and TER', respectively) are shown in Fig. 5.3. At temperatures outside species' thermal range, both TEM' and TER' are set to 0 representing local extinction. Species' thermal and vertical ranges are listed in Table 5.1.

5.2.2 Model parameters and input

We attempted to include as many species as possible of the top 20 species caught by the Hawaii deep-set longline fishery, regardless of species' commercial value. The 12 species listed in Table 5.1 are those for which there was sufficient life history and thermal tolerance information available to parameterize the model. Together, these species account for 76% of the fishery's observed catch.

5.2.2.1 Parameters and calibration

Global model parameters are left unchanged from the default *mizer* settings (Blanchard et al. 2014; Scott et al. 2014), with the exception of κ which we set at 10^{12}. This variable is used in determining species' initial size spectra (Blanchard et al. 2014). Also as in Blanchard et al. (2014), all teleosts enter the model as larvae weighing 1 mg. Blue sharks enter at 354 g, an average of mean male and female birth weights (344g and 362 g, respectively; Shark Working Group Report 2017). The additional species-specific parameters are listed in Table 5.1. Values in Table 5.1 are taken from the literature as noted, with the exception of the Brody growth coefficient, k_{vb}, for lancetfish. Estimates of this parameter for lancetfish are not available in the literature. Based on available values for similar species (Morales-Nin and Sena-Carvalho 1996;

Lorenzo and Pajuelo 1999; Harada and Ozawa 2003; Figueiredo et al. 2015; Froese and Pauly 2017), we use the median value of the lower quartile of teleost k_{vb} values.

Predation in *therMizer* is both species- and size- specific. All fish have a log-normal prey size preference that is dependent upon predator body size, species' predator-prey mass ratio (100 for teleosts, Blanchard et al. 2014; 400 for blue sharks, Barnes et al. 2008), and the width of the prey selection window (1 for all species, Blanchard et al. 2014). Prey selection is further informed by the interaction matrix (Table E.1). Interaction, θ_{ij}, between species i and j ranges from 0 to 1. Previous size spectrum models have determined the interaction matrix values based on horizontal overlap as inferred from bottom trawl surveys (Blanchard et al. 2014; Reum et al. 2019). Here, we determine interaction based on species' vertical overlap following equations 5.4 and 5.5 and illustrated in Fig. 5.4:

$$\theta_{ij} = D_{ij}^2 / D_i D_j \qquad (5.4)$$

$$D_{ij} = a - (a - b) - c \qquad (5.5)$$

where D_i and D_j are the depth ranges of species i and j, respectively; D_{ij} is the range of overlapping depths for species i and j; and a is the greater maximum depth, b is the lesser maximum depth, and c is the greater minimum depth for the pair of species i and j. All species have a minimum depth of 0 m, with the exception of opah which has a minimum depth of 50 m (Polovina et al. 2008). For all species pairs, the interaction matrix determines the proportion of total prey biomass of the appropriate size that is available to the predator.

Fishing mortality increases linearly from 0 to F over a size range unique to each species. Fishing mortality is phased in over a range of body sizes to account for longline gear's inefficiency in catching smaller body sizes (Polovina and Woodworth-Jefcoats 2013). To establish these sizes, we use time-averaged (2006 – 2016, pooled) catch records from the Pacific Islands Region Observer Program, which since 2006 has recorded the size of every third fish caught by Hawaii's longline bigeye tuna fleet. Roughly 20% of this fishery's effort is observed, and observer records have been found to correlate well with vessel logbooks (Woodworth-Jefcoats et al. 2018). We bin observed sizes of fish caught into equally spaced logarithmic size classes as in *therMizer* (Scott et al. 2014; Edwards et al. 2017). Each species is initially susceptible to fishing mortality at the size which contributes at least 1% toward that species' total observed catch. Fish are fully susceptible to fishing mortality at the size which contributed the

most to that species' total catch. The sizes at which each species is first and then fully susceptible to fishing mortality are listed in Table 5.1.

5.2.2.2 Climate forcing variables

We use output from a suite of earth system models included in the 5th phase of the Coupled Model Intercomparison Project (CMIP5; Taylor et al. 2012; Table E.2). Phyto- and zooplankton densities (Fig. 5.5) are vertically integrated over the upper 200 m of the water column. Numerical abundance within each size class is determined by dividing density by mean size. Plankton size spectra are created as linear fits to log-transformed abundances and sizes. Model-specific plankton size classes are listed in Table E.2.

As with the original *mizer* model, some calibration of the background resource was required (Blanchard et al. 2014). To this end, we compared the above described plankton spectra with the background spectrum generated by the semi-chemostat resource model to determine appropriate scaling for the slope (×1.2) and intercept (×0.8) of the CMIP5-generated plankton spectra. These scaled spectra were extended to *therMizer*'s full size range to determine the background resource at each time step. Initial spectra for individual fish species are determined as in the original *mizer* model (Scott et al. 2014).

Ocean temperature for each species is determined by averaging across each species' depth range. Initial temperatures are from World Ocean Atlas 2013 v2 data (Locarnini et al. 2013). Temperature changes from the CMIP5 models are then applied to these initial temperatures. This approach accounts for potential bias in the CMIP5 models.

Model input plankton densities are summed and temperatures averaged over the footprint of the Hawaii-based deep-set longline fishery targeting bigeye tuna: 0°–40°N from 180°–150°W and 15°–36°N from 150°–125°W (Fig. 5.1; Woodworth-Jefcoats et al. 2018).

5.2.3 Model verification

Model output from a run forced with a static climate (1986–2005 mean) and constant fishing mortality ($F = 0.2$) was compared to time-averaged records of observed catch (see description of the observer data above). Observed sizes were binned as in *therMizer* to create

size spectra of catch. Modeled and observed catch size spectra were well correlated, with Pearson's correlation coefficient, *r*, ranging from 0.39 to 0.85 (Fig. F.1).

5.2.4 Scenarios modeled

We evaluated the individual and joint effects of climate change and fishing on the ecosystem and on fishery catch. In all scenarios, the model was run for 600 years with a static climate (1986–2005 mean) and constant fishing mortality ($F = 0.2$) to account for spin-up effects. Projections run from 2006 through 2100. To assess the impact of climate change alone, we held fishing mortality constant at $F = 0.2$. To assess the impact of fishing alone, we use a static climate scenario. In all cases where a variable is held static, we hold the spin-up value constant over the 21st century.

We examine four scenarios in which fishing mortality changes linearly over the projection period (2006–2100): doubling from $F = 0.2$ to 0.4, increasing five-fold to 1, halving to 0.1, and declining to one fifth or 0.04 (hereafter referred to as 2F, 5F, 0.5F, and 0.2F, respectively). These scenarios were chosen based in part on trends in effort of Hawaii's deep-set longline fishery. Over the logbook record, effort has risen more than five-fold from 8.4 million hooks set in 1995 to over 47 million hooks set in 2015 (Woodworth-Jefcoats et al. 2018). Fishing effort does not translate equally to fishing mortality, and therefore we consider 5F to be a fairly aggressive future fishing scenario. We also consider the effect of fishing mortality doubling (2F) as a more moderate scenario. We simply use the reciprocals of the fishing increase scenarios to model a decline in fishing mortality. This facilitates scenario comparison. To further facilitate scenario comparison, we use the same value of *F* for all species. This approach eliminates potential confounding influences of fishing different species at different levels of intensity and replicates observed catch reasonably well (see discussion of model verification above). However, we note that *therMizer* is capable of incorporating species-specific *F* values (Scott et al. 2014).

We evaluate several measures of ecosystem structure and fishery performance. Total biomass and abundance provide species-specific measures of the fishery's catch and its relation to the ecosystem. We refer to ecosystem biomass as "biomass" and catch in weight as "yield". The large fish indicator (LFI; Blanchard et al. 2014) is a broad measure of the numerical

proportion of fish ≥ 15 kg (Polovina and Woodworth-Jefcoats 2013; Woodworth-Jefcoats et al. 2015). The LFI provides insight into both the size structure of the ecosystem as well as the potential value of fish catch, as larger fish are generally more valuable. As a complementary measure to the LFI, we also examine the change in species' mean size.

We assess these measures both through time series over the projection period as well as with 20-year averages in an effort to minimize the confounding influence of interannual variability. We average results over three 20-year time periods to capture the beginning, middle, and end of the 21st century: 1986–2005, 2041–2060, and 2081–2100 (hereafter referred to as 2000, 2050, and 2100, respectively). The 1986–2005 average corresponds to the equilibrium value at the start of the *therMizer* projections.

5.3 Results

We find that, taken as individual stressors, climate change and increasing fishing mortality act to reduce fish biomass and size across all species. The effects of reduced fishing mortality are generally of the opposite sign. However, when modeled jointly, there were no scenarios in which yield increased. Results for the ecosystem supporting the fishery are slightly more optimistic, with reduced fishing mortality somewhat offsetting the negative effects of climate change.

5.3.1 Total biomass and yield

Climate change, with constant *F*, acts to reduce bigeye biomass by 7% by 2050 and by 20% by 2100. Across all species modeled, these declines range from 3% (skipjack) to 14% (blue shark) by 2050 and from 7% (skipjack) to 37% (wahoo) percent by 2100. Declines in yield reflect declines in ecosystem biomass (Fig. 5.6).

For all species, in the absence of climate change, decreasing *F* leads to increasing biomass, and vice versa. This is because lower levels of *F* result in less biomass being removed as yield. Both scenarios with increasing *F* lead to declining yield for all species, due to declining biomass. Likewise, the 0.2F scenario also leads to declining yield, due to less fishing effort, for all but the largest species (swordfish, blue shark, and blue marlin). The yield of these three largest species increases an average of 7% by 2050 and 8% by 2100 (Fig. 5.6). The 0.5F

scenario leads to similarly little change in yield by 2050 (< 10% change). By 2100, roughly half the species modeled see an increase in yield of 25% or less, while two see no change, and three see small (<10%) declines (Fig. 5.6).

We find that when changes in *F* are paired with climate change, reducing *F* can compensate somewhat the climate-driven biomass declines for all species. Bigeye biomass increases to within 10–12% of what it would be in the absence of climate change by 2050 under the 0.5F + climate change and 0.2F + climate change scenarios. Across all species, this value ranges from 4–23% (Fig. 5.6). By 2100, biomass of all species except wahoo more than doubles (bigeye biomass increases 136%) when climate change is incorporated into the 0.2F scenario. When climate change is included in the 5F scenario, yield increases over the initial ~15 years and then declines. Other than this short-term increase, there is a decline in yield for all species under all fishing scenarios; none of the modeled fishing scenarios were able to compensate for the climate-driven declines in yield. Furthermore, climate change amplified the biomass declines seen under scenarios with increasing fishing mortality.

5.3.2 Total abundance

Climate change, in the absence of changing *F*, increases the abundance of a number of species (Fig. 5.7). By 2050, all species except blue shark experience an increase in abundance of 1–9%. By 2100, all species except blue shark, yellowfin, wahoo, striped marlin, and swordfish experience increases in abundance of 1–17%. Blue shark abundance declines by 10% and 21% across these time points. Yellowfin, wahoo, and striped marlin abundance decline by 9%, 9%, and 10%, respectively. Swordfish abundance is unchanged by 2100, despite increasing earlier in the century (Fig. 5.7).

The effects of changing *F* on abundance are essentially the same as those on biomass: declining fishing mortality leads to increased fish abundance and vice versa. The effects on the number of fish caught, however, are different than those of biomass (i.e., decreasing fishing mortality leads to a decline in the number of fish caught, Fig. 5.7).

The effects on abundance of pairing climate change and changes in *F* varied by species. For species that saw abundance increase under climate change, the climate effect somewhat dampened the abundance declines resulting from increasing *F* and amplified increases in

abundance under decreasing *F*. For species that saw abundance decline under climate change, these declines were exacerbated by increasing *F*. When *F* was reduced, climate change dampened the expected increases in abundance (Fig. 5.7).

5.3.3 Large fish indicator

The effect of climate change on the large fish indicator (LFI) was small in the absence of changing *F*. LFI declines from 0.129 to 0.119 by 2050 and to 0.105 by 2100. Catch LFI declines as well, falling from 0.218 to 0.201 by 2050 and to 0.173 by 2100 (Fig. 5.8).

The effects of changing *F* on LFI were greater than those from climate change. Reducing *F* led to LFI increasing from 0.129 in 2000 to 0.143–0.162 by 2050 and to 0.153–0.191 by 2100, across both the 0.5F and 0.2F scenarios. Increasing *F* had a greater effect on LFI, reducing it to 0.069–0.107 by 2050 and to 0.046–0.091 by 2100, across both the 2F and 5F scenarios. The effects on catch LFI were similar (Fig. 5.8).

We found that when paired with climate change, halving *F* almost equally offset the decreased LFI caused by climate change alone (Fig. 5.8). Climate change acted to undermine the increase in LFI caused by decreasing *F* to one fifth the initial value. Climate change also exacerbated the decline in LFI caused by increasing *F*. When looking at modeled catch, we found that neither modeled decrease in *F* was able to offset the decline in LFI after 2050. By 2100, catch LFI declined to 0.208 under the 0.2F + climate change scenario and to 0.109 under the 5F + climate change scenario.

5.3.4 Mean size

Mean size declined for all species under climate change alone. By 2050, mean size declined by 4–13% across species with bigeye mean size declining by 11%. By 2100, mean size declines by 8–38% across species, with wahoo experiencing the greatest decline in mean size (bigeye declines by 23%). Declines in the mean size of fish caught are slightly smaller (Fig. 5.9).

Because fishing targets a species' largest body sizes, the effects on mean size of changing *F* are fairly straightforward: In the absence of climate change, increasing *F* leads to mean body sizes decreasing by 11–62% by 2050 across both the 2F and 5F scenarios, with bigeye size

decreasing by 19–48% across these scenarios. By 2100, increasing *F* leads to mean body size decreasing by 19–77% (bigeye by 32–64%). Decreasing *F* has the opposite effect on mean size. By 2050, the increase is somewhat less than opposite that of the reciprocal fishing scenario. However, by 2100, reciprocal fishing scenarios result in nearly opposite effects on mean size. As with other indicators, these effects are somewhat dampened in the catch relative to the ecosystem due to the size-selective nature of fishing (Fig. 5.9).

The joint effect of fishing and climate change on species' mean size varied by species. Reduced *F* was able to offset the climate-induced decline in mean size, to some degree, for all species. By 2100, the 0.2F + climate change scenario led to increases in mean size for all species except wahoo. The 0.5F + climate change scenario allowed mean size to increase for roughly half the species modeled. These results were dampened in the modeled catch. By 2050, the mean size of fish caught changed by -8 – +11% across species under the 0.5F + climate change and 0.2F + climate change scenarios. The size of bigeye caught in 2050 ranged from -2 – +2% across these two scenarios. By 2100, the 0.5F + climate change scenario allowed mean size of fish caught to increase in four species (lancetfish, blue shark, swordfish, and blue marlin). The 0.2F + climate change scenario allowed mean size caught to increase in all but four species (mahi, yellowfin, wahoo, and striped marlin; Fig. 5.9).

5.4 Discussion

We used *therMizer*, a size-structured food web model with individual species that is capable of capturing the metabolic effects of rising ocean temperatures, to assess the effects of climate change and fishing on Hawaii's deep-set longline fishery and its supporting ecosystem. Our results show that while a decline in this fishery's yield seems likely, this may mask resilience in the ecosystem supporting the fishery. The contrast between changes in catch and changes to the ecosystem is particularly noteworthy as it highlights the limited ability of some fishery dependent data to fully capture ecosystem trends.

5.4.1 Outlook for future yield and ecosystem

Our results show that as the climate continues to change, a decline in the yield of Hawaii's bigeye tuna fishery seems inevitable. None of the changes in fishing mortality that we

modeled, whether increasing or decreasing, allowed yield to increase after more than about 15 years. These results reinforce those of Howell et al. (2013), who found that climate change is projected to reduce the Hawaii longline fishery's target yield even when fishing mortality is halved. Their study used an Ecopath with Ecosim model to simulate food web and fishery response to climate change. That two dissimilar modeling methods produce similar projections for declining yield should be noted by regional fishery managers. Additional modeling (e.g., Cheung et al. 2016; Fu et al. 2018; Quieros et al. 2018) and empirical (Watson et al. 2012) studies of other ecosystems have led to similar projections.

In addition to total yield declining, we also find that the proportion of large fish in the catch declines in all scenarios after 2050. This suggests that not only will yield be reduced, but all else being equal, the fish caught may be less valuable because there will be fewer large fish. That said, increasing fishing mortality does lead to increased numbers of fish caught for some species (Fig. 5.7). This is likely because *therMizer* models fishing mortality as a removal of a numeric percentage rather than a biomass percentage.

Despite the poor outlook for fishery yield, we find that the ecosystem supporting the fishery fares better. Biomass of all species increases when climate change is modeled jointly with a reduction in fishing effort (Fig. 5.6). This result reinforces calls from previous authors that reduced fishing can help reduce the effects of climate change (e.g., Brander 2013). We also find that halving fishing mortality allows the LFI to remain essentially unchanged over the 21st century, and that reducing fishing mortality to one fifth initial values allows the LFI to increase (Fig. 5.8). Ultimately, the decision of whether to lower fishing mortality in favor of ecosystem resilience comes down to societal values. Models such as *therMizer* can help fishery managers and other stakeholders understand a broad range of fishery management consequences (Blanchard et al. 2014; Cheung et al. 2016).

5.4.2 Mechanisms driving change

One value in modeling studies is that they allow for investigation of the mechanisms driving change. This is particularly valuable when different stressors have the same effect; without being able to examine the underlying mechanisms it can be easy to assume that they are the same. We find that both climate change and increasing fishing mortality have similar effects

on the ecosystem and fishery yield: reduced biomass and a decline in mean body size. However, the mechanisms driving this response are different. The declining plankton biomass projected as a result of climate change reduces the amount of energy (food) available to all predators. This leads to reduced growth and, in turn, lower biomass. The shift in the plankton community's size structure also propagates through the food web, with proportionally less food available to larger body sizes, further reducing growth at larger body sizes. This disproportionate allocation of limited resources shifts the size structure toward smaller body sizes, resulting in a decline in mean body size across species (see also the discussion of species-specific effects below). Further, the disproportionate allocation of resources favoring smaller body sizes, paired with the inverse relationship between abundance and body size, explains why climate change leads to increased numerical abundance for some species.

Fishing, on the other hand, selectively removes the largest individuals from the population. Because a single large individual can be orders of magnitude larger than smaller individuals, removal of numerous large fish reduces both total biomass and mean size. Conversely, allowing more large individuals to remain in the ecosystem by reducing fishing effort more than counteracts the effect of removing them (Figs. 5.6 and 5.9).

Modeling climate change and fishing jointly highlights the different mechanisms at work to drive ecosystem change. Regardless of how fishing mortality changes, climate change acts to lower the system's carrying capacity, thereby reducing potential biomass, abundance, and yield. This interaction of stressors is only apparent when they're modeled together. Such interaction may explain the diminished impact of climate change as fishing mortality increases. As fishing increases, its effects may overshadow the lower carrying capacity resulting from climate change (Blanchard et al. 2012). This result is somewhat surprising given that a number of studies have found that the effects of climate change are stronger on more heavily fished systems (e.g., Blanchard et al. 2012; Brander 2013). One possible explanation for this disparity may be tied to model structure (Woodworth-Jefcoats et al. 2015). Application of *mizer* to another ecosystem produced results similar to ours. Fu et al. (2018) found that higher trophic level fish were more likely than those at lower trophic levels to see dampened effects when fishing and climate change were combined. The species considered in our study are nearly all high trophic level species. We encourage further ecosystem modeling comparisons across modeling frameworks

and ecosystems to help separate model structure from ecosystem structure (e.g., Tittensor et al. 2018). We also encourage further studies to consider the joint effects of stressors, especially in the open ocean beyond the limits of EEZs and Large Marine Ecosystems given the relative paucity of studies doing so (Ortuño Crespo and Dunn 2017).

Another mechanism that we investigate in this study is the role that temperature plays in driving species' response to climate change. We find that shallower-living species, most notably wahoo, see the greatest effect from climate change. On the other hand, species projected to see the least warming (e.g., lancetfish, swordfish, and blue shark) experience an increase in mean body size under both scenarios where decreasing fishing mortality is paired with climate change. Rising temperatures exacerbate the effect of reduced food availability by both increasing metabolic demand and reducing aerobic scope. This means that as climate change progresses fish will need more food despite there being less available, and that they'll be less able to successfully forage for this food. The large effect that rising temperature has on wahoo and, to some degree, on mahi mahi, suggests that shallower-living species may be bellwethers of larger ecosystem changes. It also creates the potential for a shifting species composition of both the ecosystem and catch as species are differentially affected by rising ocean temperatures. Conducting additional *therMizer* simulations with more spatially discrete temperature projections, both vertically and horizontally, or with temperature exposure varying across life stages could provide further insight into how species may be affected by the ocean's warming.

Our method for incorporating temperature's effect on metabolic demand and aerobic scope requires only minimal parameterization (universal constants and species' thermal tolerance limits). This potentially increases the utility of the approach across other modeling frameworks. Similarly, it could provide an independent first approximation of how individual marine species may be affected by climate change. Others have highlighted the need to better incorporate aerobic scope into projections of climate effects (e.g., Pörtner 2012). If a similarly simple approach could be applied to the relationship between oxygen or carbon dioxide and aerobic scope, this would significantly enhance our abilities to meet this challenge.

Food web interactions are also an integral mechanism in the response to fishing and climate change. We find that the impact of warming is somewhat offset by the effect of body size on predation. For example, blue marlin, the largest species in our simulations, experiences

an increase in mean size when climate change is paired with increasing fishing mortality, despite being a fairly shallow-living species (Table 5.1). This is likely due to the lack of competition between blue marlin and other species for prey, as its maximum body size exceeds those of other species (Kitchell et al. 2002). Conversely, yellowfin tuna, which has a maximum body size nearly one-fifth that of blue marlin sees its mean size decrease or remain constant under these scenarios despite having a deeper vertical range. This might be a result of yellowfin tuna being both predator and prey simultaneously (Cox et al. 2002; Kitchell et al. 2006). We note also that food web interactions would perhaps be more important in scenarios where different species are subject to different levels of fishing mortality, as they are in real systems. In this case, food web interactions could act to amplify or dampen fishing effects or the effects of climate change.

5.4.3 Sources of uncertainty

Three primary sources of uncertainty emerged in this study. The first is linked to the range of the CMIP5 models' plankton densities. While there is broad agreement across CMIP5 models regarding change in temperature, these models vary substantially in their values for plankton densities (Woodworth-Jefcoats et al. 2017). We've presented the multi-model mean across CMIP5 models in this study for clarity. However, the range of plankton values and change in plankton values leads to quite a wide range in *therMizer* output forced by different CMIP5 models. To some degree, this is expected as CMIP5 was the first CMIP to include zooplankton among the output variables. Skill will likely improve in future generations of earth system models and CMIP6 has intercomparisons planed toward this goal (Eyring et al. 2016). We note, though, that a reliable baseline to which modeled changes could be applied (which is how temperature is treated in this study) would be valuable to future earth system and ecosystem modeling efforts. It could also help reconcile differences in the magnitude of observed and modeled size spectra (Fig. F.1). Such an empirical baseline exists for physical oceanographic variables in the World Ocean Atlas. While there are global plankton databases (e.g., COPEPOD; O'Brien 2010), their coverage is fairly limited.

The second major source of uncertainty is the species-specific model parameters. For example, the effect of rising temperature depends in part on where thermal habitat places species' metabolic scope (Rountrey et al. 2014). For species with narrow thermal ranges (e.g.,

wahoo), a small change in temperature can have a large impact on metabolic scope. We note that our modeled metabolic scope is dependent on the accuracy of species' thermal tolerance limits. For well-studied fish such as tuna, these tolerance limits are likely accurate. However, for other species, particularly those of no commercial value, these tolerance limits are inferred from data such as diet or vertical range. Better understanding of how species use their full three-dimensional habitat would reduce model uncertainty.

Uncertainty around other species-specific parameters such as maximum recruitment, growth rate, and size-at-maturity also likely influences the model's results. A *mizer* sensitivity analysis found uncertainty around life history parameters to be the second greatest source of model uncertainty (Zhang et al. 2015). Furthermore, we know very little about how these parameters may change as climate changes. Improved understanding of species' life history and its relationship with environmental influences would not only reduce model uncertainty, but also improve fisheries management more broadly by enabling it to incorporate the effects of climate change (Brander 2007; Koenigstein et al. 2016; Pentz et al. 2018). Such information would also better inform ecosystem-based approaches to fisheries management by allowing for more accurate parameterization, especially for non-target and bycatch species.

The third source of uncertainty is that linked to fundamental assumptions about the nature of the central North Pacific's pelagic ecosystem. The most critical assumption is that this is a food-limited system. If this weren't the case, then declines in biomass at the base of the food web wouldn't necessarily result in reduced biomass across the food web. A number of factors may be contributing to this apparent food limitation. Competition and prey switching can result in bottom-up forcing and aren't well captured in *therMizer*. It's also possible that there's a benefit to be had for fish being less than fully satiated. Perhaps they're better able to evade predators (MacLeod et al. 2007). Or perhaps feeding to a level below that of satiation optimizes the risks and benefits of foraging (Heithaus et al. 2008) or the balance of energy gained from food ingested with that needed to forage further (Enberg et al. 2012). While delving further into this question is beyond the scope of the present study, it is important to highlight that this assumption underpins this and likely many other projections about the ecosystem impacts of climate change. Additionally, uncertainty around feeding levels was found to be the greatest source of uncertainty in a set of *mizer* simulations (Zhang et al. 2015). Ecosystem models such

as *mizer* and *therMizer* are one tool that can be used to evaluate the validity of this assumption and others. Future work on this topic is encouraged.

5.4.4 Model limitations and future directions

Our results raise several interesting questions that *therMizer*'s limitations make challenging to address in this study. For example, food supply (via plankton) and temperature are only two variables shaping pelagic habitat. Oxygen concentration is important and isn't included in this variation of *mizer*. Beyond shaping pelagic habitat, oxygen concentration also influences aerobic scope, as do both carbon dioxide concentration and pH (Pörtner 2012). Including any of these variables may provide a clearer picture of how different species will respond to climate change. Additionally, marine species can move in response to environmental change (Pinsky et al. 2013; Montero-Serra et al. 2015), and climate change has the potential to redistribute marine species (Cheung et al. 2010; Lehodey et al. 2010, 2013; Jones and Cheung 2014; Woodworth-Jefcoats et al. 2017). Incorporating two or three spatial dimensions into *therMizer* would allow us to address questions related to fish movement. For example, can fish simply exploit deeper depths to escape rising temperatures, or will decreasing light levels at depth diminish their foraging success? How might spatial changes in species' pelagic habitat affect their catchability? Finally, our representation of the fishery is quite simplistic in that it does not include fisher behavior. We recognize that this is a critical aspect of modeling fishery response to climate change (Haynie and Pfeiffer 2012), and look forward to exploring this dimension in future work.

This study models the effects of declining food availability and rising ocean temperatures on species caught by Hawaii's deep-set longline fishery for bigeye tuna. We show how these climate effects interact with a range of changes in fishing mortality. While increasing the yield of Hawaii's longline fishery may not be possible, projections for potential ecosystem resilience are encouraging.

Table 5.1. Species-specific model parameters. Weights (w) are in grams. Unless otherwise indicated, weight-at-maturity (w_{mat}) and maximum weight (w_{max}) are calculated using the length-weight conversions detailed in Table E.3. k_{vb} is the Brody growth coefficient. Maximum recruitment (R_{max}) is scaled from maximum size as $10^{11} \times w_{max}^{-1.5}$ following Blanchard et al. (2014). w_{F0} and w_{F1} are the sizes at which species are initially and fully susceptible to fishing mortality. Species are listed in rank order of their numeric abundance in catch of Hawaii's deep-set longline fishery for bigeye tuna (1995 – 2016, pooled).

Species	w_{mat}	w_{max}	k_{vb}	R_{max}	w_{F0}	w_{F1}	T_{min} (°C)	T_{max} (°C)	Max Depth (m)	Proportion of Observed Catch
Lancetfish (*Alepisaurus ferox*)	109	8 273	0.235	132 894	229	631	2[a]	30[a]	1 200[a]	0.2215
Bigeye tuna (*Thunnus obesus*)	29 000	95 200[b]	0.354[c]	3 404	4 771	13 122	3[d]	29[d, e]	500[f]	0.1913
Mahi mahi (*Coryphaena hippurus*)	1 024[*]	29 800[g]	1.2991[h, **]	19 439	1 417	2 124	21[e]	30[e]	85[e]	0.0885
Male	1 112	-	1.1871[h]	-	-	-	-	-	-	-
Female	936	-	1.411[h]	-	-	-	-	-	-	-
Blue shark (*Prionace glauca*)	38 880[*]	104 604[*]	0.132[i, **]	2 956	5 841	16 065	5[e]	23[e]	980[j]	0.0854
Male	43 113	126 876	0.117[i]	-	-	-	-	-	-	-
Female	34 647	82 332	0.147[i]	-	-	-	-	-	-	-
Skipjack tuna (*Katsuwonus pelamis*)	1 200	10 400[b]	0.7[k, l]	94 287	2 124	3897	10[m]	33[d]	300[m]	0.0394
Yellowfin tuna (*Thunnus albacares*)	28 480	93 400[b]	0.724[n]	3 503	2 600	7 151	7[d]	31[d, e]	250[e]	0.0385
Albacore tuna (*Thunnus alalunga*)	15 220	37 200[b]	0.2483[o]	13 938	5 841	13 122	7[d]	25[e]	600[e]	0.0243
Opah (*Lampris guttatus*)	20 050[*]	89 000[p]	0.218[q]	3 766	13 122	19 668	8[r]	22[r]	400[r]	0.0204

Table 5.1. (continued) Species-specific model parameters. Weights (w) are in grams. Unless otherwise indicated, weight-at-maturity (w_{mat}) and maximum weight (w_{max}) are calculated using the length-weight conversions detailed in Table E.3. k_{vb} is the Brody growth coefficient. Maximum recruitment (R_{max}) is scaled from maximum size as $10^{11} \times w_{max}^{-1.5}$ following Blanchard et al. (2014). w_{F0} and w_{F1} are the sizes at which species are initially and fully susceptible to fishing mortality. Species are listed in rank order of their numeric abundance in catch of Hawaii's deep-set longline fishery for bigeye tuna (1995 – 2016, pooled).

Species	w_{mat}	w_{max}	k_{vb}	R_{max}	w_{F0}	w_{F1}	T_{min} (°C)	T_{max} (°C)	Max Depth (m)	Proportion of Observed Catch
Striped marlin (*Kajikia audax*)	59 400	68 000[b]	0.24[u]	5 639	7 151	10 718	11[d]	30[d]	200[e]	0.0178
Swordfish (*Xiphiaus gladius*)	33 699[*]	181 604[*]	0.259[v, **]	1 292	1 735	3 183	2[d]	30[d]	1 200[w]	0.0080
Male	17 493	154 644	0.271[v]	-	-	-	-	-	-	-
Female	49 905	208 564	0.246[v]	-	-	-	-	-	-	-
Blue marlin (*Makaira nigricans*)	77 560[*]	455 400[b]	0.26[x, **]	325	16 065	29 479	17[d]	31[d, e]	200[e]	0.0052
Male	69 890	-	0.29[x]	-	-	-	-	-	-	-
Female	85 230	-	0.23[x]	-	-	-	-	-	-	-

[*]Average of male and female size, calculated using the values found in Table E.3.

[**]Average of male and female values.

[a]Estimated from Portner et al. 2017 [b]Uchiyama and Kazama 2003 [c]Nicol et al. 2011 [d]Boyce et al. 2008 [e]Froese and Pauly 2017; Boettiger et al. 2012 [f]Howell et al. 2010 [g]Uchiyama and Boggs 2006 [h]Uchiyama et al. 1986 [i]Shark Working Group Report 2017 [j]Stevens et al. 2010 [k]Maunder 2001 [l]Bayliff 1988 [m]Schaefer and Fuller 2007 [n]Wild 1986 [o]Billfish Working Group Report 2014b [p]Hawn and Collette 2012 [q]Francis et al. 2004 [r]Polovina et al. 2008 [s]Zischke et al. 2013b [t]Sepulveda et al. 2011 [u]Billfish Working Group Report 2015 [v]DeMartini et al. 2007 [w]Abecassis et al. 2012 [x]Shimose et al. 2015

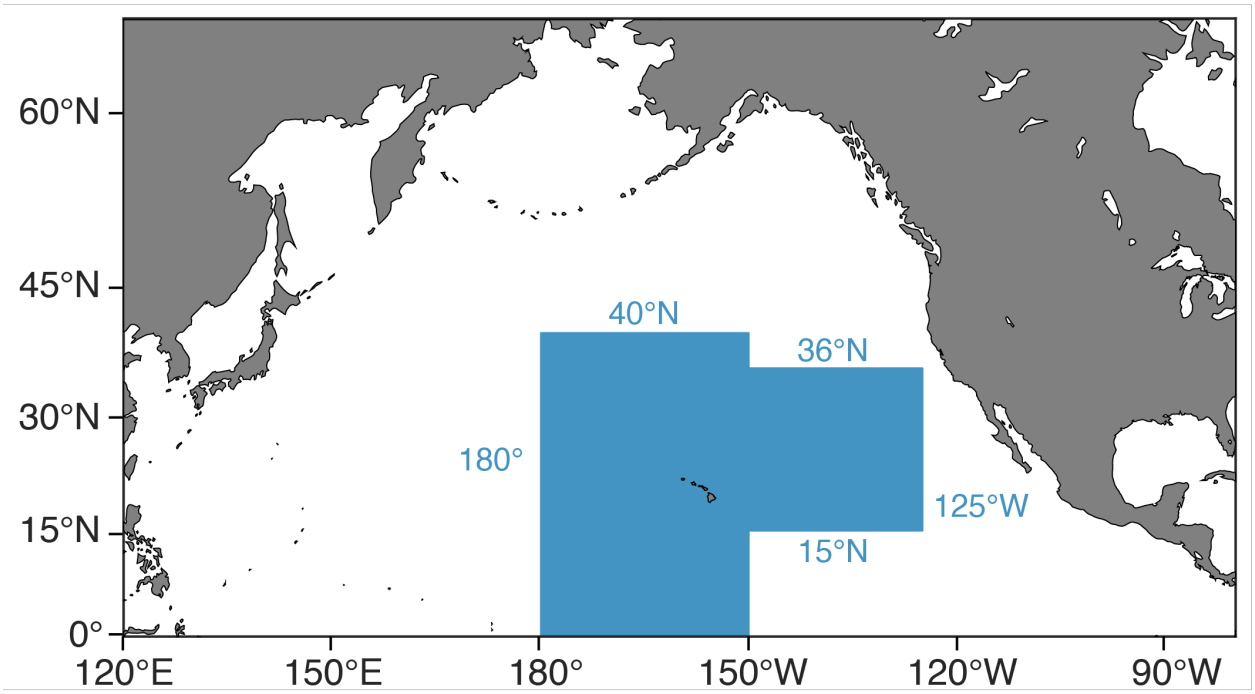

Figure 5.1 Illustration of the fishing grounds of Hawaii's deep-set longline fishery for bigeye tuna (shaded blue).

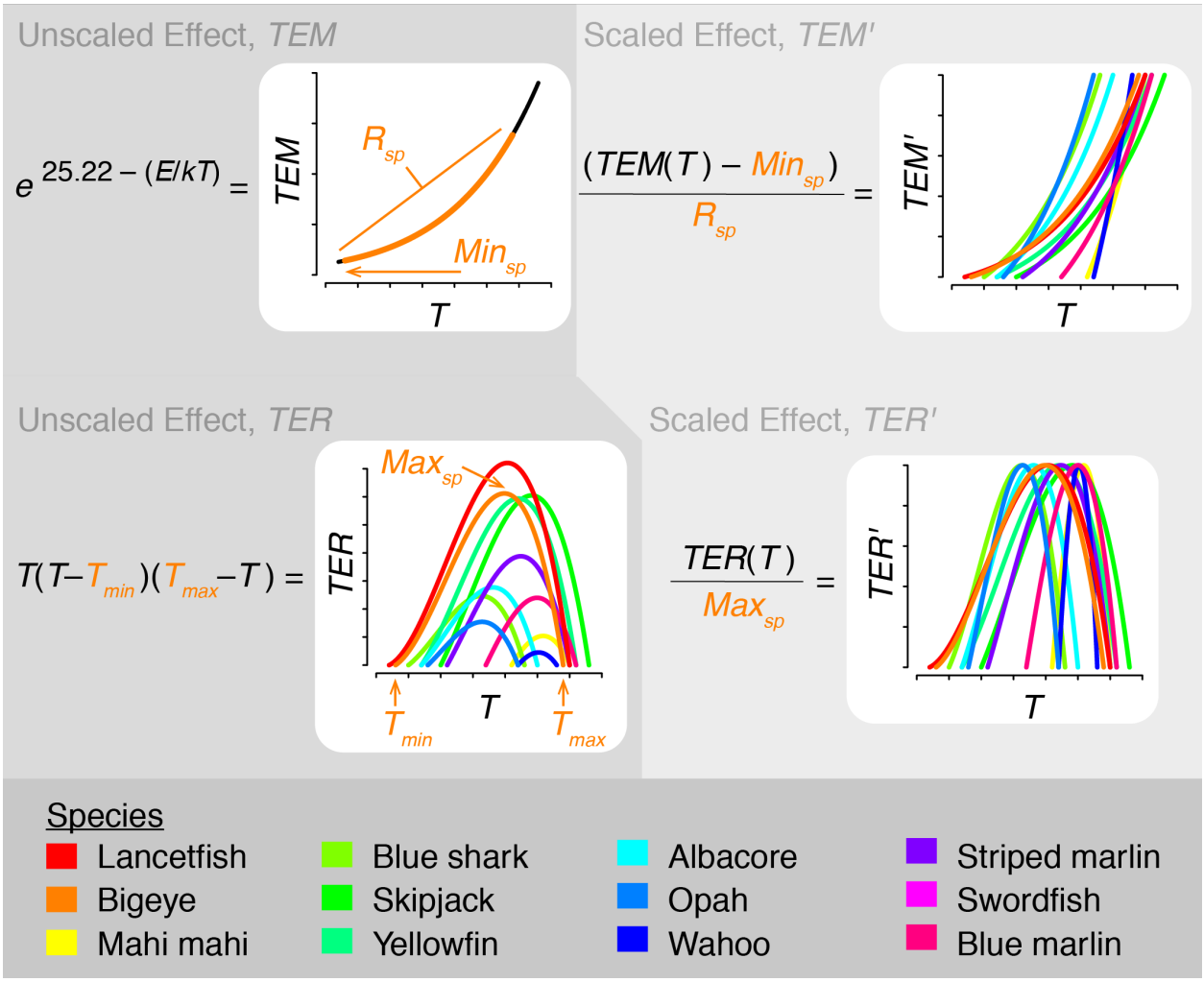

Figure 5.2 Schematic diagram illustrating how temperature is incorporated into *therMizer*. *TEM*, *TEM′*: unscaled and scaled temperature effect on metabolic rate, respectively. R_{sp}, Min_{sp}: range and minimum value of *TEM*, respectively, for species *sp*. *TER*, *TER′*: unscaled and scaled temperature effect on encounter rate, respectively. T_{min}, T_{max}: lower and upper limits of a given species' thermal tolerance range. Max_{sp}: Maximum value of *TER* for species *sp*.

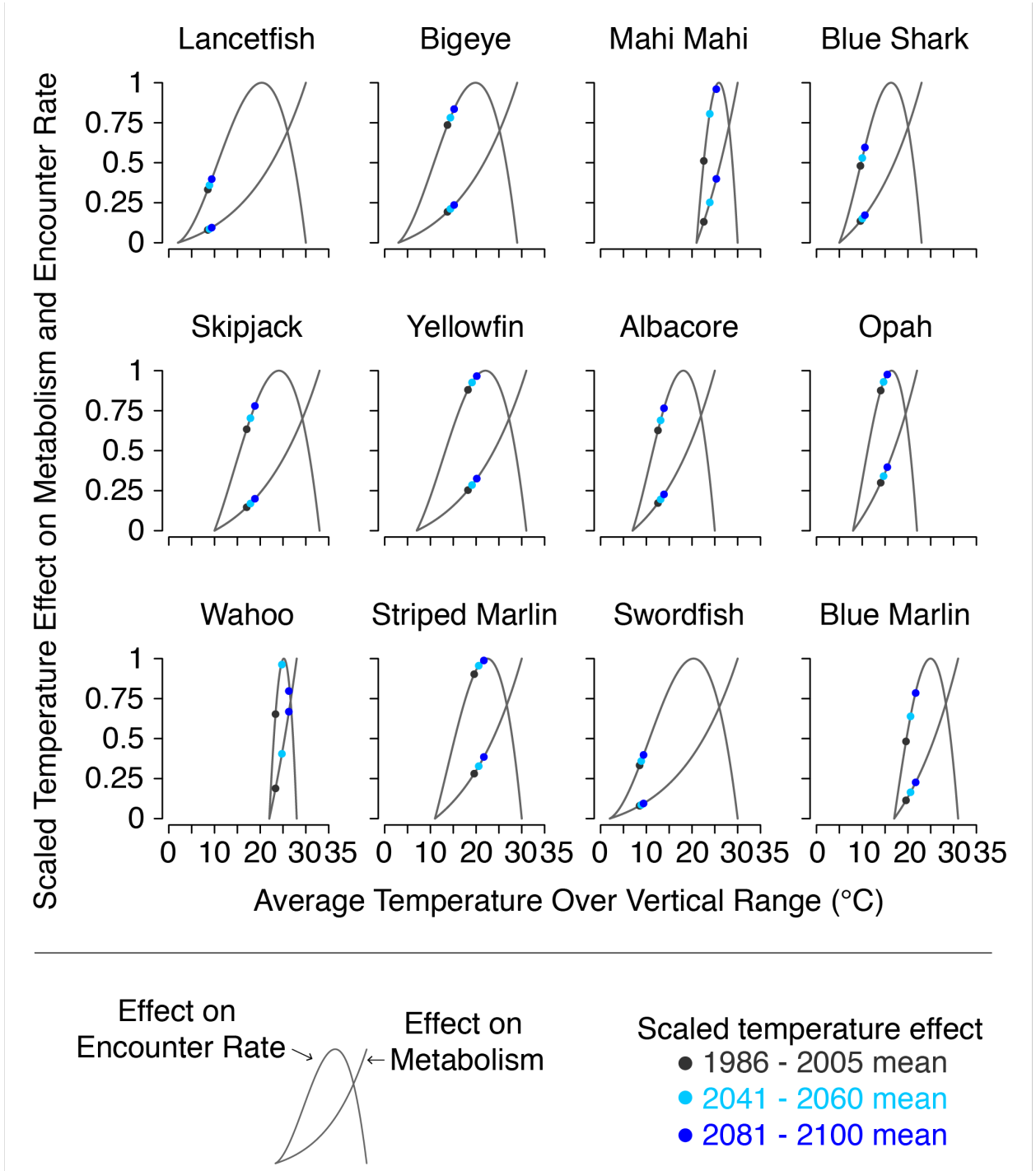

Figure 5.3 Scaled thermal effects on metabolic and encounter rates for each species at the beginning, middle, and end of the 21st century. Values plotted are the multi-model mean from the CMIP5 models used in this study. Grey lines show the full range of values possible for each species.

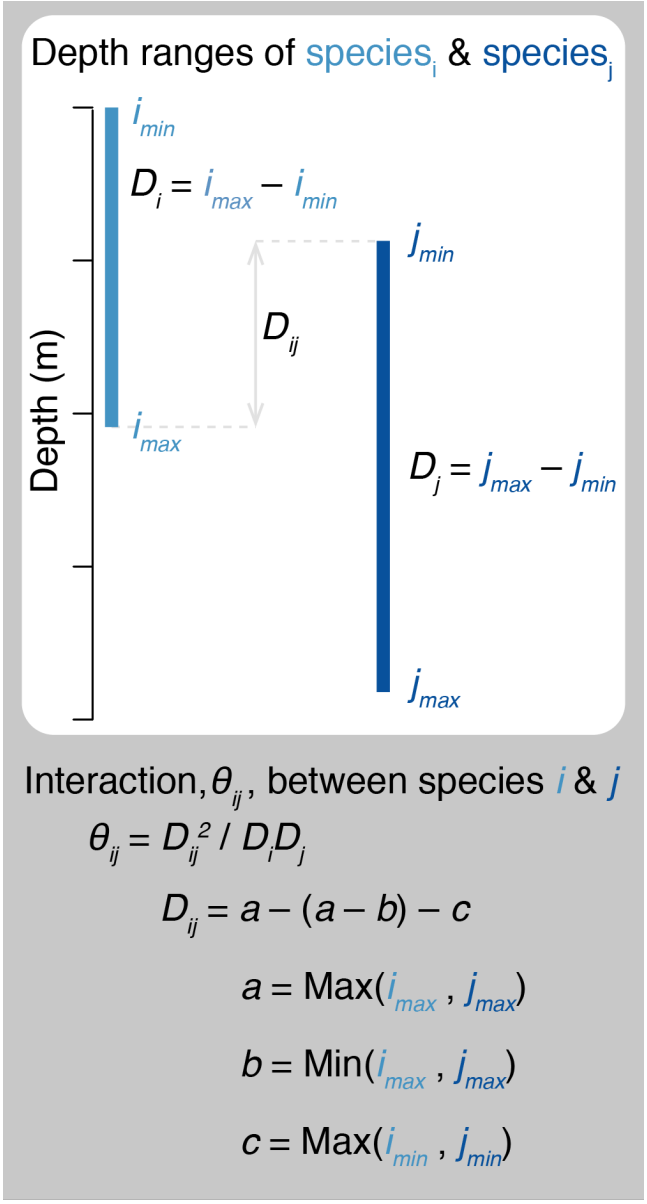

Figure 5.4 Schematic diagram illustrating how predator – prey interactions are calculated. θ_{ij}: interaction between species i and j. D_i, D_j: depth ranges of species i and j, as determined from species' minimum and maximum depths (e.g., i_{min} and i_{max}). D_{ij}: range of overlapping depths for species i and j.

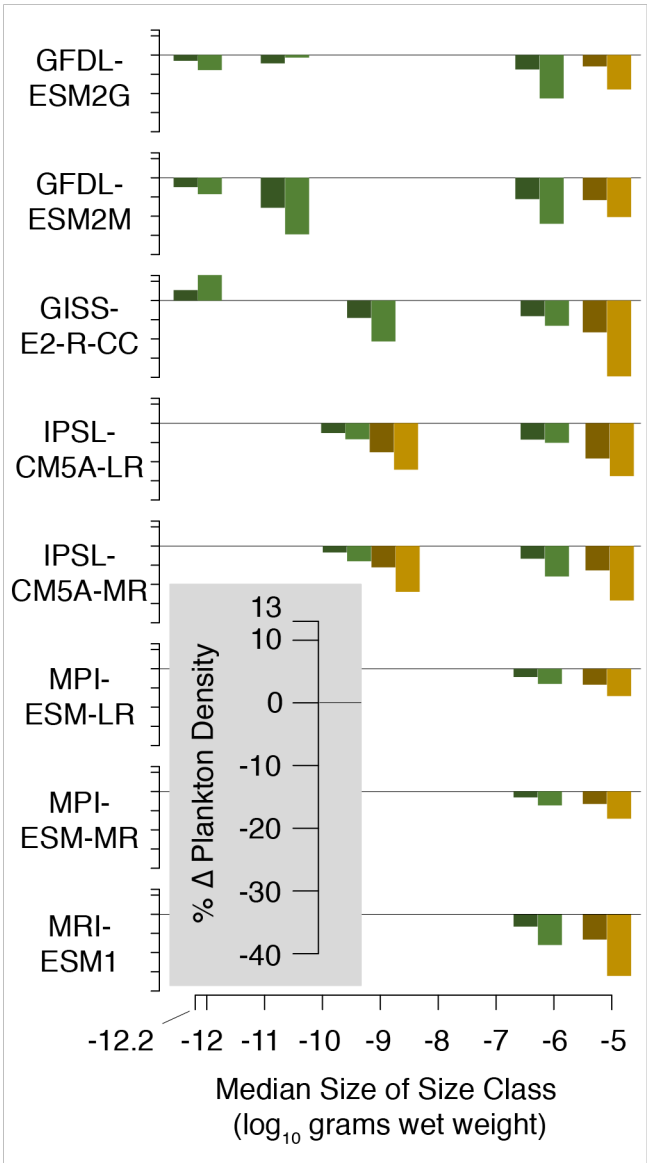

Figure 5.5 Change in phyto- (green) and zooplankton (brown) densities projected by CMIP5 models by the middle (dark shading) and end (light shading) of the 21st century. Change is relative to the average of the last 20 years of the historical run (1986–2005).

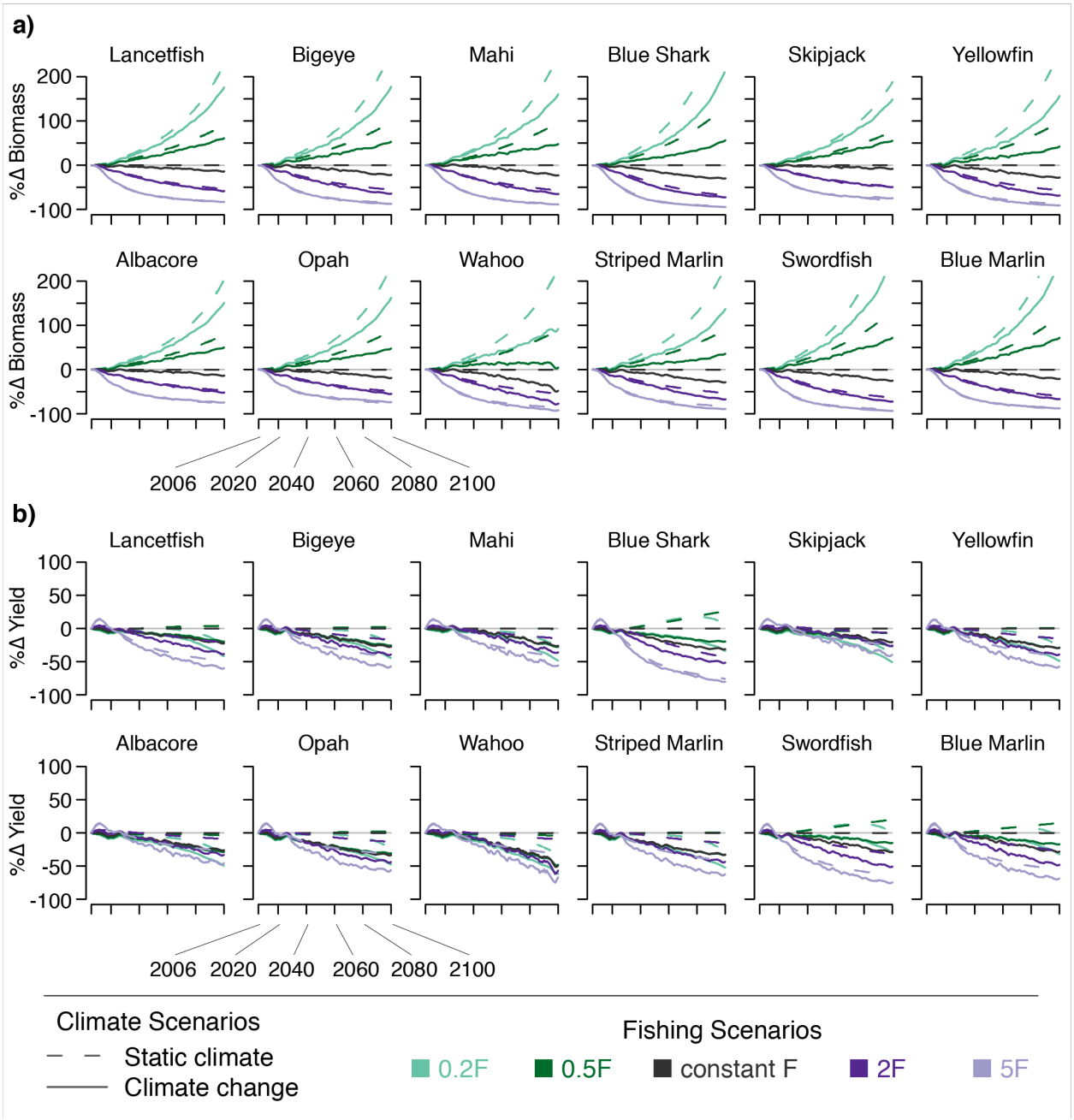

Figure 5.6 Percent change in species' A) biomass and B) yield under five fishing scenarios (indicated by line color) both with (solid lines) and without (dashed lines) climate change.

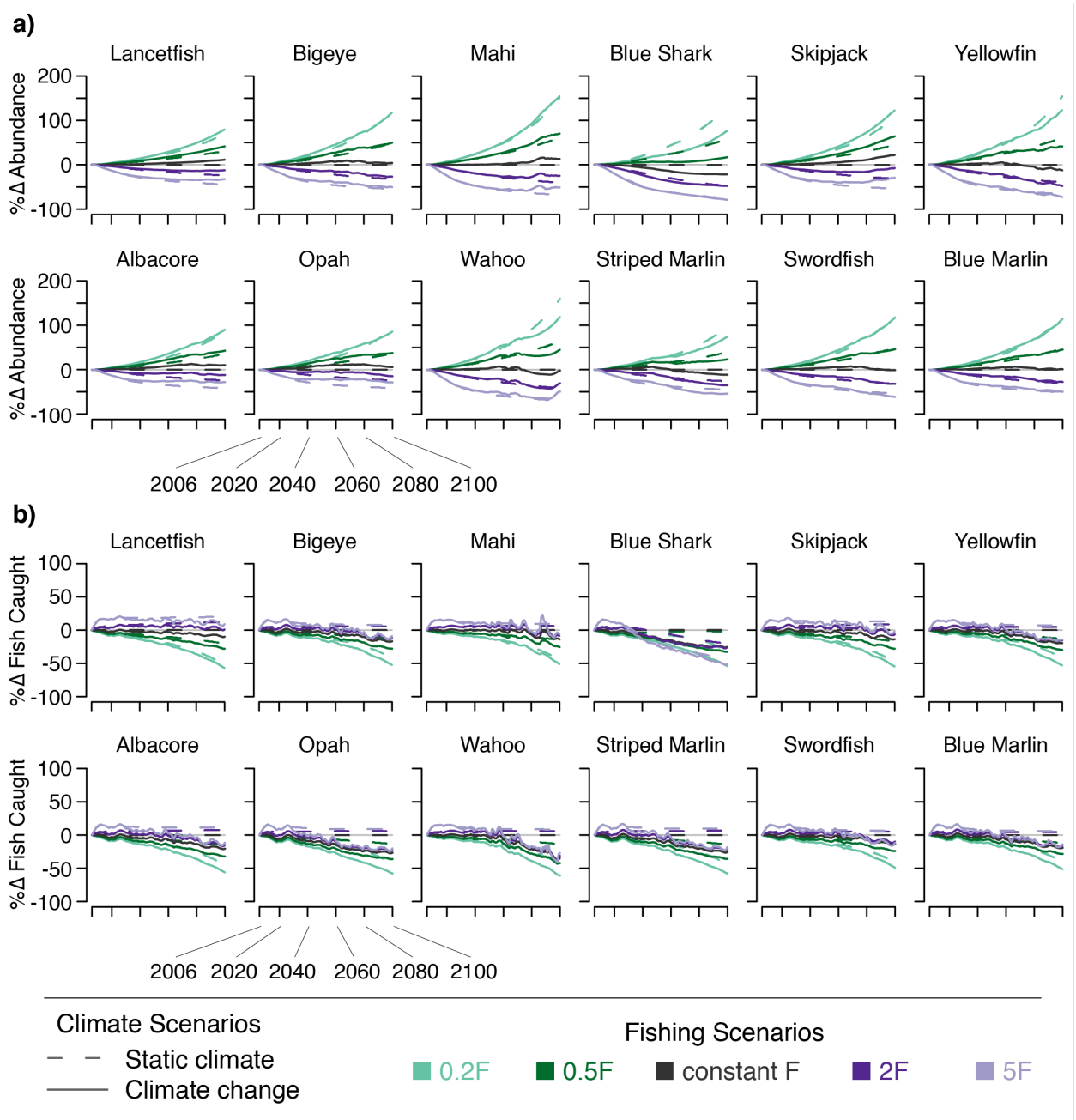

Figure 5.7 Percent change in A) species' numerical abundance and B) number of fish caught under five fishing scenarios (indicated by line color) both with (solid lines) and without (dashed lines) climate change.

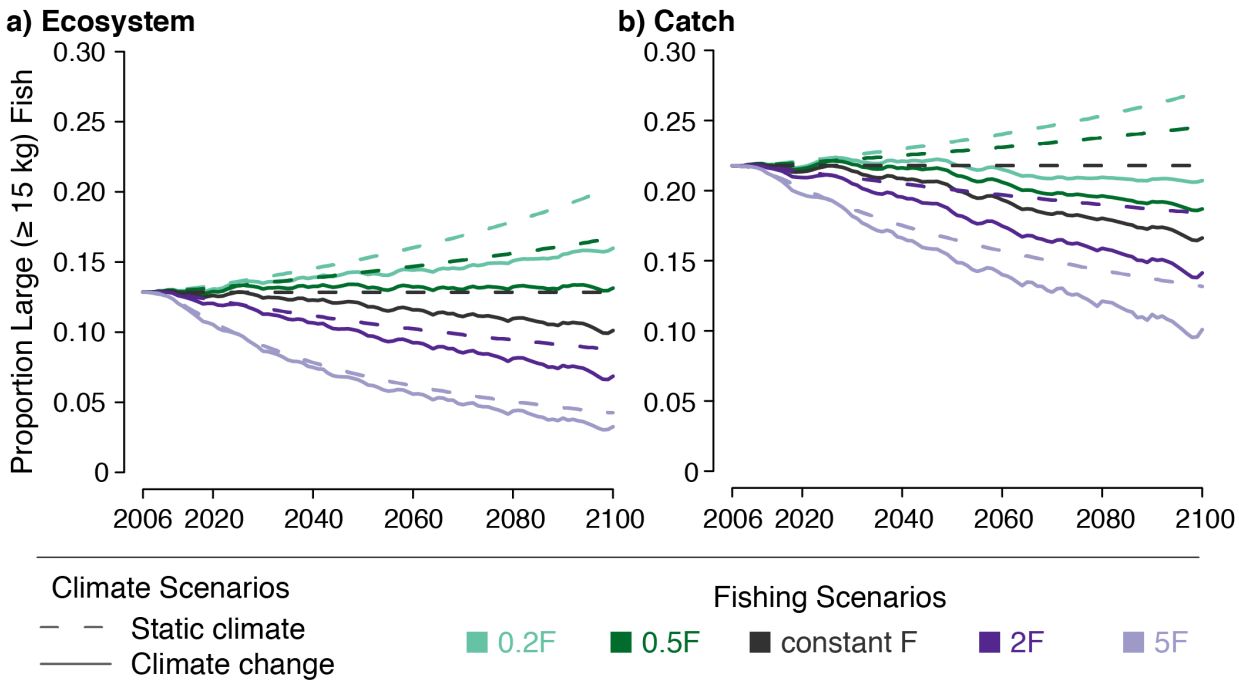

Figure 5.8 Large fish indicator (LFI) for a) the ecosystem and b) the catch under five fishing scenarios (indicated by line color) both with (solid lines) and without (dashed lines) climate change.

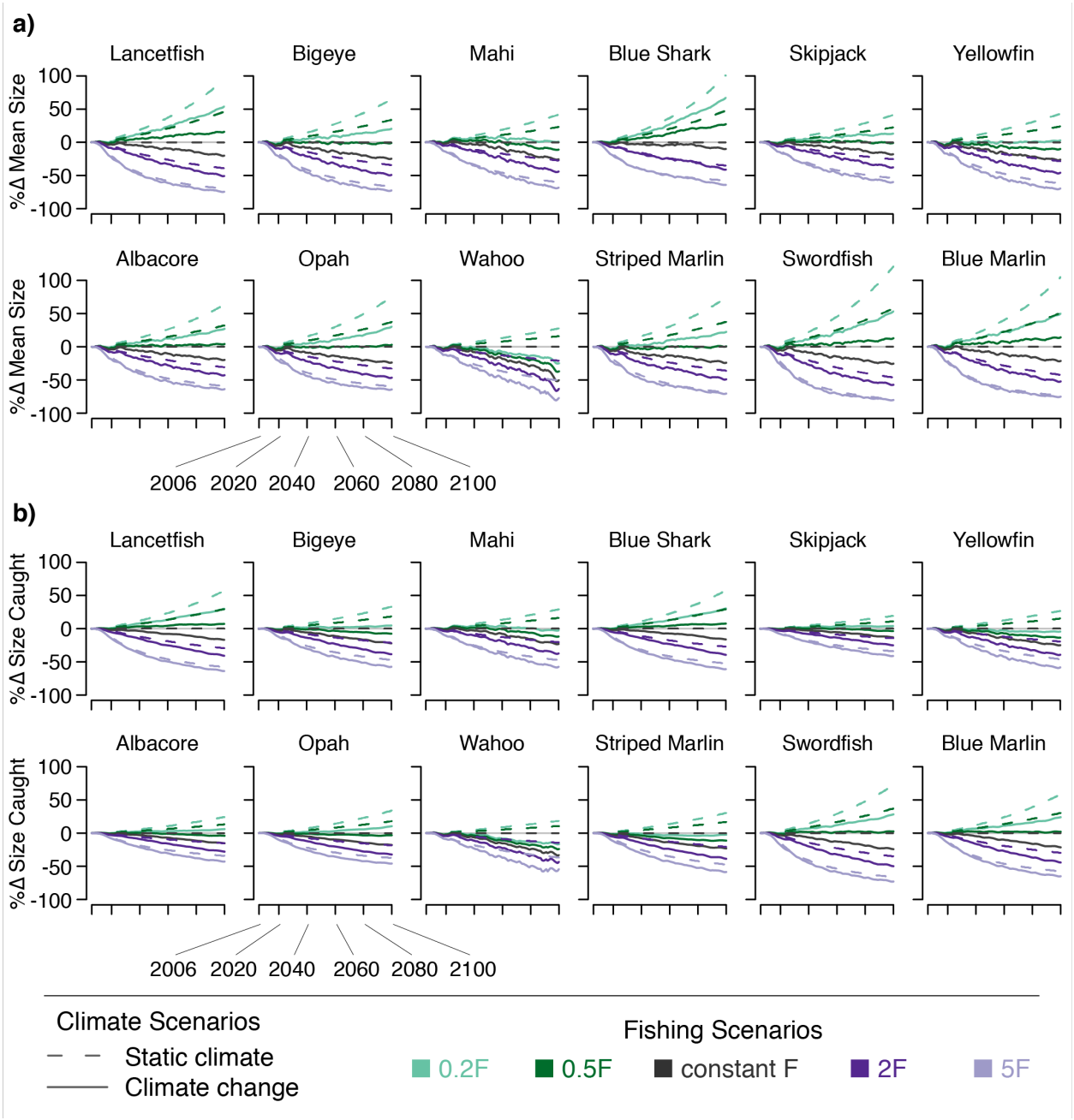

Figure 5.9 Percent change in A) species' mean size and B) the mean size of fish caught under five fishing scenarios (indicated by line color) both with (solid lines) and without (dashed lines) climate change.

CHAPTER 6

Synopsis

The research detailed in this dissertation discusses the effects of climate change and fishing on the central North Pacific's pelagic ecosystem and Hawaii's longline fishery. Climate change is projected to reduce the ecosystem's carrying capacity and, in turn, fishery yield. Rising ocean temperatures will increase fishes' metabolic demand. At the same time, biomass at the base of the food web is projected to decline, limiting fishes' ability to meet this increased demand. Increasing levels of fishing mortality, which could occur if Hawaii's longline fishing effort continues to increase, are likely to exacerbate the effects of climate change. However, it may be possible to reduce fishing mortality, have a minimal impact on yield, and allow some capacity for ecosystem resilience in the face of climate change.

The use of both earth system and ecosystem models allowed multiple facets of anthropogenic stress to be examined, both individually and in concert with one another. The ability to isolate the response of individual stressors is one benefit of modeling studies. This approach allows us to better understand the mechanisms driving change. Modeling studies can also illuminate implicit assumptions. For example, the modeling results presented in this dissertation are predicated on the assumption that the pelagic central North Pacific ecosystem is a food limited system. If this weren't the case, change at the base of the food web wouldn't necessarily result in change among apex predators. Evaluating the validity of this assumption is critical for accurately projecting the degree to which climate change will alter this ecosystem and the fishery which it supports.

Modeling studies can also highlight the limits of our present knowledge. For example, parameterizing and validating the integrated model developed in Chapter 5 highlights several limits. First, data in the pelagic realm are relatively sparse (Ortuño Crespo and Dunn 2017) and nearly all fishery-dependent. While ecosystem models can contribute to filling this gap, they cannot replace empirical, fishery-independent data. Model parameterization and validation also highlighted how little we know about how marine species use their full three-dimensional habitat. Numerous studies have linked pelagic fish to preferred sea surface temperatures (e.g., Hazen et al. 2013). However, fish spend almost no time at the ocean's surface. To accurately project how fish abundance, biomass, fitness, and distribution will change under climate change,

we have to understand where these fish are when they're below the surface. As the previous chapter shows, fish living at different depths may be affected very differently by rising ocean temperatures. Telemetry is perhaps the best option for collecting data toward this question (Metcalfe et al. 2012). Even just satellite tags recording only temperature and depth would do a great deal to address this limitation. Finally, we need to expand our knowledge about fishes' life history. Chapter 4 shows that lancetfish are caught at levels equal to Hawaii's deep-set longline fishery's target species, bigeye tuna. However, we know almost nothing about this species' life history, including its growth rate, size-at-maturity, or maximum age. This is an extreme example of fishery exploitation without knowledge of species-specific or ecosystem implications, but it isn't unique. Three of the top ten species caught by this fishery (pomfret, snake mackerel, and escolar) lacked the basic life history parameters necessary to add them to the modeling work summarized in the previous chapter. Fisheries management policies that better support observers are one way to obtain the data needed to establish this information (Nicol et al. 2013).

Despite the limits of our knowledge about pelagic fish and how they use their marine habitat, we do know that they will be affected by climate change. Where the challenge lies with regard to climate change is in how to respond to it. This challenge is heightened by the fact that "none of us acting alone as ethical individuals can do anything … to slow the change" (Nordhaus 2018). Rather, meaningful responses can only come at a societal scale. So far, we have chosen a response that can be most simply summarized as no response. This is primarily because our current course of inaction is the least expensive course of action and that which meets with the least resistance. When we buy gas for our cars or an airline ticket to travel, we're able to do so for relatively little cost because we defer most of the cost to the future when the full effects of climate change will be realized. Only when we incorporate such future costs into the prices we pay today will society begin to meaningfully, positively address climate change (Nordhaus 2013, 2018). One model for doing this can be seen in the United States, which in 1990 put a price on sulfur dioxide emissions in order to address acid rain. Doing so allowed us to address acid rain in a short amount of time, for a lower-than-projected cost (Chan et al. 2012; Nordhaus 2013). It also spurred both technical and financial innovation as firms sought to avoid costly emissions and markets arose for emissions trading (Chan et al. 2012).

Beyond curbing climate change, putting a price on carbon would likely allow us to address the fishery management challenges identified both in this dissertation and by others such as Howell et al. (2013). This is because carbon, via fossil fuels, is a necessary component of longline fishery operations. Looking more broadly, fossil fuels facilitate nearly all resource extraction, resources of which the United States consumes a disproportionate (Dietz et al. 2007) and unsustainable (Czech 2008) share. For this reason, it could be argued that the United States has the most to gain through such a carbon pricing mechanism, especially if the pricing were to take the form of a tax that could be used toward our national debt and other domestic programs (Nordhaus 2013). While a broader discussion of this topic is beyond the scope of this dissertation, the point is made here simply to illustrate that seemingly unrelated policies could have a direct effect on the management challenges discussed herein.

Another critical aspect of climate change is the planet's growing human population. It has been linked to a decline in the mean trophic level of marine ecosystems (Clausen and York 2008) and degradation of biodiversity (Mills and Waite 2009). In fact, a recent study of the most effective things individuals in developed nations could do to address climate change identified having smaller families as the most effective action by far (Wynes and Nicholas 2017). While birth rates in the United States have been below replacement for several decades (Hamilton et al. 2018), this is not the case for most of the planet (GBD 2017). Therefore, we must move toward embracing the mechanisms which have been shown to reduce fertility rates. These are primarily educational access for women and women's access to reproductive health services (GBD 2017).

Ecosystem scientists have a clear role to play in addressing the knowledge gaps and societal responses discussed in this chapter. To help address the limitations of fishery-dependent data and to create more robust future projections, we should partner with economists and other social scientists (Clausen and York 2008; Haynie and Pfeiffer 2012). To evaluate underlying assumptions and more accurately model fishes' response to a changing ocean, we should work more closely with physiologists, biologists, and ecologists (Koenigstein et al. 2016; Pörtner 2012). We must also lend our voices to conversations on society's response to climate change. We need to better engage with policy makers and those in positions to effect real change. The threats facing our planet are stark and the window for addressing them is rapidly closing (Moore et al. 2018). Therefore, we should embrace these new roles and step into them quickly.

This dissertation has shown that climate change is accelerating fishery-driven resource depletion in the central North Pacific. Yet, there are some bright spots where fishery management could be particularly effective. As Chapter 4 shows, a considerable portion of Hawaii's longline fishing ground is fished predominately by Hawaii's vessels. This means that, unlike most portions of the Pacific where international fleets dominate, local-scale reductions in catch have the potential to effect broad ecosystem change. Ecosystem models can help inform decisions around such management measures.

APPENDIX A

Ecosystem model descriptions

This appendix provides supplementary details on the key features of both the Ecopath with Ecosim (EwE) and size-based food web (SBFW) models used in the comparison detailed in Chapter 2. Full model descriptions are provided by Christensen et al. (2008, EwE) and Blanchard et al. (2012, SBFW).

Both models were run from 1991 to 2100, with the first 20 years of output removed so as not to include spin-up effects. Biomass of mid- and high-trophic level fish in EwE was calibrated with values and time series both from the literature and from stock assessments (Howell et al. 2013, ESM 1). SBFW model consumer biomass compared well to both EwE output (Figs. 2.2 and 2.3) and to regional estimates (Jennings et al. 2008, S4).

A.1 Ecopath with Ecosim

The EwE model used in the comparison in Chapter 2 is that used by Howell et al. (2013), modified as described below. This model includes 21 species/functional groups, with those listed in Appendix B subject to fishing mortality. A schematic figure of the EwE model is shown in Fig. A.1.

For straightforward comparison with the SBFW model, the EwE model was simplified in the following ways. Epipelagic mollusc predation on juvenile skipjack tuna was removed as it was not supported by the literature (Seki 1993; Cox et al. 2002; Essington 2006). Negative billfish bioaccumulation was removed as a comparable term is not included in the SBFW model. Fishing effort was adjusted such that all exploited species/functional groups experienced equal size-dependent levels of fishing mortality. This was done by replacing the species- and fleet-specific fishing mortalities used by Howell et al. (2013) with a size-dependent fishing mortality applied to all exploited species/functional groups. Finally, all vulnerabilities were set to the default value of two. This was done both to use the model's default linear functional response and to reduce as much as possible potential confounding influences of species-specific interactions.

A.2 Size-based food web model

The SBFW model used in Chapter 2 is that by Blanchard et al. (2012), as modified for the North Pacific by Woodworth-Jefcoats et al. (2013). This model consists of both a primary producer and consumer spectrum. The primary producer spectrum is discretized in $\log_{10}$ 0.1 grams wet weight (gww) bins from $\log_{10}$(-14.25 to -5.25) gww. The consumer spectrum is discretized in the same way. The minimum consumer size is set as two times (on a $\log_{10}$ scale) the median phytoplankton size, in keeping with the predator – prey mass relationship used throughout the consumer spectrum. Median phytoplankton size is determined as the cell size that represents half the phytoplankton biomass when integrating the full primary producer spectrum (see Woodworth-Jefcoats et al. 2013 for full derivation). Maximum consumer size is $\log_{10}$(5.75) gww. A schematic figure of the SBFW model is shown in Fig. A.2.

For comparison with the EwE model, the SBFW model was run without including the effects of temperature on physiological rates. This was done because the EwE model used does not include these temperature effects.

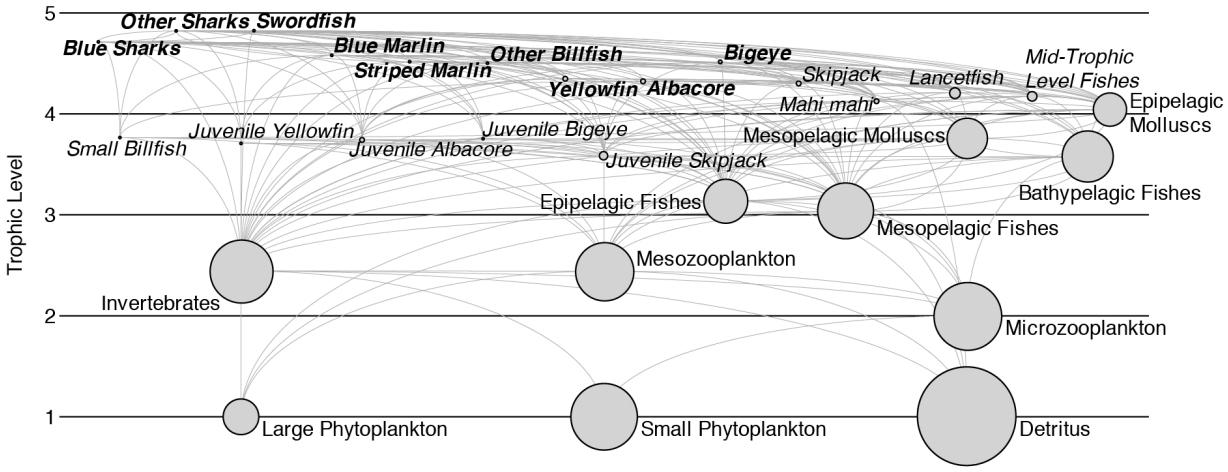

Figure A.1 A schematic diagram of the EwE model. Circle sizes represent relative biomass of each species/functional group. Connecting lines indicate diet relationships. Species/functional groups in italics are subject to fishing mortality, with large fish (>15 kg) in bold.

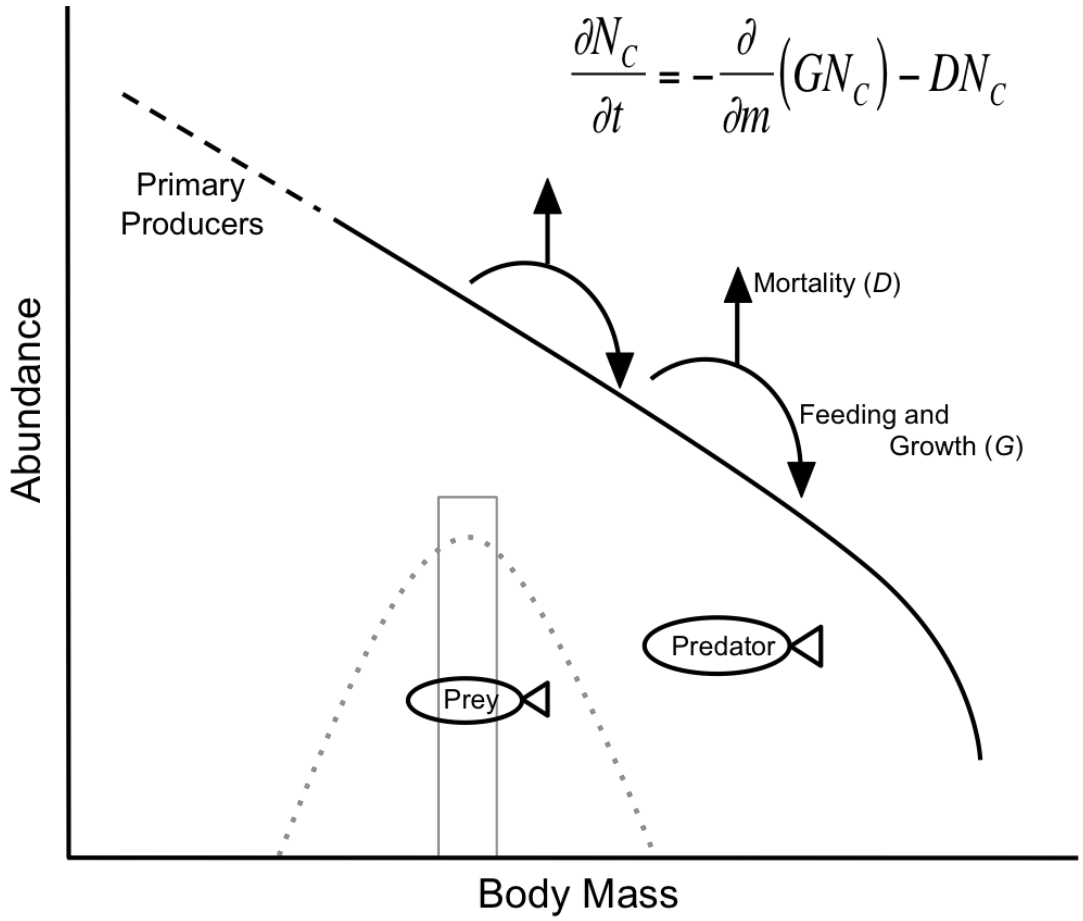

Figure A.2 A schematic diagram of the SBFW model. The dashed black line represents the primary producer spectrum and the solid black line represents the modeled consumer spectrum. Energy moves through the food web via size-based feeding. Prey are log-normally distributed (grey dotted line) about a preferred relative size (grey rectangle).

APPENDIX B

Species/Groups experiencing fishing mortality and their mean weights

Table B.1. Table of species/functional groups experiencing fishing mortality in EwE simulations and their mean weights. Mean weights were determined following the methodology used by Polovina and Woodworth-Jefcoats (2013). For a full description of these functional groups, the reader is referred to Howell et al. (2013) Electronic Supplementary Material Section 1.

EwE functional group	Mean weight (kg)	Reference
Blue Sharks	104.5	Froese and Pauly (2012)
Other Sharks	22.6	Froese and Pauly (2012) and Liu et al. (1998)
Swordfish	38.4	Griggs and Richardson (2005) and Uchiyama et al. (1999)
Blue Marlin	52.5	Ortega-Garcia et al. (2006), Prince (1991) and Uchiyama and Kazama (2003)
Striped Marlin	26.3	Uchiyama and Kazama (2003)
Other Billfish	15.7	Uchiyama and Kazama (2003)
Small Billfish	1.2	Uchiyama and Kazama (2003)
Yellowfin	40.8	Hampton (2000), Moore (1951), Uchiyama and Kazama (2003) and Zhu et al. (2008)
Juvenile Yellowfin	6.9	
Albacore	16.7	Griggs and Richardson (2005) and Zhu et al. (2008)
Juvenile Albacore	2.3	
Bigeye	31.7	Froese and Pauly (2012), Uchiyama and Kazama (2003) and Zhu et al. (2008)
Juvenile Bigeye	4.1	
Skipjack	8.0	Froese and Pauly (2012), Hampton (2000), Uchiyama and Kazama (2003)
Juvenile Skipjack[1]	0.3	
Mahi Mahi	5.9	Froese and Pauly (2012), Sundberg and Underkoffler (2011) and Uchiyama and Boggs (2006)
Lancetfish	2.8	Uchiyama and Kazama (2003)
Mid-trophic-level Fish	5.1	Froese and Pauly (2012), Sundberg and Underkoffler (2011), Uchiyama and Boggs (2006) and Uchiyama and Kazama (2003)

[1]Juvenile skipjack were subject to fishing mortality in the EwE model despite being <1 kg to more closely approximate the model used by Howell et al. (2013).

APPENDIX C

Variance for each output time series examined in Chapter 2

Table C.1. Variance (t km^{-2}) for each output time series listed[1]. Time series include climate change.

		Ecopath with Ecosim						Size-Based Food Web					
F:		0	0.2	0.4	0.6	0.8	1.0	0	0.2	0.4	0.6	0.8	1.0
Catch	Small	-	7.28×10^{-7}	2.87×10^{-6}	9.26×10^{-6}	1.62×10^{-5}	2.24×10^{-5}	-	3.57×10^{-6}	1.49×10^{-5}	3.32×10^{-5}	5.68×10^{-5}	8.41×10^{-5}
	Large	-	2.59×10^{-7}	4.35×10^{-7}	2.01×10^{-7}	1.09×10^{-7}	2.46×10^{-7}	-	4.24×10^{-6}	8.05×10^{-6}	8.83×10^{-6}	7.89×10^{-6}	6.37×10^{-6}
	Total	-	1.84×10^{-6}	5.48×10^{-6}	1.21×10^{-5}	1.85×10^{-5}	2.71×10^{-5}	-	1.58×10^{-5}	4.62×10^{-5}	7.98×10^{-5}	1.14×10^{-4}	1.47×10^{-4}
Exploitable Biomass	Small	2.68×10^{-4}	2.91×10^{-4}	2.87×10^{-4}	4.12×10^{-4}	4.06×10^{-4}	3.59×10^{-4}	7.83×10^{-4}	8.96×10^{-4}	9.70×10^{-4}	1.01×10^{-3}	1.01×10^{-3}	1.00×10^{-3}
	Large	7.40×10^{-6}	6.48×10^{-6}	2.72×10^{-6}	5.57×10^{-7}	1.70×10^{-7}	2.46×10^{-7}	2.24×10^{-4}	1.06×10^{-4}	5.03×10^{-5}	2.45×10^{-5}	1.23×10^{-5}	6.37×10^{-6}
	Total	3.63×10^{-4}	3.83×10^{-4}	3.44×10^{-4}	4.41×10^{-4}	4.19×10^{-4}	3.77×10^{-4}	1.75×10^{-3}	1.57×10^{-3}	1.43×10^{-3}	1.33×10^{-3}	1.24×10^{-3}	1.16×10^{-3}

[1]Input variance with climate change:
Small phytoplankton: 1.53×10^{-3} g C m^{-2}
Large phytoplankton: 9.64×10^{-5} g C m^{-2}

APPENDIX D

Supplemental figures for Chapter 4

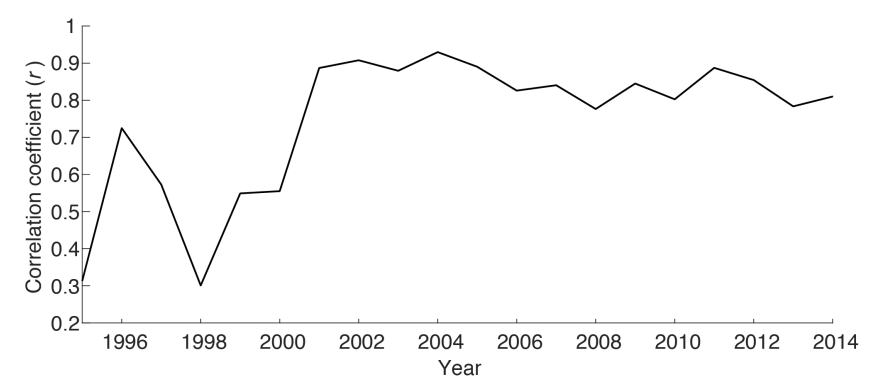

Figure D.1 Time series of correlation coefficients (r) between 1° × 1° grids of total annual effort reported in logbook and observer records of the Hawaii-based longline fishery from 1995 through 2014. When time series of summed total annual effort are compared, logbook and observer data have an r value of 0.97. Time series of mean latitude and longitude of annual effort are both correlated with an r value of 0.97.

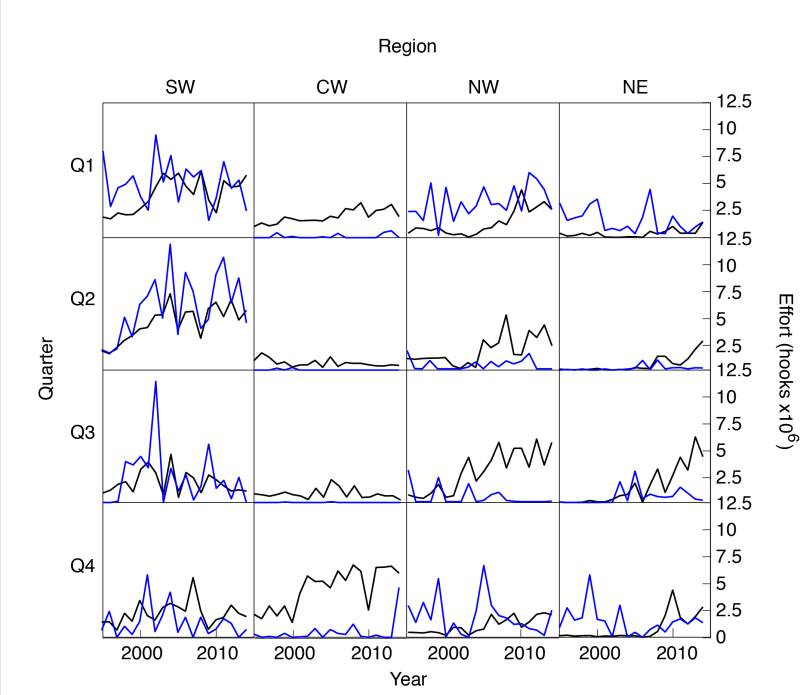

Figure D.2 The total effort (number of hooks set) by the Hawaii-based (black) and international (blue) longline fisheries in each region and quarter, for all grid cells with Hawaii-based effort from 1995 through 2014. Note that both deep-set and shallow-set effort are included because data of international effort do not provide information on the number of hooks per float. The regions are southwest (SW), central west (CW), northwest (NW), and northeast (NE).

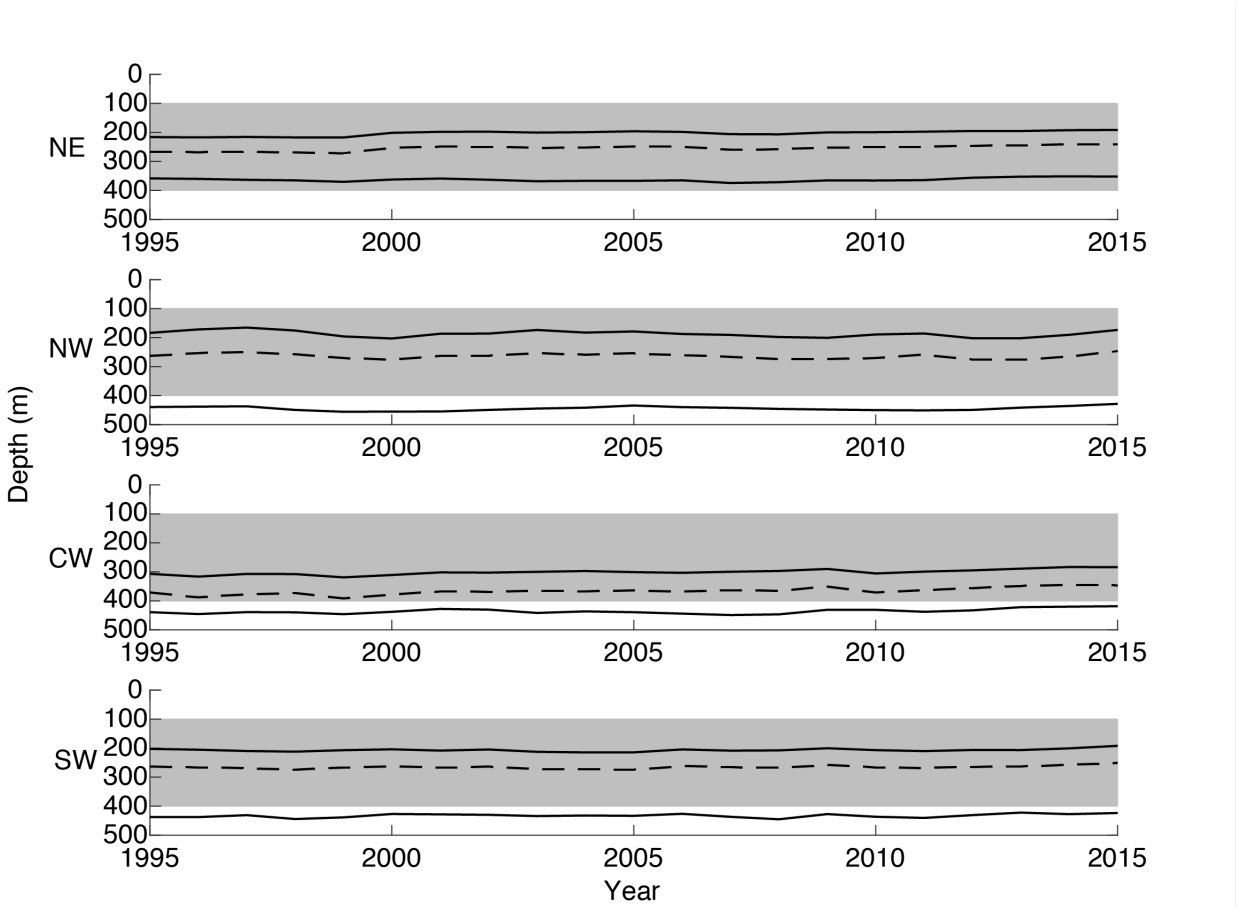

Figure D.3 Annual time series of the vertical extent (solid lines) and median depth (dashed lines) of preferred thermal habitat for bigeye tuna (*Thunnus obesus*) (8–14°C) for all grid cells in each region with any effort, based on logbook data, by the Hawaii-based longline fishery from 1995 through 2015. Grey shading indicates the average vertical range of deep-set hooks. The regions are southwest (SW), central west (CW), northwest (NW), and northeast (NE).

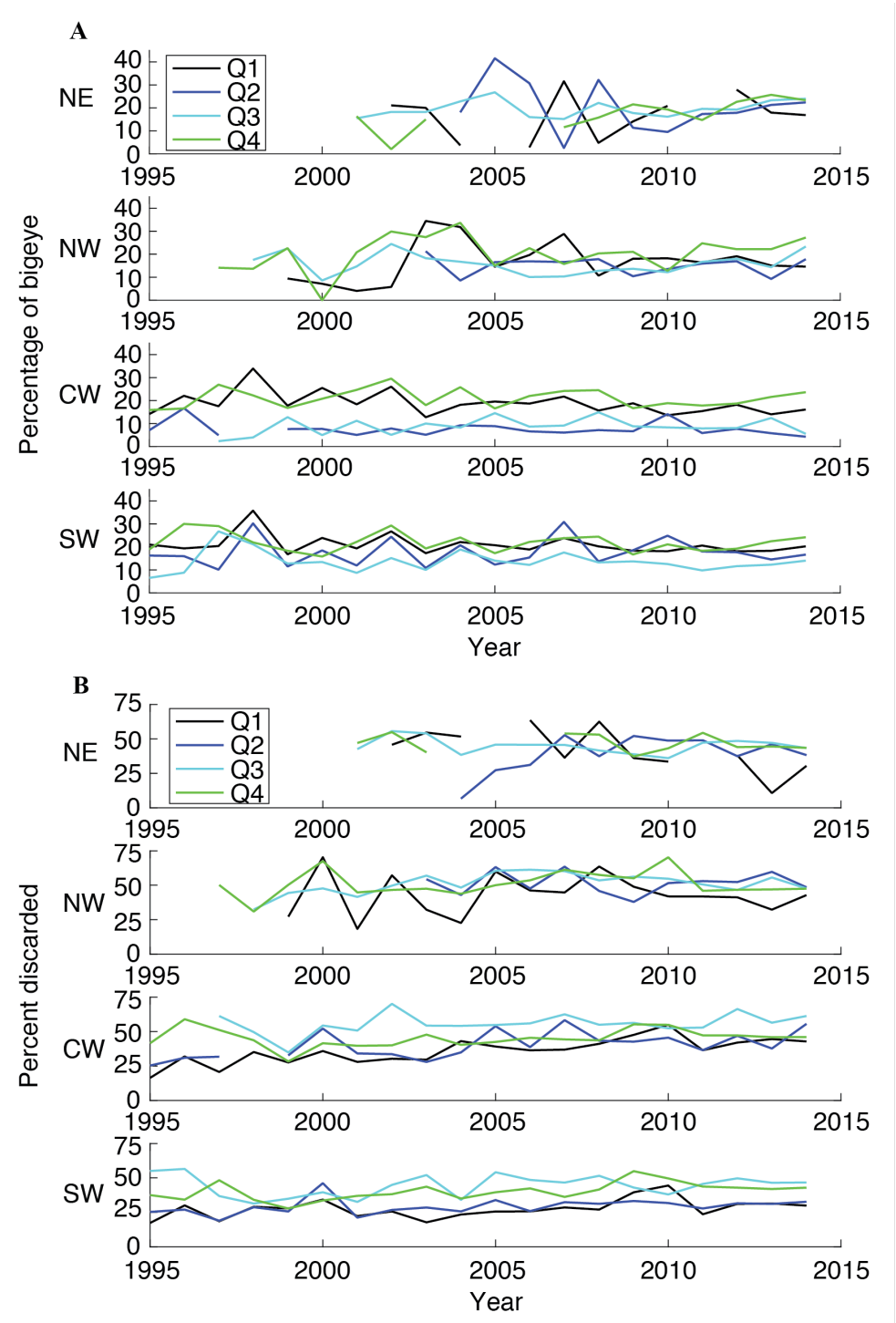

Figure D.4 Quarterly (A) percent contribution of bigeye tuna (*Thunnus obesus*) to total catch and (B) percentage of total catch (all species) discarded, based on observer data, in four regions of the Hawaii-based longline fishery from 1995 through 2014. The regions are southwest (SW), central west (CW), northwest (NW), and northeast (NE). Note that the y-axes are different in each panel.

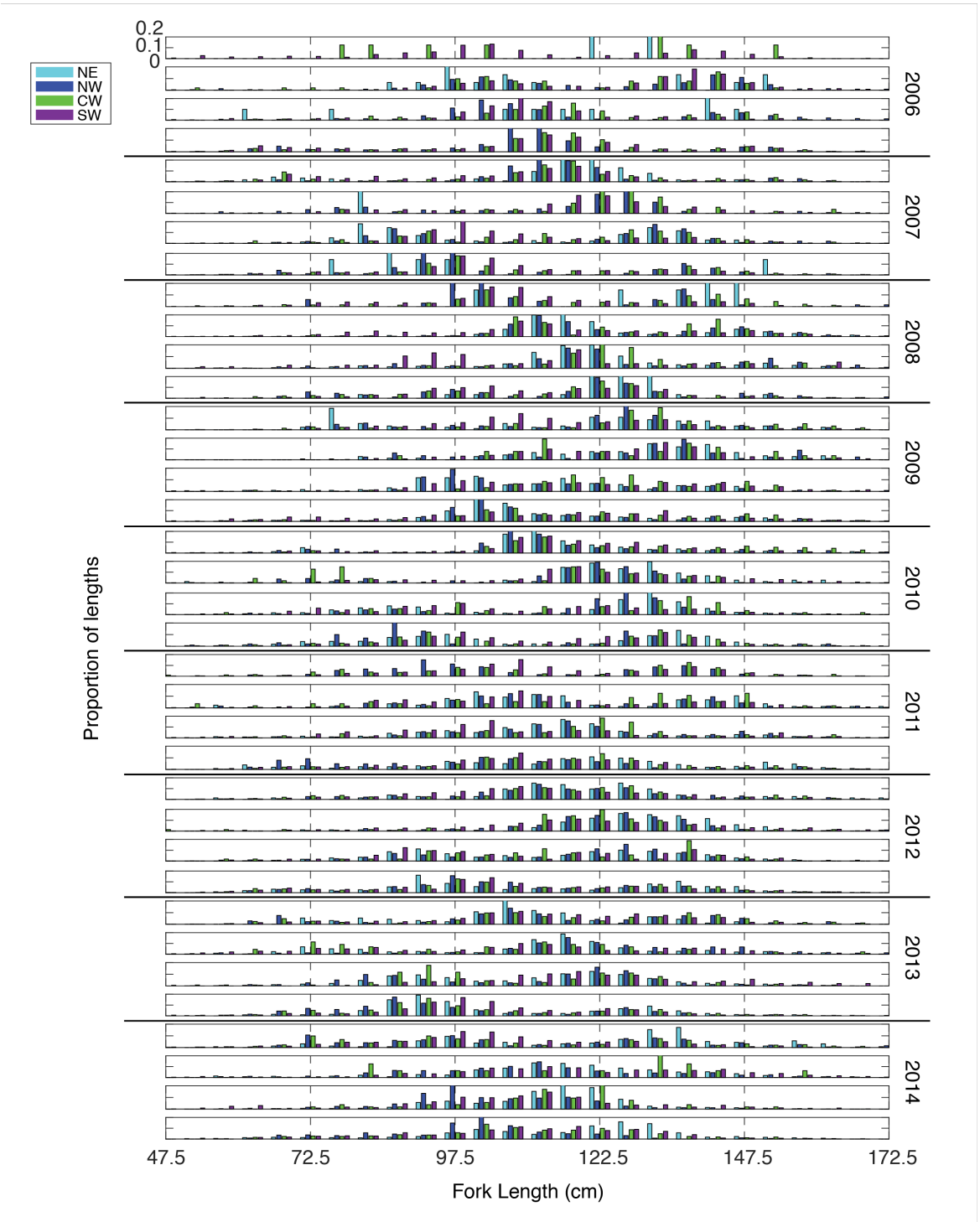

Figure D.5 The quarterly size distribution of bigeye tuna (*Thunnus obesus*) across the fishing grounds of the Hawaii-based longline fishery for the years (2006–2014) during which longline observers followed a consistent protocol of measuring every third fish caught. The regions are northeast (NE), northwest (NW), central west (CW), and southwest (SW). Proportions are shown for each region and quarter.

APPENDIX E

Supplemental tables for Chapter 5

Table E.1. Interaction matrix. Values represent the proportion of appropriately sized prey of a given species that are available to predators of a given species. The table is broken for ease of presentation.

		Prey					
		Bigeye Tuna	Mahi Mahi	Blue Shark	Skipjack Tuna	Yellowfin Tuna	Albacore Tuna
Predator	Bigeye Tuna	1	0.17	0.5102041	0.6	0.5	0.8333333
	Mahi Mahi	0.17	1	0.08673469	0.28333333	0.34	0.14166667
	Blue Shark	0.5102041	0.08673469	1	0.30612245	0.25510204	0.61224490
	Skipjack Tuna	0.6	0.28333333	0.30612245	1	0.83333333	0.5
	Yellowfin Tuna	0.5	0.34	0.25510204	0.83333333	1	0.4166667
	Albacore Tuna	0.8333333	0.14166667	0.61224490	0.5	0.4166667	1
	Striped Marlin	0.4	0.425	0.20408163	0.66666667	0.8	0.33333333
	Wahoo	0.04	0.23529412	0.02040816	0.06666667	0.08	0.03333333
	Swordfish	0.4166667	0.07083333	0.81666667	0.25	0.2083333	0.5
	Blue Marlin	0.4	0.425	0.20408163	0.66666667	0.8	0.33333333
	Lancetfish	0.4166667	0.07083333	0.81666667	0.25	0.2083333	0.5
	Opah	0.7	0.04117647	0.35714286	0.59523810	0.4571429	0.58333333

Table E.1. (continued) Interaction matrix. Values represent the proportion of appropriately sized prey of a given species that are available to predators of a given species. The table is broken for ease of presentation.

		Prey					
		Striped Marlin	Wahoo	Swordfish	Blue Marlin	Lancetfish	Opah
Predator	Bigeye Tuna	0.4	0.04	0.4166667	0.4	0.4166667	0.7
	Mahi Mahi	0.425	0.23529412	0.07083333	0.425	0.07083333	0.04117647
	Blue Shark	0.20408163	0.02040816	0.81666667	0.20408163	0.81666667	0.35714286
	Skipjack Tuna	0.66666667	0.06666667	0.25	0.66666667	0.25	0.59523810
	Yellowfin Tuna	0.8	0.08	0.2083333	0.8	0.2083333	0.4571429
	Albacore Tuna	0.33333333	0.03333333	0.5	0.33333333	0.5	0.58333333
	Striped Marlin	1	0.1	0.1666667	1	0.1666667	0.3214286
	Wahoo	0.1	1	0.01666667	0.1	0.01666667	0
	Swordfish	0.1666667	0.01666667	1	0.16666667	1	0.29166667
	Blue Marlin	1	0.1	0.16666667	1	0.1666667	0.3214286
	Lancetfish	0.1666667	0.01666667	1	0.1666667	1	0.29166667
	Opah	0.3214286	0	0.29166667	0.3214286	0.29166667	1

Table E.2. Plankton size classes. Plankton classes available from each CMIP5 model used and their size ranges, as determined from the literature. Sizes are given in equivalent spherical diameter (ESD) measured in μm. The primary reference for each CMIP5 model is noted next to the model's name. References used to determine plankton size classes are listed in the right-most column.

Earth System Model	Phytoplankton	Zooplankton	References
NOAA Geophysical Fluid Dynamics Laboratory Earth System Model Generalized ocean layer dynamics[a] (GFDL-ESM2G)	picophytoplankton: 0.2–2 miscellaneous phytoplankton: 2–5 diatoms, diazotrophs: 5–200	zooplankton 2 – 500	a, b, c
NOAA Geophysical Fluid Dynamics Laboratory Earth System Model Modular Ocean Model 4[a] (GFDL-ESM2M)	picophytoplankton: 0.2–2		
NASA Goddard Institute for Space Studies ModelE2 Earth System Model with carbon cycle coupled to the Russell ocean model[d, e] (GISS-E2-R-CC)	calcareous, miscellaneous phytoplankton: 2–20 diatoms, diazotrophs: 2–500	zooplankton 2 – 500	f, g, h, i, j
Institut Pierre-Simon Laplace Low Resolution CM5A[k] (IPSL-CM5A-LR)	miscellaneous phytoplankton: 2–20	microzooplankton: 2 – 20	k, l, m
Institut Pierre-Simon Laplace Medium resolution CM5A[k] (IPSL-CM5A-MR)	diatoms: 20–200	mesozooplankton: 20 – 500	
Max-Planck-Institute für Meteorologie Earth System Model low resolution[n] (MPI-ESM-LR)	phytoplankton 0.2–200	zooplankton 2 – 500	o
Max-Planck-Institute für Meteorologie Earth System Model medium resolution[n] (MPI-ESM-MR)			
Meteorological Research Institute Earth System Model Version 1[p] (MRI-ESM1)	phytoplankton 0.2–200	zooplankton 2 – 500	p

[a]Dunne et al. 2013 [b]Dunne et al. 2005 [c]Dunne et al. 2012 [d]Romanou et al. 2014 [e]Schmidt et al. 2014 [f]Gregg and Casey 2007 [g]Bricaud and Morel 1986 [h]Bricaud et al. 1983 [i]Ahn et al. 1992 [j]Sathyendranath et al. 1987 [k]Dufresne et al. 2013 [l]Aumont and Bopp 2006 [m]Séférian et al. 2012 [n]Giorgetta et al. 2013 [o]Ilyina et al. 2013 [p]Yukimoto et al. 2011

Table E.3. Length-weight conversions. Lengths (l) are converted to weights following the standard exponential equation $W = aL^b$. References for both a and b values are indicated in the column for b. For length-weight conversion, lengths are in cm and weights in kg for all species except wahoo where lengths are in mm. Billfish lengths are eye-fork lengths. Shark lengths are precaudal lengths. All other lengths are fork lengths.

Species	l_{min}	l_{mat}	l_{max}	a	b
Albacore tuna (*Thunnus alalunga*)	-	90[d]	-	*	*
Bigeye tuna (*Thunnus obesus*)	-	107.8[e]	-	3.66×10^{-5}	2.90182[p]
Bigeye thresher shark (*Alopias superciliosus*)	68[a]	154[a]	195[a]	9.11×10^{-6}	3.0802[a]
Blue marlin (*Makaira nigricans*)	-	179.46[f]	-	-	-
Male	-	-	-	1.37×10^{-5}	2.975[f]
Female	-	-	-	1.84×10^{-5}	2.956[f]
Blue shark (*Prionace glauca*)	36[b]	-	-	-	-
Male	-	161[b]	225[b]	3.29×10^{-6}	3.225[b]
Female	-	156.6[b]	207[b]	5.39×10^{-6}	3.102[b]
Lancetfish (*Alepisaurus ferox*)	-	35[g]	168[n]	6.01×10^{-6}	2.78949[p]
Mahi mahi (*Coryphaena hippurus*)	-	-	-	-	-
Male	-	50.57[h]	-	8.09×10^{-6}	3.0157[q]
Female	-	48.38[h]	-	1.07×10^{-5}	2.9337[q]
Opah (*Lampris guttatus*)	-	80[t]	-	**	**
Shortfin mako shark (*Isurus oxyrinchus*)	60[c]	277.5[c]	321[c]	1.67×10^{-5}	2.847[c]
Skipjack tuna (*Katsuwonus pelamis*)	-	40[i]	-	7.65×10^{-6}	3.24281[p]
Striped marlin (*Kajikia audax*)	-	177[j]	-	4.68×10^{-6}	3.16[j]
Swordfish (*Xiphiaus gladius)*	-	-	-	1.37×10^{-5}	3.04[r]
Male	-	102[k]	208.9[o]	-	-
Female	-	144[k]	230.5[o]	-	-
Wahoo (*Acanthocybium solandri*)	-	104.6[l]	-	8.77×10^{-10}	3.28[s]
Yellowfin tuna (*Thunnus albacares*)	-	115[m]	-	3.17×10^{-5}	2.88938[p]

*Albacore lengths are converted using Uchiyama and Kazama (2003)'s equation: $W = 6.16388 - 0.323931(L) + 0.00600216(L)^{1.94647}$

** Opah lengths were converted using Sundberg and Underkoffler (2011)'s equations: $\ln(W_{female}) = 2.5815 \times \ln(L_{female}) - 8.3379$ and $\ln(W_{male}) = 2.5692 \times \ln(L_{male}) - 8.2368$

[a]Young et al. 2016 [b]Shark Working Group Report 2017 [c]Froese and Pauly 2017; Boettiger et al. 2012 [d]Billfish Working Group Report 2014b [e]Nicol et al. 2011 [f]Billfish Working Group Report

2016 [g]Estimated: the average size between adult and “small” lancetfish in Gibbs 1960 [h]Alejo-Plata et al. 2011 [i]Rice et al. 2014 [j]Billfish Working Group Report 2015 [k]DiMartini et al. 2000 [l]Zischke et al. 2013a [m]Itano 2000 [n]Portner et al. 2017 [o]DeMartini et al. 2007 [p]Uchiyama and Kazama 2003 [q]Uchiyama and Boggs 2006 [r]Billfish Working Group 2014a [s]Zischke et al. 2013b [t]Francis et al. 2004

APPENDIX F

Modeled and observed catch size spectra

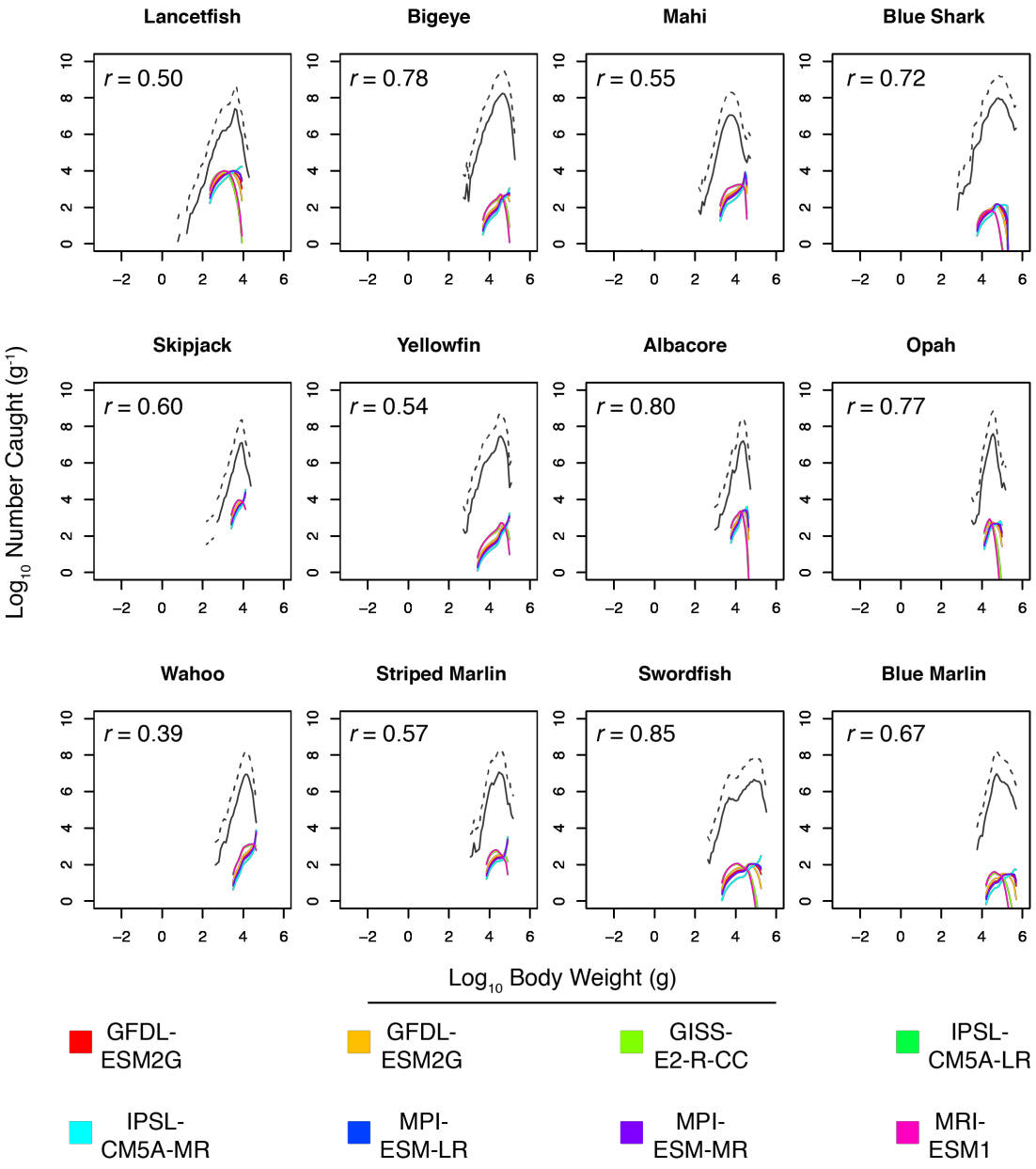

Figure F.1 Modeled (color) and observed (black) catch size spectra. The solid line is the observed abundance. The dashed line is scaled to represent the full catch. Observed catch is scaled by dividing by 0.06 (on average, 20% of the fishery is observed and observers measure every third fish). The average Pearson correlation coefficient, *r*, across CMIP5 models is noted for each species.

Literature Cited

Abecassis M, Dewar H, Hawn D, Polovina J, 2012. Modeling swordfish daytime vertical habitat in the North Pacific Ocean from pop-up archival tags. Marine Ecology Progress Series, 452: 219–236. doi: 10.3354/meps09583

Ahn Y-H, Bricaud A, Morel A, 1992. Light backscattering efficiency and related properties of some phytoplankters. Deep-Sea Research, 39(11/12): 1835-1855

Ainsworth CH, Samhouri JF, Busch DS, Cheung WWL, Dunne J, Okey TA, 2011. Potential impacts of climate change on Northeast Pacific marine foodwebs and fisheries. ICES Journal of Marine Science, 68(6): 1217-1229. doi: 10.1093/icesjms/fsr043.

Aires-da-Silva A, Maunder MN, 2015. Status of bigeye tuna in the eastern Pacific Ocean in 2014 and outlook for the future. Inter-American Tropical Tuna Commission Stock Assess. Rep. 16, 13 p. Available at https://www.iattc.org/PDFFiles/StockAssessmentReports/_English/SAR16-1-BET-assessment-2014.pdf

Alejo-Plata C, Díaz-Jaimes P, Salgado-Ugarte IH, 2011. Sex ratios, size at sexual maturity, and spawning seasonality of dolphinfish (*Coryphaena hippurus*) captured in the Gulf of Tehuantepec, Mexico. Fisheries Research, 110: 207-216. doi: 10.1016/j.fishres.2011.04.008

Andersen KH, Pedersen M, 2010. Damped trophic cascades driven by fishing in model marine ecosystems. Proceedings of the Royal Society B: Biological Sciences, 277(1682): 795-802.

Aumont O, Bopp L, 2006. Globalizing results from ocean in situ iron fertilization studies. Global Biogeochemical Cycles, 20: GB2017, doi:10.1029/2005GB002591.

Barnes C, Bethea DM, Brodeur RD, Spitz J, Ridoux V, Pusineri C, Chase BC, Hunsicker ME, Juanes F, Kellermann A, Lancaster J, Ménard F, Bard F-X, Munk P, Pinnegar JK, Scharf FS, Rountree RA, Stergiou KI, Sassa C, Sabates A, Jennings S, 2008. Predator and prey body sizes in marine food webs. Ecology, 89: 881.

Bayliff WH, 1988. Growth of skipjack, *Katsuwonus pelamis*, and yellowfin, *Thunnus albacares*, tunas in the Eastern Pacific Ocean as estimated from tagging data. Inter-American Tropical Tuna Commission Bulletin, 19(4): 311-385.

Bell JD, Ganachaud A, Gehrke PC, Griffiths SP, Hobday AJ, Hoegh-Guldberg O, Johnson JE, Le Borgne R, Lehodey P, Lough JM, Matear RJ, Pickering TD, Pratchett MS, Sen Gupta A, Senina I, Waycott M, 2013. Mixed responses of tropical Pacific fisheries and aquaculture to climate change. Nature Climate Change, 3: 591–599. doi: 10.1038/NCLIMATE1838

Benoît E, Rochet M-J, 2004. A continuous model of biomass size spectra governed by predation and the effects of fishing on them. Journal of Theoretical Biology, 226: 9-21.

Bigelow K, Musyl MK, Poisson F, Kleiber P, 2006. Pelagic longline gear depth and shoaling. Fisheries Research, 77: 173-183. doi: 10.1016/j.fishres.2005.10.010

Billfish Working Group Report, 2014a. North Pacific swordfish (*Xiphiaus gladius*) stock assessment in 2014. International Scientific Committee for Tuna and Tuna-like Species in the North Pacific Ocean, Taipei, Chinese-Taipei. 85p.

Billfish Working Group Report, 2014b. Stock assessment of albacore tuna in the North Pacific Ocean in 2014. International Scientific Committee for Tuna and Tuna-like Species in the North Pacific Ocean. Taipei, Taiwan. 131p.

Billfish Working Group Report, 2015. Stock assessment update for striped marlin (*Kajikia audax*) in the Western and Central North Pacific Ocean through 2013. International Scientific Committee for Tuna and Tuna-like Species in the North Pacific Ocean, Kona, HI. 97p.

Billfish Working Group Report, 2016. Stock assessment update for blue marlin (*Makaira nigricans*) in the Pacific Ocean through 2014. International Scientific Committee for Tuna and Tuna-like Species in the North Pacific Ocean, Sapporo, Hokkaido, Japan. 90p.

Blanchard JL, Andersen KH, Scott F, Hintzen N, Piet G, Jennings S, 2014. Evaluating targets and trade-offs among fishieries and conservation objectives using a multispecies size spectrum model. Journal of Applied Ecology, 51(3): 612-622. doi: 10.1111/1365-2664.12238.

Blanchard JL, Dulvy NK, Jennings S, Ellis JR, Pinnegar JK, Tidd A, Kell LT, 2005. Do climate and fishing influence size-based indicators of Celtic Sea fish community structure? ICES Journal of Marine Science, 62(3): 405-411.

Blanchard JL, Heneghan RF, Everett JD, Trebilco R, Richardson AJ, 2017. From bacteria to whales: using functional size spectra to model marine ecosystems. Trends in Ecology and Evolution, 32(3): 174-186. doi: 10.1016/j.tree.2016.12.003

Blanchard JL, Jennings S, Holmes R, Harle J, Merino G, Allen JI, Holt J, Dulvy NK, Barange M, 2012. Potential consequences of climate change for primary productions and fish productions in large marine ecosystems. Philosophical Transactions of the Royal Society B, 367: 2979-2989. doi: 10.1098/rstb.2012.0231.

Blanchard JL, Jennings S, Law R, Castle MD, McCloghie P, Rochet M-J, Benoît E, 2009. How does abundance scale with body size in coupled size-structured food webs? Journal of Animal Ecology, 78: 270-280. doi: 10.1111/j.1365-2656.2008.01466.x.

Blanchard JL, Law R, Castle MD, Jennings S, 2011. Coupled energy pathways and the resilience of size-structured food webs. Theoretical Ecolology, 4: 289-300. doi: 10.1007/s12080-010-0078-9.

Block BA, Jonsen ID, Jorgensen SJ, Winship AJ, Shaffer SA, Bograd SJ, Hazen EL, Foley DG, Breed GA, Harrison A-L, Ganong JE, Swithenbank A, Castleton M, Dewar H, Mate BR, Shillinger GL, Schaefer KM, Benson SR, Weise MJ, Henry RW, Costa DP, 2011. Tracking apex marine predator movements in a dynamic ocean. Nature, 475: 86–90. doi:10.1038/nature10082

Boettiger C, Lang DT, Wainwright PC, 2012. rfishbase: exploring, manipulating, and visualizaing FishBase from R. Journal of Fish Biology, 81: 2030–2039. doi:10.1111/j.1095-8649.2012.03464.x

Boggs CH, 1992. Depth, capture time, and hooked longevity of longline-caught pelagic fish: timing bites of fish with chips. Fishery Bulletin 90: 642-658.

Bond AL, Lavers JL, 2014. Climate change alters the trophic niche of a declining, apex marine predator. Global Change Biology, 20: 2100–2107.

Bopp L, Resplandy L, Orr JC, Doney SC, Dunne JP, Gehlen M, Halloran P, Heinze C, Ilyina T, Séférian R, Tjiputra J, Vichi M, 2013. Multiple stressors of ocean ecosystems in the 21st century: projections with CMIP5 models. Biogeosciences, 10: 6225–6245. doi:10.5194/bg-10-6225-2013

Boyce DG, Tittensor DP, Worm B, 2008. Effects of temperature on global patterns of tuna and billfish richness. Marine Ecology Progress Series, 355: 267–297.

Brander KM, 2007. Global fish production and climate change. Proceedings of the National Academy of Sciences, 104(50): 19709–19714.

Brander K, 2013. Climate and current anthropogenic impacts on fisheries. Climatic Change, 119(1): 9–21. doi: 10.1007/s10584-012-0541-2

Bricaud A, Morel A, 1986. Light attenuation and scattering by phytoplanktonic cells: a theoretical modeling. Applied Optics, 25(4): 571-580.

Bricaud A, Morel A, Prieur L, 1983. Optical Efficiency Factors of Some Phytoplankters. Limnology and Oceanography, 28(5): 816-832.

Brown JH, Gillooly JF, Allen AP, Savage VM, West GB, 2004. Toward a metabolic theory of ecology. Ecology, 85: 1771–1789.

Burrows MT, Schoeman DS, Buckley LB, Moore P, Poloczanska ES, Brander KM, Brown C, Bruno JF, Duarte CM, Halpern BS, Holding J, Kappel CV, Kiessling W, O'Connor MI, Pandolfi MJ, Parmesan C, Schwing FB, Sydeman WJ, Richardson AJ, 2011. The pace of

shifting climate in marine and terrestrial ecosystems. Science, 334: 652-655. doi: 10.1126/science.1210288.

Cabré A, Marinov I, Bernardello R, Bianchi D, 2015a. Oxygen minimum zones in the tropical Pacific across CMIP5 models: mean state differences and climate change trends. Biogeosciences, 12: 5429-5454. doi: 10.5194/bg-12-5429-2015

Cabré A, Marinov I, Leung S, 2015b. Consistent global responses of marine ecosystems to future climate change across the IPCC AR5 earth system models. Climate Dynamics, 45: 1253–1280.

Chan G, Stavins R, Stowe R, Sweeney R, 2102. The SO_2 allowance trading tystem and the Clean Air Act amendments of 1990: reflections on twenty years of policy innovation. Cambridge, Mass.: Harvard Environmental Economics Program, January 2012.

Chang EKM, Guo Y, Xia X, 2012. CMIP5 multimodel ensemble projection of storm track change under global warming. Journal of Geophysical Research, 117: D23118.

Cheung WWL, Lam VWY, Sarmiento JL, Kearney K, Watson R, Zeller D, Pauly D, 2010. Large-scale redistribution of maximum fisheries catch potential in the global ocean under climate change. Global Change Biology, 16: 24-35. doi: 10.1111/j.1365-2486.2009.0195.x.

Cheung WWL, Reygondeau G, Frölicher TL, 2016. Large benefits to marine fisheries of meeting the 1.5°C global warming target. Science, 354(6319): 1591–1594. doi: 10.1126/science.aag2331

Cheung WWL, Sarmiento JL, Dunne J, Frölicher TL, Lam VWY, Palomares MLD, Watson R, Pauly D, 2013. Shrinking of fishes exacerbates impacts of global ocean changes on marine ecosystems. Nature Climate Change, 3: 254-258. doi: 10.1038/NCLIMATE1691.

Christensen V, Walters CJ, 2004. Ecopath with Ecosim: methods, capabilities and limitations. Ecological Modelling, 172: 109-139.

Christensen V, Walters CJ, Pauly D, Roffest R, 2008. Ecopath with Ecosim Version 6 User Guide. University of British Columbia, Vancouver.

Christian JR, Arora VK, Boer GJ, Curry CL, Zahariev K, Denman KL, Flato GM, Lee WG, Merryfield WJ, Roulet NT, Scinocca JF, 2010. The global carbon cycle in the Canadian Earth system model (CanESM1): preindustrial control simulation. Journal of Geophysical Research, 115: G03014. doi:10.1029/2008JG000920

Chust G, Allen JI, Bopp L Schrum C, Holt J, Tsiaras K, Zavatarelli M, Chifflet M, Cannaby H, Dadou I, Daewel U, Wakelin SL, Machu E, Pushpadas D, Butenschon M, Artioli Y, Petihakis G, Smith C, Garçon V, Goubanova K, Le Vu B, Fach BA, Salihoglu B, Clementi E, Irigoien X, 2014. Biomass changes and trophic amplification of plankton in a warmer ocean. Global Change Biology, 20: 2124–2139. doi: 10.1111/gcb.12562

Clausen R, York R, 2008. Economic Growth and Marine Biodiversity: Influence of Human Social Structure on Decline of Marine Trophic Levels. Conservation Biology, 22(2): 458–466. doi: 10.1111/j.1523-1739.2007.00851.x

Collins WJ, Bellouin N, Doutriaux-Boucher M, Gedney N, Halloran P, Hinton T, Hughes J, Jones CD, Joshi M, Liddicoat S, Martin G, O'Connor F, Rae J, Senior C, Sitch S, Totterdell I, Wiltshire A, Woodward S, 2011. Development and evaluation of an Earth-system model – HadGEM2. Geoscientific Model Development, 4: 1051–1075. doi:10.5194/gmd-4-1051-2011

Cox SP, Essington TE, Kitchell JF, Martell SJD, Walters CJ, Boggs C, Kaplan I, 2002. Reconstructing ecosystem dynamics in the central Pacific Ocean, 1952–1998. II. A preliminary assessment of the trophic impacts of fishing and effects on tuna dynamics. Canadian Journal of Fisheries and Aquatic Science, 59: 1736-1747. doi: 10.1139/F02-138.

Czech B, 2008. Prospects for Reconciling the Conflict between Economic Growth and Biodiversity Conservation with Technological Progress. Conservation Biology, 22(6): 1389–1398. doi: 10.1111/j.1523-1739.2008.01089.x

Daufresne M, Lengfellner K, Sommer U, Carpenter SR, 2009. Global warming benefits the small in aquatic ecosystems. Proceedings of the National Academy of Sciences of the United States of America, 106(31): 12788-12793. doi: 10.1073/pnas.0902080106.

Del Raye G, Weng KC, 2015. An aerobic scope-based habitat suitability index for predicting the effects of multi-dimensional climate change stressors on marine teleosts. Deep-Sea Research II: 113, 280-290. doi: 10.1016/j.dsr2.2015.01.014

Delworth TL, Broccoli AJ, Rosati A, Stouffer RJ, Balaji V, Beesley JA, Cooke WF, Dixon KW, Dunne J, Dunne KA, Durachta JW, Findell KL, Ginoux P, Gnanadesikan A, Gordon CT, Griffies SM, Gudgel R, Harrison MJ, Held IM, Hemler RS, Horowitz LW, Klein SA, Knutson TR, Kushner PJ, Langenhorst AR, Lee H-C, Lin S-J, Lu J, Malyshev SL, Milly PCD, Ramaswamy V, Russell J, Schwarzkopf MD, Shevliakova E, Sirutis JJ, Spelman MJ, Stern WF, Winton M, Wittenberg AT, Wyman B, Zeng F, Zhang R, 2006. GFDL's CM2 global coupled climate models. Part I: formulation and simulation characteristics. Journal of Climate, 19: 643–674.

DeMartini EE, Uchiyama JH, Humphreys RL, Sampaga JD, Williams HA, 2007. Age and growth of swordfish (*Xiphias gladius*) caught by the Hawaii-based pelagic longline fishery. Fishery Bulletin, 105: 356-367.

DeMartini EE, Uchiyama JH, Williams HA, 2000. Sexual maturity, sex ratio, and size composition of swordfish, *Xiphias gladius*, caught by the Hawaii-based pelagic longline fishery. Fishery Bulletin, 98(3): 489-506.

Dietz T, Rosa EA, York R, 2007. Driving the human ecological footprint. Frontiers in Ecology and the Environment, 5(1): 13–18.

Doney SC, Bopp M, Long MC, 2014. Historical and future trends in ocean climate and biogeochemistry. Oceanography, 27: 108–119. doi: 10.5670/oceanog.2014.14

Dufresne J-L, Foujols M-A, Denvil S, Caubel A, Marti O, Aumont O, Balkanski Y, Bekki S, Bellenger H, Benshila R, Bony S, Bopp L, Braconnot P, Brockmann P, Cadule P, Cheruy F, Codron F, Cozic A, Cugnet D, de Noblet N, Duvel J-P, Ethé C, Fairhead L, Fichefet T, Flavoni S, Friedlingstein P, Grandpeix J-Y, Guez L, Guilyardi E, Hauglustaine D, Hourdin F, Idelkadi A, Ghattas J, Joussaume S, Kageyama M, Krinner G, Labetoulle S, Lahellec A, Lefebvre M-P, Lefevre F, Levy C, Li ZX, Lloyd J, Lott F, Madec G, Mancip M, Marchand M, Masson S, Meurdesoif Y, Mignot J, Musat I, Parouty S, Polcher J, Rio C, Schulz M, Swingedouw D, Szopa S, Talandier C, Terray P, Voivy N, Vuichard N, 2013. Climate change projections using the IPSL-CM5 Earth System Model: from CMIP3 to CMIP5. Climate Dynamics, 40, 2123–2165. doi: 10.1007/s00382-012-1636-1

Dunne JP, Armstrong RA, Gnanadesikan A, Sarmiento JL, 2005. Empirical and mechanistic models for the particle export ratio. Global Biogeochemical Cycles, 19: GB4026.

Dunne JP, Hales B, Toggweiler JR, 2012. Global calcite cycling constrained by sediment preservation controls. Global Biogeochemical Cycles, 26, GB3023. doi: 10.1029/2010GB003935

Dunne JP, John JG, Shevliakova E, Stouffer RJ, Krasting JP, Malyshev SL, Milly PCD, Sentman LT, Adcroft AJ, Cooke W, Dunne KA, Griffies SM, Hallberg RW, Harrison MJ, Levy H, Wittenberg AT, Phillips PJ, Zadeh N, 2013. GFDL's ESM2 global coupled climate-carbon Earth System Models. Part II: carbon system formulation and baseline simulation characteristics. Journal of Climate, 26: 2247–2267. doi: 10.1175/JCLI-D-12-00150.1

Edwards AM, Robinson JPW, Plank MJ, Baum JK, Blanchard JL, 2017. Testing and recommending methods for fitting size spectra to data. Methods in Ecology and Evolution, 8(1): 57–67. doi: 10.1111/2041-210X.12641

Enberg K, Jørgensen C, Dunlop ES, Varpe Ø, Boukal DS, Baulier L, Eliassen S, Heino M, 2012. Fishing-induced evolution of growth: concepts, mechanism, and the empirical evidence. Marine Ecology, 33: 1-25. doi: 10.1111/j.1439-0485.2011.00460.x

Essington TE, 2006. Pelagic ecosystem response to a century of commercial fishing and whaling. In: Estes, J.A., (Ed.), Whales, whaling, and ocean ecosystems, vol. xvi, 402 p. University of California Press, Berkeley, pp. 38-49.

Essington TE, 2007. Evaluating the sensitivity of a trophic mass-balance model (Ecopath) to imprecise data inputs. Canadian Journal of Fisheries and Aquatic Sciences, 64: 628-637. doi: 10.1139/F07-042.

Evans MR, Bithell M, Cornell SJ, Dall SRX, Díaz S, Emmott S, Ernande B, Grimm V, Hodgson DJ, Lewis SL, Mace GM, Morecroft M, Moustakas A, Murphy E, Newbold T, Norris KJ, Petchey O, Smith M, Travis JMJ, Bentin TG, 2013. Predictive systems ecology. Proceedings of the Royal Society B, 280: 20131452. doi: 10.1098/rspb.2013.1452.

Eyring V, Bony S, Meehl GA, Senior CA, Stevens B, Stouffer RJ, Taylor KE, 2016. Overview of the Coupled Model Intercomparison Project Phase 6 (CMIP6) experimental design and organization. Geoscientific Model Development, 9(5): 1937–1958. doi: 10.5194/gmd-9-1937-2016

Federal Register, 2016. Papahānaumokuākea Marine National Monument expansion. Fedederal Register, 81: 60227-60234.

Figueiredo C, Diogo H, Pereira JG, Higgins RM, 2015. Using information-based methods to model age and growth of the silver scabbardfish, *Lepidopus caudatus*, from the mid-Atlantic Ocean. Marine Biology Research, 11: 86-96. doi: 10.1080/17451000.2014.889307

Food and Agriculture Organization of the United Nations (FAO), 2012. FAO Yearbook, Fishery and Aquaculture Statistics, Capture Production. FAO, Rome, Italy.

Francis M, Griggs L, Maolagáin CO, 2004. Growth rate, age at maturity, longevity and natural mortality rate of moonfish (*Lampris guttatus*). Final Research Report for the Ministry of Fisheries Research Project TUN2003-01, Objective 1, 28p.

Froese R, Pauly D (Eds.), 2012 and 2017. FishBase. Available at http://www.fishbase.org

Fu C, Travers-Trolet M, Velez L, Grüss A, Bundy A, Shannon LJ, Fulton EA, Akoglu E, Houle JE, Coll M, Verley P, Heymans JJ, John E, Shin Y-J, 2018. Risky business: The combined effects of fishing and changes in primary productivity on fish communities. Ecological Modelling, 368: 265–276. doi: 10.1016/j.ecolmodel.2017.12.003

Garcia HE, Locarnini RA, Boyer TP, Antonov JI, Mishonov AV, Baranova OK, Zweng MM, Reagan JR, Johnson DR, 2013. World ocean atlas 2013. Volume 3: dissolved oxygen, apparent oxygen utilization, and oxygen saturation. NOAA Atlas NESDIS 75, 27 p.

Gårdmark A, Lindegren M, Neuenfeldt S, Blencker T, Heikinheimo O, Müller-Karulis B, Niiranen S, Tomczak MT, Aro E, Wikström A, Möllmann C, 2013. Biological ensemble modeling to evaluate potential futures of living marine resources. Ecological Applications, 23(4): 742-754.

Gardner JL, Peters A, Kearney MR, Joseph L, Heinsohn R, 2011. Declining body size: a third universal response to warming? Trends in Ecology and Evolution, 26(6): 285-291. doi: 10.1016/j.tree.2011.03.005

Gibbs RH, 1960. *Alepisaurus brevirostris*, a new species of lancetfish from the western North Atlantic. Museum of Comparative Zoology, 1-16.

Gilman E, Chaloupka M, Read A, Dalzell P, Holetschek J, Curtice C. 2012. Hawaii longline tuna fishery temporal trends in standardized catch rates and length distributions and effects on pelagic and seamount ecosystems. Aquatic Conservation, 22: 446-488. doi: 10.1002/acq.2237

Giorgetta MA, Jungclaus J, Reick CH, Legutke S, Bader J, Böttinger M, Brovkin V, Crueger T, Esch M, Fieg K, Glushak K, Gayler V, Haak H, Hollweg H-D, Ilyina T, Kinne S, Kornblueh L, Matei D, Mauritsen T, Mikolajewicz U, Mueller W, Notz D, Pithan F, Raddatz T, Rast S, Redler R, Roeckner E, Schmidt H, Schnur R, Segschneider J, Six KD, Stockhause M, Timmreck C, Wegner J, Widmann H, Weiners K-H, Claussen M, Marotzke J, Stevens B, 2013. Climate and carbon cycle changes from 1850 to 2100 in MPI-ESM simulations for the Coupled Model Intercomparison Project phase 5. Journal of Advances in Modeling Earth Systems, 5: 572–597. doi: 10.1002/jame.20038

Global Burden of Disease (GBD), 2017. Population and Fertility Collaborators, 2018. Population and fertility by age and sex for 195 countries and territories, 1950 – 2017: a systematic analysis for the Global Burden of Disease Study 2017. Lancet, 392(10159): 1995-2051. doi: 10.1016/S0140-6736(18)32278-5

Gnanadesikan A, Dixon KW, Griffies MS, Balaji V, Barriero M, Beesley JA, Cooke WF, Delworth TL, Gerdes R, Harrison MJ, Held IM, Hurlin WJ, Lee H-C, Liang Z, Nong G, Pacanowski RC, Rosati A, Russell J, Samuels BL, Song Q, Spelman MJ, Stouffer RJ, Sweeney CO, Vecchi G, Winton M, Wittenberg AT, Zeng F, Zhang F, Dunne JP, 2006. GFDL's CM2 global coupled climate models. Part II: the baseline ocean simulation. Journal of Climate, 19: 675-697.

Gnanadesikan A, Dunne JP, John J, 2011. What ocean biogeochemical models can tell us about bottom-up control of ecosystem variability. ICES Journal of Marine Science, 68(6): 1030-1044. doi: 10.1093/icesjms/fsr068.

Gregg WW, Casey NW, 2007. Modeling coccolithophores in the global ocean. Deep-Sea Research II 54: 447-477. doi:10.1016/j.dsr2.2006.12.007

Grenouillet G, Comte L, 2014. Illuminating geographical patterns in species' range shifts. Global Change Biology, 20: 3080–3091.

Griggs LH, Richardson K, 2005. New Zealand tuna fisheries, 2001 and 2002. New Zealand Fisheries Assessment Report 2005/4. 58 p.

Hamilton BE, Martin JA, Osterman MJK, Driscoll AK, Rossen LM, 2018. Births: Provisional data for 2017. Vital Statistics Rapid Release; no 4. Hyattsville, MD: National Center for Health Statistics. May 2018. Available at https://www.cdc.gov/nchs/data/vsrr/report004.pdf.

Hampton J, 2000. Natural Mortality rates in tropical tunas: size really does matter. Canadian Journal of Fisheries and Aquatic Science, 57: 1002-1010.

Harada T, Ozawa T, 2003. Age and growth of *Lestrolepis japonica* (Aulopiformes: Paralepididae) in Kagoshima Bay, southern Japan, Ichthyology Research, 50: 182-185. doi: 10.1007/s10228-002-0144-4

Harley S, Davies N, Hampton J, McKechnie S, 2014. Stock assessment of bigeye tuna in the western and central Pacific Ocean. West. Cent. Pac. Fish. Comm. WCPFC-SC10-2014/SA-WP-01, 115 p. Available at https://www.wcpfc.int/system/files/SC10-SA-WP-01%20%5BBET%20Assessment%5D_rev1_25July.pdf

Hawn DR, Collette BB, 2012. What are the maximum size and live body coloration of opah (Teleostei: Lampridae: *Lampris* species)? Ichthyology Research, 59(3): 272-275. doi: 10.1007/s10228-012-0277z

Haynie AC, Pfeiffer L, 2012. Why economics matters for understanding the effects of climate change on fisheries. ICES Journal of Marine Science, 69(7): 1160–1167. doi: 10.1093/icesjms/fss021

Hazen EL, Jorgensen S, Rykaczewski RR, Bograd SJ, Foley DG, Jonsen ID, Shaffer SA, Dunne JP, Costa DP, Crowder LB, Block BA, 2013. Predicted habitat shifts of Pacific top predators in a changing climate. Nature Climate Change, 3, 234–238. doi: 10.1038/NCLIMATE1686

Heithaus MR, Frid A, Wirsing AJ, Worm B, 2008. Predicting ecological consequences of marine top predator declines. Trends in Ecology and Evolution, 23(4): 202–210. doi: 10.1016/j.tree.2008.01.003

Howell EA, Bograd SJ, Hoover AL, Seki MP, Polovina JJ, 2015. Variation in phytoplankton composition between two North Pacific frontal zones along 158°W during winter–spring 2008–2011. Progress in Oceanography, 150: 3-12. doi: 10.1016/j.pocean.2015.06.003.

Howell EA, Hawn DR, Polovina JJ, 2010. Spatiotemporal variability in bigeye tuna (*Thunnus obesus*) dive behavior in the central North Pacific Ocean. Progress in Oceanography, 86: 81–93.

Howell EA, Wabnitz CCC, Dunne JP, Polovina JP, 2013. Climate-induced primary productivity and fishing impacts on the Central North Pacific ecosystem and Hawaii-based pelagic longline fishery. Climatic Change, 119: 79-83. doi: 10.1007/s10584-012-0597-z.

Ilyina T, Six KD, Segschneider J, Maier-Reimer E, Li H, Núñez-Riboni I, 2013. Global ocean biogeochemistry model HAMOCC: Model architecture and performance as component of the MPI-Earth system model in different CMIP5 experimental realizations, Journal of Advances in Modeling Earth Systems, 5: doi:10.1029/2012MS000178.

Itano DG, 2000. The reproductive biology of yellowfin tuna (*Thunnus albacares*) in Hawaiian waters and the western tropical Pacific Ocean: project summary. University of Hawaii School of Ocean and Earth Science and Technology Report 00-01. Honolulu, HI. 69.

Jennings S, Blanchard JL, 2004. Fish abundance with no fishing: predictions based on macroecological theory. Journal of Animal Ecology, 73, 632-642.

Jennings S, Brander K, 2010. Predicting the effects of climate change on marine communities and the consequence for fisheries. Journal of Marine Systems, 79: 418-426. doi: 10.1016/j.jmarsys.2008.12.016.

Jennings S, Mélin F, Blanchard JL, Forster RM, Dulvy NK, Wilson RW, 2008. Global-scale predictions of community and ecosystem properties from simple ecological theory. Proceedings of the Royal Society B, 275: 1375-1383. doi: 10.1098/rspb.2008.0192.

Jones MC, Cheung WWL, 2014. Multi-model ensemble projections of climate change effects of global marine biodiversity. ICES Journal of Marine Science, 72(3): 741-752. doi: 10.1093/icesjms/fsul72.

Kearney KA, Stock C, Sarmiento JL, 2013. Amplification and attenuation of increased primary production in a marine food web. Marine Ecology Progress Series, 491: 1-14. doi: 10.3354/meps10484.

Kitchell JF, Essington TE, Boggs CH, Schindler DE, Walters CJ, 2002. The role of sharks and longline fisheries in a pelagic ecosystem of the central Pacific. Ecosystems, 5: 202-216. doi: 10.1007/s10021-001-0065-5

Kitchell JF, Martell SJD, Walters CJ, Jensen OP, Kaplan IC, Watters J, Essington TE, Boggs CH, 2006. Billfishes in an ecosystem context, Bulletin of Marine Science, 79(3): 669–682.

Koenigstein S, Mark FC, Gößling-Reisemann S, Reuter H, Pörtner H-O, 2016. Modelling climate change impacts on marine fish populations: process-based integration of ocean warming, acidification and other environmental drivers. Fish and Fisheries, 17(4): 972–1004. doi: 10.1111/faf.12155

Koslow JA, Goericke R, Lara-Lopez A, Watson W, 2011. Impact of declining intermediate-water oxygen on deepwater fishes in the California Current. Marine Ecology Progress Series, 436: 207–218.

Kume S, 1969. Ecologial studies on bigeye tuna—V: A critical review on distribution, size composition and stock structure of bigeye tuna in the North Pacific Ocean (north of 16°N). Bulletin of the Far Seas Fishery Research Laboratory, 1: 57-75.

Law R, Plank MJ, James A, Blanchard JL, 2009. Size-spectra dynamics from stochastic predation and growth of individuals. Ecology, 90(3): 802-811.

Lefort S, Aumont O, Bopp L, Arsouze T, Gehlen M, Maury O, 2015. Spatial and body-size dependent response of marine pelagic communities to projected global climate change. Global Change Biology, 21, 154–164.

Lehodey P, Hampton J, Brill RW, Nicol S, Senina I, Calmettes B, Pörtner HO, Bopp L, Ilyina T, Bell JD, Sibert J, 2011. Vulnerability of oceanic fisheries in the tropical Pacific to climate change. In: Vulnerability of Tropical Pacific Fisheries and Aquaculture to Climate Change (eds Bell JD, Johnson JE, Hobday AJ), pp. 433–492. Secretariat of the Pacific Community, Noumea, New Caledonia.

Lehodey P, Semoma I, Calmettes B, Hampton J, Nicol S, 2013. Modeling the impact of climate change on Pacific skipjack tuna population and fisheries. Climatic Change, 119: 95–109.

Lehodey P, Senina I, Sibert J, Bopp L, Calmettes B, Hampton J, Mutugudde R, 2010. Preliminary forecasts of Pacific bigeye tuna population trends under the A2 IPCC scenario. Progress in Oceanography, 86: 302-315. doi: 10.1016/j.pocean.2010.021.

Liu K-M, Chiang P-J, Chen C-T, 1998. Age and growth estimates of the bigeye thresher shark, Alopias superciliosus, in northeastern Taiwan waters. Fishery Bulletin, 96: 482-491.

Locarnini RA, Mishonov AV, Antonov JI, Boyer TP, Garcia HE, Baranova OK, Zweng MM, Paver CR, Reagan JR, Johnson DR, Hamilton M, Seidov D, 2013. World Ocean Atlas 2013, Volume 1: Temperature. Levitus S, Ed., Mishonov A, Technical Ed., NOAA Atlas NESDIS 73. National Oceanographic Data Center, Silver Spring, MD, USA.

Lorenzo J, Pajuelo J, 1999. Biology of a deep benthopelagic fish, roudi escolar *Promethichthys prometheus* (Gempylidae), off the Canary Islands, Fishery Bulletin: 97, 92-99.

Mackinson S, Daskalov G, Heymans JJ, Neira S, Arancibia H, Zetina-Rejón M, Jiang H, Cheng HQ, Coll M, Arreguin-Sanchez F, Keeble K, Shannon L, 2009. Which forcing factors fit? Using ecosystem models to investigate the relative influence of fishing and changes in primary productivity on the dynamics of marine ecosystems. Ecological Modelling, 220: 2972-2987. doi: 10.1016/j.ecolmodel.2008.10.021.

MacLeod R, MacLeod CD, Learmonth JA, Jepson PD, Reid RJ, Deaville R, Pierce GJ, 2007. Mass-dependent predation risk and lethal dolphin–porpoise interactions. Proceedings of the Royal Society B: Biological Sciences, 274(1625): 2587–2593. doi: 10.1098/rspb.2007.0786

Maunder MN, 2001. Growth of skipjack tuna (*Katsuwonus pelamis*) in the Eastern Pacific Ocean, as estimated from tagging data. Inter-American Tropical Tuna Commission Bulletin, 22(2): 95-131.

Metcalfe JD, Le Quesne WJF, Cheung WWL, Righton DA, 2012. Conservation physiology for applied management of marine fish: an overview with perspectives on the role and value of telemetry. Philosophical Transactions of the Royal Society B: Biological Sciences, 367(1596): 1746–1756. doi: 10.1007/s00360-009-0442-5

Mills JH, Waite TA, 2009. Economic prosperity, biodiversity conservation, and the environmental Kuznets curve. Ecological Economics, 68(7): 2087–2095. doi: 10.1016/j.ecolecon.2009.01.017

Montero-Serra I, Edwards M, Genner MJ, 2015. Warming shelf seas drive the subtropicalization of European pelagic fish communities. Global Change Biology, 21: 144–153.

Moore HL, 1951. Estimation of age and growth of yellowfin tuna (Neothunnus macropterus) in Hawaiian waters by size frequencies. Fishery Bulletin, 52: 131-149.

Moore JK, Fu W, Primeau F, Britten GL, Lindsay K, Long M, Doney SC, Mahowald N, Hoffman F, Randerson JT, 2018. Sustained climate warming drives declining marine biological productivity. Science, 359(6380): 1139–1143. doi: 10.1126/science.aao6379

Morales-Nin B, Sena-Carvalho D, 1996. Age and growth of the black scabbard fish (*Aphanopus carbo*) off Madeira, Fisheries Research, 25: 239-251.

Morán XAG, López-Urrutia A, Calvo-Díaz A, Li WKW, 2010. Increasing importance of small phytoplankton in a warmer ocean. Global Change Biology, 16: 1137-1144. doi: 10.1111/j.1365-2486.2009.01960.x.

Morris DJ, Speirs DC, Cameron AI, Heath MR, 2014. Global sensitivity analysis of an end-to-end marine ecosystem model of the North Sea: factors affecting the biomass of fish and benthos. Ecological Modelling, 273: 251-263. doi: 10.1016/j.ecolmodel.2013.11.019.

Nakićenović N, Alcamo J, Davis G, de Vries B, Fenhann J, Gaffin S, Gregory K, Grübler A, Jung TY, Kram T, La Rovere EL, Michaelis L, Mori S, Morita T, Pepper W, Pitcher H, Price L, Riahi K, Roehrl A Rogner H-H, Sankovski A, Schlesinger M, Shukla P, Smith S, Swart R, van Rooijen S, Victor N, Dadi Z, 2000. IPCC Special Report on Emissions Scenarios. Cambridge University Press, Cambridge, UK, and New York, USA, 599 pp.

National Marine Fisheries Service (NMFS), 2016a. Annual Commercial Landing Statistics, National Marine Fisheries Service, Available at http://www.st.nmfs.noaa.gov/commercial-fisheries/commercial-landings/annual-landings/index

National Marine Fisheries Service (NMFS), 2016b. Total Commercial Fishery Landings At Major U. S. Ports Summarized By Year And Ranked By Dollar Value, Available at https://www.st.nmfs.noaa.gov/commercial-fisheries/commercial-landings/other-specialized-programs/total-commercial-fishery-landings-at-major-u-s-ports-summarized-by-year-and-ranked-by-dollar-value/index

National Marine Fisheries Service (NMFS), 2017. Fisheries of the United States, 2016. U.S. Department of Commerce, NOAA Current Fishery Statistics No. 2016.

National Marine Fisheries Service (NMFS), 2018. Fisheries Economics of the United States, 2016. U.S. Dept. of Commerce, NOAA Tech. Memo. NMFS-F/SPO-187, 243 p.

Nicol SJ, Allain V, Pilling GM, Polovina J, Coll M, Bell J, Dalzell P, Sharples P, Olson R, Griffiths S, Dambacher JM, Young J, Lewis A, Hampton J, Molina JJ, Hoyle S, Briand K, Bax N, Lehodey P, Williams P, 2013. An ocean observation system for monitoring the affects of climate change on the ecology and sustainability of pelagic fisheries in the Pacific Ocean. Climatic Change, 119(1): 131–145. doi: 10.1007/s10584-012-0598-y

Nicol S, Hoyle S, Farley J, Muller B, Retalmai S, Sisior K, Williams A, 2011. Bigeye tuna age, growth and reproductive biology (Project 35). Western and Central Pacific Fisheries Commission report WCPRC-SC7-2011/SA-WP-01, Revision 1 3 August 2011. Secretariat of the Pacific Community, Pohnpei, Federated States of Micronesia. 13p.

Nordhaus WD, 2013. The Climate Casino: Risk, Uncertainty, and Economics for a Warming World. Yale University Press, New Haven and London. 378.

Nordhaus WD, 2018. Prize Lecture. NobelPrize.org. Nobel Media AB 2018. Available at https://www.nobelprize.org/prizes/economic-sciences/2018/nordhaus/lecture/

O'Brien TD, 2010. COPEPOD: The Global Plankton Database. An overview of the 2010 database contents, processing methods, and access interface. U.S. Dep. Commerce, NOAA Tech. Memo., NMFS-F/ST-36, 28 pp.

Ockendon N, Baker DJ, Carr JA, White EC, Almond REA, Amano T, Bertram E, Bradbury RB, Bradley C, Butchart SHM, Doswald N, Foden W, Gill DJC, Green RE, Sutherland WJ, Tanner EVJ, Pearce-Higgins JW, 2014. Mechanisms underpinning climatic impacts on natural populations: altered species interactions are more important than direct effects. Global Change Biology, 20: 2221–2229. doi: 10.1111/gcb.12559

Olson RJ, Duffy LM, Kuhnert PM, Galván-Magaña F, Bocanegra-Castillo N, Alatorre-Ramírez V, 2014. Decadal diet shift in yellowfin tuna *Thunnus albacares* suggests broad-scale food web changes in the eastern tropical Pacific Ocean. Marine Ecology Progress Series, 497: 157-178. doi:10.3354/meps10609.

Ortega-Garcia S, Klett-Traulsen A, Rodriguez-Sanchez R, 2006. Some biological aspects of blue marlin (*Makaira nigricans*) in the recreational fishery at Cabo San Lucas, Baja California Sur, Mexico. Bulletin of Marine Science, 79: 739-746.

Ortuño Crespo G, Dunn DC, 2017. A review of the impacts of fisheries on open-ocean ecosystems. ICES Journal of Marine Science, 74(9): 2283–2297. doi: 10.1093/icesjms/fsx084

Pauly D, Christensen V, Dalsgaard J, Froese R, Torres F, 1998. Fishing down marine food webs. Science, 279: 860-863. doi: 10.1126/science.279.5352.860.

Pentz B, Klenk N, Ogle S, Fisher JAD, 2018. Can regional fisheries management organizations (RFMOs) manage resources effectively during climate change? Marine Policy, 92: 13–20. doi: 10.1016/j.marpol.2018.01.011

Perry RI, Cury P, Brander K, Jennings S, Möllmann C, Planque B, 2010. Sensitivity of marine systems to climate and fishing: Concepts, issues and management responses. Journal of Marine Systems, 79: 427-435. doi: 10.1016/j.marsys.2008.12.017.

Pikitch EK, Santora C, Babcock EA, Bakun A, Bonfil R, Conover DO, Dayton P, Doukakis P, Fluharty D, Heneman B, Houde ED, Link J, Livingston PA, Mangel M, McAllister MK, Pope J, Sainsbury KJ, 2004. Ecosystem-Based Fishery Management. Science, 305(5682): 346–347. doi: 10.1126/science.1098222

Pinsky ML, Worm B, Fogarty MJ, Sarmiento JL, Levin SA, 2013. Marine taxa track local climate velocities. Science, 341: 1239-1242. doi: 10.1126/science.1239352.

Polovina JJ, 1984. Model of a coral reef ecosystem I. The ECOPATH model and its application to French Frigate Shoals. Coral Reefs, 3: 1-11.

Polovina JJ, Abecassis M, Howell EA, Woodworth P, 2009. Increases in the relative abundance of mid-trophic level fishes concurrent with declines in apex predators in the subtropical North Pacific, 1996–2006. Fishery Bulletin, 107: 523-531.

Polovina JJ, Dunne JP, Woodworth PA, Howell EA, 2011. Projected expansion of the subtropical biome and contraction of the temperature and equatorial upwelling biomes in the North Pacific under global warming. ICES Journal of Marine Science, 68: 986–995.

Polovina JJ, Hawn D, Abecassis M, 2008. Vertical movement and habitat of opah (*Lampris guttatus*) in the central North Pacific recorded with pop-up archival tags. Marine Biology, 153(3): 257-267. doi: 10.1007/s00227-007-0801-2

Polovina JJ, Howell E, Kobayashi DR, Seki MP, 2001. The transition zone chlorophyll front, a dynamic global feature defining migration and forage habitat for marine resources. Progress in Oceanography, 49: 469–483.

Polovina JJ, Howell E, Kobayashi DR, Seki MP, 2015. The transition zone chlorophyll front updated: advances from a decade of research. Progress in Oceanography, 150: 79-85. doi: 10.1016/j.pocean.20105.01.006.

Polovina JJ, Woodworth PA, 2012. Declines in phytoplankton cell size in the subtropical oceans estimated from satellite remotely-sensed temperature and chlorophyll, 1998-2007. Deep-Sea Research II, 77-80: 82-88. doi: 10.1016/j.dsr2.2012.04.006

Polovina JJ, Woodworth-Jefcoats PA, 2013. Fishery-induced changes in the subtropical Pacific pelagic ecosystem: observations and theory. PLoS ONE, 8: e62341. doi: 10.1371/journal.pone.0062341.

Pörtner HO, 2012. Integrating climate-related stressor effects on marine organisms: unifying principles linking molecule to ecosystem-level changes. Marine Ecology Progress Series. 470: 273-290. doi: 10.3354/meps10123

Pörtner HO, Peck MA, 2010. Climate change effects on fishes and fisheries: toward a cause-and-effect understanding. Journal of Fish Biology. 77: 1745-1779. doi: 10.1111/j.1095-8649.2010.02783.x

Portner EJ, Polovina JJ, Choy CA, 2017. Patterns of micronekton diversity across the North Pacific Subtropical Gyre observed from the diet of longnose lancetfish (*Alepisaurus ferox*). Deep-Sea Research Part I, 125: 40-51. doi: 10.1016/j.dsr.2017.04.013

Prince ED, 1991. Estimating age and growth of young Atlantic blue marlin *Makaira nigricans* from otolith microstructure. Fishery Bulletin, 89: 441-459.

Queirós AM, Fernandes J, Genevier L, Lynam CP 2018. Climate change alters fish community size-structure, requiring adaptive policy targets. Fish and Fisheries, 19(4): 613–621. doi: 10.1111/faf.12278

Reum JCP, Blanchard JL, Holsman KK, Aydin A, Punt AE, 2019. Species-specific ontogenetic diet shifts attenuate trophic cascades and lengthen food changes in exploited systems. Oikos, In Press. doi: 10.1111/oik.05630

Riahi K, Rao S, Krey V, Cho C, Chirkov V, Fischer G, Kindermann G, Nakicenovic N, Rafaj P, 2011. RCP 8.5 – a scenario of comparatively high greenhouse gas emissions. Climatic Change, 109: 33–57. doi: 10.1007/s10584-011-0149-y

Rice J, Harley S, Davies N, Hampton J, 2014. Stock assessment of skipjack tuna in the Western and Central Pacific Ocean. Western and Central Pacific Fisheries Commission report WCPFC-SC10-2014/SA-WP-05, Rev1 25 July 2014. Secretariat of the Pacific Community, Noumea, New Caledonia. 125 p.

Rochet M-J, Benoît E, 2012. Fishing destabilized the biomass flow in the marine size spectrum. Proceedings of the Royal Society B, 279: 284-292. doi: 10.1098/rspb.2011.0893.

Romanou A, Romanski J, Gregg WW, 2014. Natural ocean carbon cycle sensitivity to the parameterizations of the recycling in a climate model. Biogeosciences, 11: 1137–1154.

Rountrey AN, Coulson PG, Meeuwig JJ, Meekan M, 2014. Water temperature and fish growth: otoliths predict growth patterns of a marine fish in a changing climate. Global Change Biology, 20(8): 2450–2458. doi: 10.1111/gcb.12617

Rykaczewski RR, Dunne JP, 2010. Enhanced nutrient supply to the California Current Ecosystem with global warming and increased stratification in an earth system model. Geophysical Research Letters 37, L21606. doi: 10.1029/2010GL045019.

Saha S, Nadiga S, Thiaw C, Wang J, Wang W, Zhang Q, Van den Dool HM, Pan H-L, Moorthi S, Behringer D, Stokes D, Peña M, Lord S, White G, Ebisuzaki W, Peng P, Xie P, 2006. The NCEP Climate Forecast System. Journal of Climate, 19: 3483-3517. doi: 10.1175/JCLI3812.1

Sarmiento JL, Slater R, Barber R, Bopp L, Doney SC, Hirst AC, Kleypas J, Matear R, Mikolajewicz U, Monfray P, Soldatov V, Spall SA, Stouffer R, 2004. Response of ocean ecosystems to climate warming. Global Biogeochemical Cycles, 18: GB3003. doi: 10.1029/2003GB002134

Sathyendranath S, Lazzara L, Prieur L, 1987. Variations in the Spectral Values of Specific Absorption of Phytoplankton. Limnology and Oceanography, 32(2): 403-415.

Schaefer KM, Fuller DW, 2007. Vertical movement patterns of skipjack tuna (*Katsuwonus pelamis*) in the eastern equatorial Pacific Ocean, as revealed with archival tags. Fishery Bulletin, 105: 379-389.

Schaefer K, Fuller D, Hampton J, Caillot S, Leroy B, Itano D. 2015. Movements, dispersion, and mixing of bigeye tuna (*Thunnus obesus*) tagged and released in the equatorial Central Pacific Ocean, with conventional and archival tags. Fisheries Research, 161: 336-355. doi: 10.1016/j.fishres.2014.08.018

Scheff J, Frierson DMW, 2012. Robust future precipitation declines in CMIP5 largely reflect the poleward expansion of model subtropical dry zones. Geophysical Research Letters, 39: L18704.

Schmidt GA, Kelley M, Nazarenko L, Ruedy R, Russell GL, Aleinov I, Bauer M, Bauer SE, Bhat MJ, Bleck R, Canuto V, Chen Y-H, Cheng Y, Clune TL, Del Genio A, de Fainchtein R, Faluvegi G, Hansen JE, Healy RJ, Kiang NY, Koch D, Lacis AA, LeGrande AN, Lerner J, Lo KK, Matthews EE, Menon S, Miller RL, Oinas V, Oloso AO, Perlwitz JP, Puma MJ, Putman WM, Rind D, Romanou A, Sato M, Shindell DT, Sun S, Syed RA, Tausnev N, Tsigaridis K, Unger N, Voulgarakis A, Yao M-S, Zhang J, 2014. Configuration and assessment of GISS ModelE2 contributions to the CMIP5 archive. Journal of Advances in Modeling Earth Systems, 6: 141–184. doi: 10.1002/2013MS000265

Scott F, Blanchard JL, Andersen KH, 2014. mizer: an R package for multispecies, trait-based and community size spectrum ecological modelling. Methods in Ecology and Evolution, 5(10): 1121-1125. doi: 10.1111/2041-210X.12256

Séférian R, Bopp L, Gehlen M, Orr JC, Ethé C, Cadule P, Aumont O, Salas y Mélia D, Voldoire A, Madec G, 2012. Skill assessment of three earth system models with common marine biogeochemistry. Climate Dynamics, 40: 2549-2573. doi: 10.1007/s00382-012-1362-8

Seki MP, 1993. The role of the Neon Flying Squid, *Ommastrephes bartimi*, in the North Pacific Pelagic Food web. International Bulletin of the North Pacific Commission, 53(2): 207-215.

Sen Gupta A, Jourdain NC, Brown JN, Monselesan D, 2013. Climate drift in the CMIP5 models. Journal of Climate, 26: 8597–8615.

Sepulveda CA, Aalbers SA, Ortega-Garcia S, Wegner NC, Bernal D, 2011. Depth distribution and temperature preferences of wahoo (*Acanthocybium solandri*) off Baja California Sur, Mexico. Marine Biology, 158: 917-926. doi: 10.1007/s00227-010-1618-y

Shark Working Group Report, 2017. Stock assessment and future projections of blue shark in the North Pacific Ocean through 2015. International Scientific Committee for Tuna and Tuna-like Species in the North Pacific Ocean, Vancouver, Canada. 95p.

Sheridan JA, Bickford D, 2011. Shrinking body size as an ecological response to climate change. Nature Climate Change, 1(8), 401-406. doi: 10.1038/nclimate1259.

Shimose T, Yokawa K, Tachihara K, 2015. Age determination and growth estimation from otolith micro-increments and fin spine sections of blue marlin (*Makaira nigricans*) in the western North Pacific. Marine and Freshwater Research, 66: 1116-1127. doi: 10.1071/MF14305

Shin Y-J, Shannon LJ, Cury PM, 2004. Simulations of fishing effects on the southern Benguela fish community using an individual-based model: learning from a comparison with ECOSIM. African Journal of Marine Science, 26: 95-114.

Sibert J, Hampton J, Kleiber P, Maunder M, 2006. Biomass, size, and trophic status of top predators in the Pacific Ocean. Science, 314: 1773-1776. doi: 10.1126/science.1135347

Smith ADM, Brown CJ, Bulman CM, Fulton EA, Johnson P, Kaplan IC, Lozano-Montes H, Mackinson S, Marzloff M, Shannon LJ, Shin Y-J, Tam J, 2011. Impacts of fishing low-trophic level species on marine ecosystems. Science, 333: 1147-1150. doi: 10.1126/science.1209395.

Speirs DC, Guirey EJ, Gurney WSC, Heath MR, 2010. A length-structured partial ecosystem model for cod in the North Sea. Fisheries Research, 106: 474-494.

Steinacher M, Joos F, Frölicher TL, Bopp L, Cadule P, Cocco V, Doney SC, Gehlen M, Lindsay K, Moore JK, Schneider B, Segschneider J, 2010. Projected 21st century decrease in marine productivity: a multi-model analysis. Biogeosciences, 7: 979–1005.

Steneck RS, Graham MH, Bourque BJ, Corbett D, Erlandson JM, Estes JA, Tegner MJ, 2002. Kelp forest ecosystems: biodiversity, stability, resilience and future. Environmental Conservation, 29(4): 436-459. doi: 10.1017/S0376892902000322.

Stevens JD, Bradford RW, West GJ, 2010. Satellite tagging of blue sharks (*Prionace glauca*) and other pelagic sharks off eastern Australia: depth behavior, temperature experience and movements. Marine Biology, 157: 575-591. doi: 10.1007/s00227-009-1343-6

Stock CA, Dunne JP, John JG, 2014. Drivers of trophic amplification of ocean productivity trends in a changing climate. Biogeosciences, 11: 7125–7135.

Storch D, Menzel L, Frickenhaus S, Pörtner H-O, 2014. Climate sensitivity across marine domains of life: limits to evolutionary adaptation shape species interactions. Global Change Biology, 20: 3059–3067.

Stramma L, Johnson GC, Sprintall J, Mohrholz V, 2008. Expanding oxygen-minimum zones in the tropical oceans. Science, 320: 655-658. doi: 10.1126/science.1153847

Sundberg M, Underkoffler K, 2011. Size composition and length-weight data for bottomfish and pelagic species sampled and the United Fishing Agency fish auction in Honolulu, Hawaii from October 2007 through December 2009. PIFSC Administrative Report H-11-04. 38 p.

Tans P, Keeling R, 2014. Mauna Loa CO_2 annual mean data. NOAA/ERSL. Available at http://www.esrl.noaa.gov/gmd/ccgg/trends/ and scrippsco2.ucsd.edu/

Taylor KE, Stouffer RJ, Meehl GA, 2012. An overview of CMIP5 and the experiment design. Bulletin of the American Meteorological Society, 93(4): 485-498. doi: 10.1175/BAMS-D-11-00094.1.

Tittensor DP, Eddy TD, Lotze HK, Galbraith ED, Cheung W, Barange M, Blanchard JL, Bopp L, Bryndum-Buchholz A, Büchner M, Bulman C, Carozza DA, Christensen V, Coll M, Dunne JP, Fernandes JA, Fulton EA, Hobday AJ, Huber V, Jennings S, Jones M, Lehodey P, Link JS, Mackinson S, Maury O, Niiranen S, Oliveros-Ramos R, Roy T, Schewe J, Shin Y-J, Silva T, Stock CA, Steenbeek J, Underwood PJ, Volkholz J, Watson JR, Walker ND, 2018. A protocol for the intercomparison of marine fishery and ecosystem models: Fish-MIP v1.0. Geoscientific Model Development, 11(4): 1421–1442. doi: 10.5194/gmd-11-1421-2018

Travers M, Shin Y-J, Jennings S, Machu E, Huggett JA, Field JG, Cury PM, 2009. Two-way coupling versus one-way forcing of plankton and fish models to predict ecosystem changes in the Benguela. Ecological Modelling, 220: 3089-3099. doi: 10.1016/j.ecolmodel.2009.08.016.

Travers M, Watermeyer K, Shannon LJ, Shin Y-J, 2010. Changes in food web structure under scenarios of overfishing in the southern Benguela: Comparison of the Ecosim and OSMOSE modelling approaches. Journal of Marine Systems, 79: 101-111. doi: 10.1016/j.jmarsys.2009.07.005.

Uchiyama JH, Boggs CH, 2006. Length-weight relationships of dolphinfish, *Coryphaena hippurus*, and wahoo, *Acanthocybiom solandri*: seasonal effects of spawning and possible migration in the central North Pacific. Marine Fisheries Review, 68: 19-29.

Uchiyama JH, Burch RK, Kraul SA, 1986. Growth of dolphins, *Coryphaena hippurus* and *C. equiselis*, in Hawaiian waters as determined by daily increments on otoliths. Fishery Bulletin, 84(1): 186-191.

Uchiyama JH, DeMartini EE, Williams HA, 1999. Length-weight interrelationships for swordfish, *Xiphas gladius*, caught in the central North Pacific. NMFS Tech. Memo. 284, 91 p.

Uchiyama JH, Kazama TK, 2003. Updated weight-on-length relationships for pelagic fishes caught in the central North Pacific Ocean and bottomfishes from the Northwestern Hawaiian Islands. PIFSC Administrative Report H-03-01. 46 p.

United Nations (UN), 2011. Seven billion and growing: the role of population policy in achieving sustainability. Technical Paper No. 2011/13. 36 pp.

van der Heide T, Roijackers RMM, van New EH, Peeters ETHM, 2006. A simple equation for describing the temperature dependent growth of free-floating macrophytes. Aquatic Botany, 84: 171-175. doi: 10,1016/j.aquabot.2005.09.004

Van Vuuen DP, Edmonds J, Kainuma M, Raihi K, Thompson A, Hibbard K, Hurtt GC, Kram T, Krey V, Lamarque J-F, Masui T, Meinshausen M, Nakicenovic N, Smith SJ, Rose SK, 2011. The representative concentration pathways: An overview. Climatic Change, 109: 5-31. doi: 10.1007/s10584-011-0148-z

Vasconcellos M, Mackinson S, Sloman K, Pauly D, 1997. The stability of trophic mass-balance models of marine ecosystems: a comparative analysis. Ecological Modelling, 100: 125-134.

Walsh WA, Brodziak J, 2015. Billfish CPUE standardization in the Hawaii longline fishery: model selection and multimodel inference. Fisheries Research, 166: 151-162. doi: 10.1016/j.fishres.2014.07.015

Walsh WA, Ito RY, Kawamoto KE, McCracken M, 2005. Analysis of logbook accuracy for blue marlin (*Makaira nigricans*) in the Hawaii-based longline fishery with a generalized additive model and commercial sales data. Fisheries Research, 75: 175-192. doi: 10.1016/j.fishres.2004.11.007

Walsh WA, Kleiber P, McCracken M, 2002. Comparison of logbook reports of incidental blue shark catch rates by Hawaii-based longline vessels to fishery observer data by application of a generalized additive model. Fisheries Research, 58: 79-94.

Walsh HJ, Richardson DE, Marancik KE, Hare JA, 2015. Long-term changes in the distributions of larval and adult fish in the Northeastern U.S. shelf ecosystem. PLoS One, 10: e0137382.

Ward P, Myers RA, 2005a. Inferring the depth distribution of catchability for pelagic fishes and correcting for variations in the depth of longline fishing gear. Canadian Journal of Fisheries and Aquatic Science, 62: 1130-1142. doi: 10.1139/F05-021

Ward P, Myers RA, 2005b. Shifts in open-ocean fish communities coinciding with the commencement of commercial fishing. Ecology, 86(4): 835-847.

Watson RA, Cheung WWL, Anticamara JA, Sumaila RU, Zeller D, Pauly D, 2012. Global marine yield halved as fishing intensity redoubles. Fish and Fisheries, 14(4): 493–503. doi: 10.1111/j.1467-2979.2012.00483.x

Watters GM, Olson RJ, Francis RC, Fiedler PC, Polovina JJ, Reilly SB, Aydin KA, Boggs CH, Essington TE, Walters CJ, Kitchell JF, 2003. Physical forcing and the dynamics of the pelagic ecosystem in the eastern tropical Pacific: simulations with ENSO-scale and global-warming climate drivers. Canadian Journal of Fisheries and Aquatic Sciences, 60: 1161-1175. doi: 10.1139/F03-100.

Wild A, 1986. Growth of yellowfin tuna, *Thunnus albacares*, in the Eastern Pacific Ocean based on otolith increments. Inter-American Tropical Tuna Commission Bulletin, 18(6): 423-482.

Wirtz KW, 2012. Who is eating whom? Morphology and feeding type determine the size relation between planktonic predators and their ideal prey. Marine Ecology Progress Series, 445: 1-12. doi: 10.3354/meps09502.

Woodworth-Jefcoats PA, Polovina JJ, Drazen JC, 2017. Climate change is projected to reduce carrying capacity and redistribute species richness in North Pacific pelagic marine ecosystems. Global Change Biology, 23(3): 1000-1008. doi: 10.1111/gcb.13471

Woodworth-Jefcoats PA, Polovina JJ, Drazen JC, 2018. Synergy among oceanographic variability, fishery expansion, and longline catch composition in the central North Pacific Ocean. Fishery Bulletin, 116(3-4): 228-239. doi: 10.7755/FB.116.3.2

Woodworth-Jefcoats PA, Polovina JJ, Dunne JP, Blanchard JL, 2013. Ecosystem size structure responses to 21st century climate projection: large fish abundance decreases in the central North Pacific and increases in the California Current. Global Change Biology, 19: 724-733. doi: 10.1111/gcb.12076.

Woodworth-Jefcoats PA, Polovina JJ, Howell EA, Blanchard JL, 2015. Two takes on the ecosystem impacts of climate change and fishing: comparing a size-based and a species-based ecosystem model in the central North Pacific. Progress in Oceanography, 138: 533–545.

Wynes S, Nicholas KA, 2017. The climate mitigation gap: education and government recommendations miss the most effective individual actions. Environmental Research Letters, 12(7): 074024–10. doi: 10.1088/1748-9326/aa7541

Xu L, Xie S-P, Lui Q, 2012. Mode water ventilation and subtropical countercurrent over the North Pacific in CMIP5 simulations and future projections. Journal of Geophysical Research, 117: C12009.

Yongyun H, Lijun T, Jiping L, 2012. Poleward expansion of the Hadley circulation in CMIP5 simulations. Advances in Atmospheric Sciences, 30: 790–795.

Young CN, Carlson J, Hutchinson M, Kobayashi D, McCandless C, Miller MH, Teo S, Warren T, 2016. Status review report: common thresher shark (*Alopias vulpinus*) and bigeye thresher shark (*Alopias superciliosus*). Final Report to National Marine Fisheries Service, Office of Protected Resources. March 2016. 199 pp.

Yukimoto S, Yoshimura H, Hosaka M, Sakami T, Tsujino H, Hirabara M, Tanaka TY, Deushi M, Obata A, Nakano H, Adachi Y, Shindo E, Yabu S, Ose T, Kitoh A, 2011. Meteorological Research Institute-Earth System Model Version 1 (MRI-ESM1) Model Description. Technical Report of the Meteorological Research Institute No. 64.

Yvon-Durocher G, Montoya JM, Trimmer M, Woodward G, 2011. Warming alters the size spectrum and shifts the distribution of biomass in freshwater ecosystems. Global Change Biology, 17: 1681-1694. doi: 10.1111/j.1365-2486.2010.02321.x.

Zhang C, Chen Y, Ren Y, 2015. Assessing uncertainty of a multispecies size-spectrum model resulting from process and observation errors. ICES Journal of Marine Science, 72(8): 2223–2233. doi: 10.1093/icesjms/fsv086

Zhu G, Xu L, Zhou Y, Dai X, 2008. Length-frequency compositions and weight-length relationships for bigeye tuna, yellowfin tuna, and albacore (Perciformes: scombrinae) in the Atlantic, Indian, and Eastern Pacific Oceans. Acta Icthyological et Piscatoria, 38: 157-161.

Zischke MT, Farley JH, Griffiths SP, Tibbetts IR, 2013a. Reproductive biology of wahoo, *Acanthocybium solandri*, off eastern Australia. Reviews in Fish Biology and Fisheries, 23: 491-506. doi: 10.1007/s11160-013-9304-1

Zischke MT, Griffiths SP, Tibbets IR, 2013b. Rapid growth of wahoo (*Acanthocybium solandri*) in the Coral Sea, based on length-at-age estimates using annual and daily increments on sagittal otoliths. ICES Journal of Marine Science, 70(6): 1128-1139. doi: 10.1093/icesjms/fst039